THE PROCEEDINGS OF
THE PHYSICAL SOCIETY

Section A

VOL. 64, PART 6 1 June 1951 No. 378 A

The Vibrations of an Infinitely Long Chain of CH_2-Groups and the Infra-Red Spectrum of Polythene

BY L. KELLNER
Imperial College, London

MS. received 31st July 1950, and in amended form 14th December 1950

ABSTRACT. An attempt has been made to interpret the infra-red spectrum of polythene as the spectrum of an infinitely long chain of CH_2-groups. The vibrations of such a chain have been calculated using a potential function which involves valence and angle forces as well as the torsional force resisting a twisting of the C–C bonds. The selection rules and states of polarization of the fourteen possible frequencies are derived. The observed bands are assigned to the calculated vibrations and the force constants are evaluated. It is shown that the oscillations involving the C–C valence force are weakly active in contradiction to the theory. In the last section, this activity has been ascribed to the presence of CH_3-groups at the ends of the polythene chain.

§1. INTRODUCTION

POLYTHENE, a condensation product of ethylene, is presumed to have the formula C_nH_{2n+2}, i.e. it consists of a very long chain of CH_2-groups with a CH_3-group at each end of the molecule. Since polythene has a molecular weight of 13,000, n is approximately 928 so that the effect of the additional third CH-linkages at the two ends can be neglected in comparison with the periodic CH_2-structure along the axis of the molecule. The crystal structure of a polythene containing 1,000 CH_2-groups has been investigated by Bunn (1939). The carbon atoms are found to be arranged in a plane zigzag structure so that the hydrogen atoms are in a plane normal to the molecular axis. The C–C bonds have an equilibrium length of 1·54A. and form a valency angle of 112°. The elementary cell contains four CH_2-groups belonging to two molecules so that every molecule can be said to possess two CH_2-groups per unit cell. Thompson and Torkington (1945) studied the infra-red spectrum of polythene in the range between 3,000 and 600 cm^{-1}, while Fox and Martin (1940) investigated the region of the C–H valence vibrations in greater detail. The infra-red bands exhibit dichroism as observations with polarized light have shown (Elliott, Ambrose and Temple 1948, 1949). The striking feature of the spectrum is the comparative paucity of bands (their number is 10) in such a large molecule. If polythene is considered as a lattice with two CH_2-groups in the elementary cell and one translational axis, the

spectrum can be expected to show at most $3\times 6=18$ bands instead of the $9n$ vibrations of the molecule C_nH_{2n+2}. In the following, an attempt is therefore made to calculate the spectrum of such a lattice and compare the results with the observations.

§2. VIBRATIONS OF AN INFINITELY LONG CHAIN C_nH_{2n}

The vibrations of an infinitely long chain of CH_2-groups have been calculated by Kirkwood (1939) for the valence and deformation frequencies of the carbon atoms only; Whitcomb, Nielsen and Thomas (1940) derived the spectrum in the case that the carbon and hydrogen atoms move in a central force field. Simanouti and Mizushima (1949) solved the problem for a Urey–Bradley field acting between the carbon and hydrogen atoms. They alone applied the solution to a very long chain, the polythene molecule, while in the other two publications the method is used to interpret the spectra of short hydrocarbon chains ($n=3$ and 11) where the method breaks down since the boundary conditions become of importance. Simanouti and Mizushima's spectrum is not complete as they do not include the forces responsible for the non-planar motions of the carbon atoms and the torsional vibrations. Consequently, they obtain only six frequencies for polythene instead of the fourteen possible vibrations given here.

Since the number of CH_3-groups in the polythene model adopted here is negligible compared with that of the CH_2-groups, the infra-red spectrum is in first approximation assumed to originate from the vibrations of an infinitely long chain C_nH_{2n}. In agreement with x-ray evidence (Bunn 1939), the carbon atoms form a zigzag line in the x, y plane where the valence angle between two consecutive C–C bonds is the tetrahedral angle θ (the crystal structure analysis gives an angle of 112°). Two hydrogen atoms are linked to every carbon atom in such a way that they are symmetrically disposed with respect to the x,y plane, C–H bonds enclosing a tetrahedral angle with the adjacent C–C linkages and with each other. The molecule C_nH_{2n} can then be described as a lattice whose elementary cell contains two CH_2-groups; the lattice is produced by a translation of the elementary cell by $2a\sin\frac{1}{2}\theta$ along the x-axis where a is the equilibrium distance of the C–C bonds. It is assumed that the potential function of this structure is dependent on valence and angle forces. It will then have the form :

$$2V=f_C\sum_{i=1}^{n-1} l_i^2+f_H\sum_{i=1}^{n}(l_i'^2+l_i''^2)+a^2\phi_C\sum_{i=2}^{n-1}\lambda_i^2+b^2\phi_H\sum_{i=1}^{n}\beta_i^2+ab\phi_{CH}\sum_{i=1}^{n}(\delta_i'^2+\delta_i''^2)$$
$$+ab\phi_{CH}\sum_{i=1}^{n}(\epsilon_i'^2+\epsilon_i''^2)+2ab\sin\tfrac{1}{2}\theta\tau\sum_{i=1}^{n-1}\psi_i^2+2a^2\sin\theta\eta\sum_{i=1}^{n-3}\alpha_i^2$$
$$(\lambda_i+\delta_i'+\delta_i''=\beta_i+\epsilon_i'+\epsilon_i''),$$

where the symbols have the following meanings: l_i = stretching of the C_i–C_{i+1} linkages, l_i' and l_i'' = stretching of the two C–H linkages attached to C_i, λ_i = change of the angle C_{i-1}–C_i–C_{i+1} from its equilibrium value, β_i = change of the angle H_i'–C_i–H_i'', δ_i', δ_i'' = change of the angle C_{i-1}–C_i–H_i', ϵ_i', ϵ_i'' = change of the angle H_i'–C_i–C_{i+1}, ψ_i = angle of twist of the C–C linkages produced by a rotation of the two CH_2 groups at the ends of each bond around it, α_i = angle between the plane containing C_{i-2}, C_{i-1} and C_i, and the plane containing the particles C_{i-1}, C_i and C_{i+1}, a = equilibrium distance of the carbon atoms, b = equilibrium distance of the hydrogen atoms, θ = tetrahedral angle. f_C, f_H etc. are the force constants associated with these movements. The coordinates used in the potential function are

$$
\begin{vmatrix}
m_C\omega^2 - 2(1-\cos\alpha) \\
\quad \times \{\sin^2\tfrac{1}{2}\theta f_C \\
\quad + \phi_{CH}(b\cos^2\tfrac{1}{2}\theta)/a + a\} \\
\quad - a\phi_{CH}/b\cos^2\tfrac{1}{2}\theta \\
\quad - 4\cos^2\tfrac{1}{2}\theta\sin^2\alpha\,\phi_C
& i\sin\alpha\sin\theta \\
\quad \times \{f_C - (\phi_{CH}/2a\cos^2\tfrac{1}{2}\theta) \\
\quad \times (2b\cos^2\tfrac{1}{2}\theta + a\sin^2\tfrac{1}{2}\theta)\} \\
\quad - 2\,i\sin\alpha\sin\theta \\
\quad \times (1+\cos\alpha)\phi_C
& \phi_{CH}(1-\cos\alpha) \\
\quad + a\phi_{CH}/b\cos^2\tfrac{1}{2}\theta
& -i\sin\alpha\sin\theta\,\phi_{CH}
& i\sin\alpha\cos^2\tfrac{1}{2}\theta\,\phi_{CH} \\
-i\sin\alpha\sin\theta \\
\quad \times \{f_C - (\phi_{CH}/2a\cos^2\tfrac{1}{2}\theta) \\
\quad \times (2b\cos^2\tfrac{1}{2}\theta + a\sin^2\tfrac{1}{2}\theta) \\
\quad - 2\phi_C(1+\cos\alpha)\}
& m_C\omega^2 - 2\cos^2\tfrac{1}{2}\theta f_H \\
\quad - 4\sin^2\tfrac{1}{2}\theta\,\phi_H \\
\quad - a\sin^2\tfrac{1}{2}\theta\,\phi_{CH}/b \\
\quad - 2(1+\cos\alpha) \\
\quad \times \{\cos^2\tfrac{1}{2}\theta f_C + \sin^2\tfrac{1}{2}\theta \\
\quad \times (\phi_{CH}/a)(b-a)\} \\
\quad - 4\sin^2\tfrac{1}{2}\theta \\
\quad \times \phi_C(1+\cos\alpha)^2
& -i\sin\alpha\tan\tfrac{1}{2}\theta\,\phi_{CH}
& 2\cos^2\tfrac{1}{2}\theta f_H + 4\sin^2\tfrac{1}{2}\theta\,\phi_H \\
\quad + (\sin^2\tfrac{1}{2}\theta/b)\phi_{CH} \\
\quad \times \{a - b(1+\cos\alpha)\}
& \sin\theta\{f_H - 2\phi_H + (\phi_{CH}/2b) \\
\quad \times [b(1+\cos\alpha) - a]\} \\
(\phi_{CH}/2b\cos^2\tfrac{1}{2}\theta) \\
\quad \times \{a + b\cos^2\tfrac{1}{2}\theta \\
\quad \times (1-\cos\alpha)\}
& (i\sin\alpha\tan\tfrac{1}{2}\theta/2)\phi_{CH}
& m_H\omega^2 - a\phi_{CH}/2b\cos^2\tfrac{1}{2}\theta
& 0
& 0 \\
(i\sin\alpha\sin\theta/4)\phi_{CH}
& \cos^2\tfrac{1}{2}\theta f_H + 2\sin^2\tfrac{1}{2}\theta\,\phi_H \\
\quad - \tfrac{1}{2}\sin^2\tfrac{1}{2}\theta(1+\cos\alpha)\phi_{CH} \\
\quad + (a\sin^2\tfrac{1}{2}\theta/2b)\phi_{CH}
& 0
& m_H\omega^2 - \cos^2\tfrac{1}{2}\theta f_H \\
\quad - 2\sin^2\tfrac{1}{2}\theta\,\phi_H \\
\quad - (a\sin^2\tfrac{1}{2}\theta/2b)\phi_{CH}
& -\tfrac{1}{2}\sin\theta(f_H - 2\phi_H \\
\quad - a\phi_{CH}/2b) \\
-(i\sin\alpha\cos^2\tfrac{1}{2}\theta/2)\phi_{CH}
& \tfrac{1}{2}\sin\theta\{f_H - 2\phi_H + (\phi_{CH}/2b) \\
\quad \times [b(1+\cos\alpha) - a]\}
& 0
& -\tfrac{1}{2}\sin\theta(f_H - 2\phi_H \\
\quad - a\phi_{CH}/2b)
& m_H\omega^2 - \sin^2\tfrac{1}{2}\theta f_H \\
\quad - 2\cos^2\tfrac{1}{2}\theta\,\phi_H \\
\quad - (a\cos^2\tfrac{1}{2}\theta/2b)\phi_{CH}
\end{vmatrix} = 0. \quad \ldots\ldots (1)
$$

$$
\begin{vmatrix}
m_C\omega^2 - 2\sin^2\tfrac{1}{2}\theta f_H & 2i\sin\alpha[(\phi_{CH}/2\cos^2\tfrac{1}{2}\theta) & \sin\theta[f_H - a\phi_{CH}/2b] & 2\sin^2\tfrac{1}{2}\theta f_H \\
\quad -(a\cos^2\tfrac{1}{2}\theta/b)\phi_{CH} & \quad +4\sin\tfrac{1}{2}\theta\tau] & \quad -\tan\tfrac{1}{2}\theta(1-\cos\alpha)\phi_{CH} & \quad +(a\cos^2\tfrac{1}{2}\theta/b)\phi_{CH} \\
\quad -[2(1-\cos\alpha)/a\cos^2\tfrac{1}{2}\theta] & & \quad -8\cos\tfrac{1}{2}\theta(1-\cos\alpha)\tau & \quad +(1-\cos\alpha)\phi_{CH} \\
\quad \times(b+a\cos^2\tfrac{1}{2}\theta)\phi_{CH} & & & \\
\quad -(16b\sin\tfrac{1}{2}\theta/a)(1-\cos\alpha)\tau & & & \\
\quad -(4\eta/\sin\tfrac{1}{2}\theta)(1-\cos\alpha)\sin^2\alpha & & & \\
-2i\sin\alpha[(1/4\cos^2\tfrac{1}{2}\theta)\phi_{CH} & m_H\omega^2 - (a/2b\cos^2\tfrac{1}{2}\theta)\phi_{CH} & (-2i\sin\alpha\, a\cos\tfrac{1}{2}\theta/b)\tau & 0 \\
\quad +2\sin\tfrac{1}{2}\theta\tau] & \quad -(2a\sin\tfrac{1}{2}\theta/b)(1+\cos\alpha)\tau & & \\
\tfrac{1}{2}\sin\theta\,[f_H - (a\phi_{CH}/2b)] & (2i\sin\alpha\, a\cos\tfrac{1}{2}\theta/b)\tau & m_H\omega^2 - \cos^2\tfrac{1}{2}\theta f_H & -\tfrac{1}{2}\sin\theta(f_H - a\phi_{CH}/2b) \\
\quad -\tfrac{1}{2}\tan\tfrac{1}{2}\theta(1-\cos\alpha)\phi_{CH} & & \quad -(a\sin^2\tfrac{1}{2}\theta/2b)\phi_{CH} & \\
\quad -4\cos\tfrac{1}{2}\theta(1-\cos\alpha)\tau & & \quad -(2a\cos^2\tfrac{1}{2}\theta/b\sin\tfrac{1}{2}\theta) & \\
 & & \quad \times(1-\cos\alpha)\tau & \\
\sin^2\tfrac{1}{2}\theta f_H + (a\cos^2\tfrac{1}{2}\theta/2b)\phi_{CH} & 0 & -\tfrac{1}{2}\sin\theta(f_H - a\phi_{CH}/2b) & m_H\omega^2 - \sin^2\tfrac{1}{2}\theta f_H \\
\quad +\tfrac{1}{2}(1-\cos\alpha)\phi_{CH} & & & \quad -(a\cos^2\tfrac{1}{2}\theta/2b)\phi_{CH}
\end{vmatrix} = 0. \quad \ldots\ldots(2)
$$

linear combinations of the displacements of the atoms along the three coordinate axes; the method adopted in determining the coordinates and in calculating the frequencies has been used in a previous paper (Kellner 1941).

The vibrations can be split up into two groups, symmetric and antisymmetric with respect to the x, y plane. In the symmetric oscillations, the carbon atoms move only in the x, y plane and the two hydrogen atoms attached to every C_i swing in unison so that $l_i'=l_i''$, $\delta_i'=\delta_i''$, $\epsilon_i'=\epsilon_i''$, $\psi_i=\alpha_i=0$. Since the angle coordinates are not independent of each other $(\lambda_i+\delta_i'+\delta_i''=\beta_i+\epsilon_i'+\epsilon_i'')$, the group of symmetric vibrations results in five frequency branches involving the stretching of the C–C bonds and of the C–H bonds and the deformations of the valence angles enclosed by them.

In the second group, the carbon atoms perform a movement parallel to the z axis while the hydrogen atoms oscillate in antiphase. Consequently, $l_i'=-l_i''$, $\delta_i'=-\delta_i''$, $\epsilon_i'=-\epsilon_i''$, $l_i=\lambda_i=\beta_i=0$. In these antisymmetric C–H vibrations, the torsional force and the shear determined by the force constants τ and η come into play. In addition, the four frequency branches of this symmetry type involve the stretching of the C–H linkages and the deformation of the valence angles between the C–C and C–H linkages.

The above potential function is used to obtain the frequencies of the C_nH_{2n} molecule assuming that the displacements of the rth particle are proportional to $\exp[i(2\pi\nu t+r\alpha)]$, where ν is the frequency of the oscillation and α is defined as the phase difference between C_i and C_{i+1} or H_i' and H_{i+1}' respectively. The five branches of symmetric vibrations are obtained from the fifth order determinant (1) and the four branches of the antisymmetric vibrations from the fourth order determinant (2).

If the C_nH_{2n} chain is assumed to be infinitely long, only those oscillations will be infra-red active in which the elementary cells swing in phase. Since the unit cell contains two CH_2-groups, i.e. six particles, the phase difference between the two carbon atoms in the cell can be 0 and π. The active vibrations are therefore calculated by evaluating the determinants (1) and (2) with $\alpha=0$ and π. As a result, eighteen vibrations are obtained in accordance with the number of particles per unit cell (the six particles have three degrees of freedom each). The calculated formulae are given below.

I. Symmetric C–H Vibrations

$\alpha=0$. (Determinant (1))

$$\left.\begin{aligned}
&\omega_1^2=0.\\
&\omega_2^2=\frac{a\phi_{CH}}{2b\cos^2\frac{1}{2}\theta}\left(\frac{1}{m_H}+\frac{2}{m_C}\right).\\
&\omega_{3,4,5}^6-\omega_{3,4,5}^4\left\{\frac{4F_C}{m_C}+f_H\left(\frac{1}{m_H}+\frac{2\cos^2\frac{1}{2}\theta}{m_C}\right)+\left(\frac{1}{m_H}+\frac{2\sin^2\frac{1}{2}\theta}{m_C}\right)\Phi\right.\\
&\qquad\left.+\frac{4\sin^2\frac{1}{2}\theta\phi_{CH}}{am_C}(b-a)\right\}+\frac{\omega_{3,4,5}^2}{m_H}\left\{\frac{4F_C}{m_C}(f_H+\Phi)\right.\\
&\qquad+f_H\Phi\left(\frac{1}{m_H}+\frac{2}{m_C}\right)+\frac{2\sin^2\frac{1}{2}\theta}{am_C}(2b-a)f_H\phi_{CH}\\
&\qquad\left.+\frac{8b\sin^2\frac{1}{2}\theta}{am_C}\phi_H\phi_{CH}\right\}-\frac{4F_Cf_H\Phi}{m_Cm_H^2}-\frac{8b\sin^2\frac{1}{2}\theta}{am_Cm_H^2}f_H\phi_H\phi_{CH}=0.
\end{aligned}\right\}\quad\ldots\ldots(3)$$

$\alpha=\pi$.

$$\omega_6^2=0.$$

$$\omega_{7,8}{}^4-\omega_{7,8}{}^2\left\{f_H\left(\frac{1}{m_H}+\frac{2\cos^2\frac{1}{2}\theta}{m_C}\right)+\Phi\left(\frac{1}{m_H}+\frac{2\sin^2\frac{1}{2}\theta}{m_C}\right)\right\}+\frac{f_H\Phi}{m_H}\left(\frac{1}{m_H}+\frac{2}{m_C}\right)=0.$$

$$\omega_{9,10}{}^4-\omega_{9,10}{}^2\left\{\frac{4\sin^2\frac{1}{2}\theta}{m_C}f_C+\frac{a\phi_{CH}}{2b\cos^2\frac{1}{2}\theta}\left(\frac{1}{m_H}+\frac{(2b\cos^2\frac{1}{2}\theta+a)^2}{a^2m_C}\right)\right\}+\frac{2a\sin^2\frac{1}{2}\theta}{b\cos^2\frac{1}{2}\theta\, m_Cm_H}f_C\phi_{CH}=0. \qquad \ldots\ldots(4)$$

II. Antisymmetric C–H Vibrations

$\alpha=0$. (Determinant (2))

$$\omega_{11}{}^2=0.$$

$$\omega_{12}{}^2=\frac{a}{2bm_H}\left(\frac{\phi_{CH}}{\cos^2\frac{1}{2}\theta}+8\sin\tfrac{1}{2}\theta\tau\right).$$

$$\omega_{13,14}{}^4-\omega_{13,14}{}^2\left\{f_H\left(\frac{1}{m_H}+\frac{2\sin^2\frac{1}{2}\theta}{m_C}\right)+\frac{a\phi_{CH}}{2b}\left(\frac{1}{m_H}+\frac{2\cos^2\frac{1}{2}\theta}{m_C}\right)\right\}+\frac{a}{2bm_H}\left(\frac{1}{m_H}+\frac{2}{m_C}\right)f_H\phi_{CH}=0. \qquad \ldots\ldots(5)$$

$\alpha=\pi$.

$$\omega_{15}{}^2=0.$$

$$\omega_{16}{}^2=a/(2b\cos^2\tfrac{1}{2}\theta\, m_H)\phi_{CH}$$

$$\omega_{17,18}{}^4-\omega_{17,18}{}^2\left\{f_H\left(\frac{1}{m_H}+\frac{2\sin^2\frac{1}{2}\theta}{m_C}\right)+\frac{a\phi_{CH}}{2b}\left(\frac{1}{m_H}+\frac{2(2b+a\cos^2\frac{1}{2}\theta)^2}{a^2\cos^2\frac{1}{2}\theta\, m_C}+\frac{4a\cos^2\frac{1}{2}\theta}{b\sin\frac{1}{2}\theta}\tau\right)\right\}+\frac{a}{2bm_H}\left(\frac{1}{m_H}+\frac{2(2b+a\cos^2\frac{1}{2}\theta)^2}{a^2\cos^2\frac{1}{2}\theta\, m_C}+\frac{2\sin^2\frac{1}{2}\theta}{m_C}\right)\times\left(f_H\phi_{CH}+4\sin\theta\cos\tfrac{1}{2}\theta f_H\tau+\frac{4a\cos^4\frac{1}{2}\theta}{b}\phi_{CH}\tau\right)=0. \qquad \ldots\ldots(6)$$

$\omega=2\pi\nu$, m_H = mass of hydrogen atom, m_C = mass of carbon atom, $F_C=\cos^2\frac{1}{2}\theta f_C+4\sin^2\frac{1}{2}\theta\phi_C$, $\Phi=2\phi_H+(a/2b)\phi_{CH}$. It will be seen that the force constant η does not appear in the above formulae but there are two zero frequencies ν_{12} and ν_{15}. The non-planar motions of the carbon atoms do not contribute to the spectrum of the infinitely long chain. As explained above, the amplitudes of the oscillations of the rth particle are proportional to $e^{ir\alpha}$. If therefore u_0, v_0, w_0 denote the amplitudes of the displacements along the x, y, z axes, the amplitudes become for $\alpha=0$:

u_0, $(-1^i)v_0$, w_0 for C_i, $\quad u_0'$, $(-1^i)v_0'$, w_0' for H_i', $\quad u_0''$, $(-1^i)v_0''$, w_0'' for H_i'',

and for $\alpha=\pi$: $(-1^i)u_0$, v_0, $(-1^i)w_0$ for C_i, $\quad (-1^i)u_0'$, v_0', $(-1^i)w_0'$ for H_i',

$(-1^i)u_0''$, v_0'', $(-1^i)w_0''$ for H_i''.

The oscillatory amplitudes for the vibrations calculated above are given in Table 1 for the carbon and hydrogen atoms.

Table 1 gives the motions of the oscillating chain associated with the calculated frequencies. Formulae (3) to (6) show that ν_2 and ν_{16} involve only a change of the C–C–H valence angles while in ν_{12} a twisting movement of the CH_2-groups is added to the distortion of the C–C–H angle. In ν_{13}, ν_{14} and ν_{17}, ν_{18} a stretching of the C–H bonds is linked with a deformation of the C–C–H angles together with a twisting of the C–C linkages in the case of the last two frequencies. In ν_7 and ν_8

Table 1

Frequency	Amplitudes				Type of vibration
ν_2	u_0,	0,	0	C_i	Symmetric, $\alpha=0$
	u_0',	0,	0	H_i'	
	u_0'',	0,	0	H_i''	
ν_3, ν_4, ν_5	0,	$(-1)^i v_0$,	0	C_i	
	0,	$(-1)^i v_0'$,	w_0'	H_i'	
	0,	$(-1)^i v_0''$,	$-w_0'$	H_i''	
ν_7, ν_8	0,	v_0,	0	C_i	Symmetric, $\alpha=\pi$
	0,	v_0',	$(-1)^i w_0'$,	H_i'	
	0,	v_0'',	$-(-1)^i w_0'$	H_i''	
ν_9, ν_{10}	$(-1)^i u_0$,	0,	0	C_i	
	$(-1)^i u_0'$,	0,	0	H_i'	
	$(-1)^i u_0''$,	0,	0	H_i''	
ν_{12}	0,	0,	0	C_i	Antisymmetric, $\alpha=0$
	u_0',	0,	0	H_i'	
	$-u_0''$,	0,	0	H_i''	
ν_{13}, ν_{14}	0,	0,	w_0,	C_i	
	0,	$(-1)^i v_0'$,	w_0'	H_i'	
	0,	$-(-1)^i v_0''$,	w_0''	H_i''	
ν_{16}	0,	0,	0	C_i	Antisymmetric, $\alpha=\pi$
	$(-1)^i u_0'$,	0,	0	H_i'	
	$-(-1)^i u_0''$,	0,	0	H_i''	
ν_{17}, ν_{18}	0,	0,	$(-1)^i w_0$	C_i	
	0,	v_0',	$(-1)^i w_0'$,	H_i'	
	0,	$-v_0''$,	$(-1)^i w_0'$	H_i''	

the C–H stretching is bound up with a contraction of the C–C–H valence angles and a corresponding expansion of the H–C–H angles. A fluctuation of the C–C bond length is accompanied by a variation of the C–C–H angles in ν_9 and ν_{10}. The vibrations ν_3, ν_4, ν_5, finally, are caused by a stretching of all the valence bonds and deformation of the valence angles.

§ 3. SELECTION RULES AND POLARIZATION OF BANDS

The intensity of the bands is proportional to the square of the dipole moments associated with the vibrations of the chain. Since the C–C linkages do not carry a dipole moment or produce one on oscillation, a change of the dipole moment of the chain can only be produced by the C–H bonds. If, therefore, e' is the effective

charge of the C–H dipole, the x-component M_x of the dipole moment is given by $M_x = e' \sum_i (u_i' + u_i'' - 2u_i)$ or, since $m_C \sum_i u_i + m_H \sum_i (u_i' + u_i'') = 0$,

$$M_x = -e' m_C \left(\frac{1}{m_H} + \frac{2}{m_C} \right) \sum_i u_i .$$

There are corresponding expressions for M_y and M_z. The dipole moments can be calculated for the infinite wavelength vibrations from the displacements in Table 1 and are tabulated in Table 2. The oscillations with vanishing dipole moment will be inactive while the state of polarization of the band is indicated by the non-vanishing component of the dipole moment. If the polythene is rolled or stretched, the molecules align themselves with their long axis (here the x-direction) roughly parallel to the surface of the film so that a frequency for which $M_x \neq 0$, may be denoted by π (parallel band) and the symbol σ (perpendicular band) may be used to refer to $M_{y,z} \neq 0$.

Table 2

Frequency	Type of vibration	Dipole moment
ν_2	Symmetric, $\alpha=0$	π $M_x = -e' m_C \left(\frac{1}{m_H} + \frac{2}{m_C} \right) n u_0$
		$M_y = M_z = 0$
ν_3, ν_4, ν_5	Symmetric, $\alpha=0$	$M_x = M_y = M_z = 0$
ν_7, ν_8	Symmetric, $\alpha=\pi$	σ $M_x = M_z = 0$
		$M_y = -e' m_C \left(\frac{1}{m_H} + \frac{2}{m_C} \right) n v_0$
ν_9, ν_{10}	Symmetric, $\alpha=\pi$	$M_x = M_y = M_z = 0$
ν_{12}	Antisymmetric, $\alpha=0$	$M_x = M_y = M_z = 0$
ν_{13}, ν_{14}	Antisymmetric, $\alpha=0$	σ $M_x = M_y = 0$
		$M_z = -e' m_C \left(\frac{1}{m_H} + \frac{2}{m_C} \right) n w_0$
ν_{16}	Antisymmetric, $\alpha=\pi$	$M_x = M_y = M_z = 0$
ν_{17}, ν_{18}	Antisymmetric, $\alpha=\pi$	$M_x = M_y = M_z = 0$

The Table shows that in an infinitely long chain of CH_2-groups, five only of the eighteen possible oscillations will be optically active. The forbidden bands include those involving the stretching and bending of the C–C chain itself and all the torsional vibrations. The result is in agreement with the selection rules due to the inner symmetry of the elementary cell consisting of two CH_2-groups and belonging to the symmetry group C_{2h}. The symmetry properties of this group are set out in the first three columns of Table 3; in column 4 are given the group theoretical selection rules for the infra-red spectrum and in column 5 the symmetry classification used above.

Table 3

Symmetry class	Symmetric	Antisymmetric	Infra-red activity	Classification
A_g	C_2, σ_z, i		forbidden	Symmetric, $\alpha=0$ and π
A_u	C_2	σ_z, i	$M_z \neq 0$	Antisymmetric, $\alpha=0$, π
B_g	i	C_2, σ_z	forbidden	Antisymmetric, $\alpha=0$, π
B_u	σ_z	C_2, i	$M_x \neq 0$, $M_y \neq 0$	Symmetric, $\alpha=0$ and π

In the usual manner, the symbol C_2 stands for the twofold symmetry axis (here the z-axis), σ_z for the symmetry plane (xy plane) and 'i' for the centre of inversion. A glance at Table 1 shows that ν_3, ν_4, ν_5, ν_9, ν_{10} fulfil the symmetry requirements of the symmetry class A_g while ν_{13}, ν_{14} and ν_{16} fall into the symmetry class A_u. ν_{12}, ν_{17} and ν_{18} are of the type B_g and ν_2, ν_7 and ν_8, finally, satisfy the conditions of the symmetry class B_u.

The theory of the vibrations of an infinitely long chain C_nH_{2n} leads therefore to the following conclusions: of the eighteen possible vibrations, five can be expected to be infra-red active, one of which will show polarization along the chain axis while the remaining four possess a polarization normal to the axis of translation.

§ 4. COMPARISON OF THEORY WITH THE OBSERVED INFRA-RED SPECTRUM OF POLYTHENE

The experiments carried out by Thompson and Torkington (1945) on the infra-red absorption spectrum of polythene of high molecular weight (13,000) show three intense bands at 2900 cm^{-1}, 1460 cm^{-1}, and 725 cm^{-1} in addition to two weaker bands 1380 and 1310 cm^{-1}. Besides, there are two faint but quite distinct maxima of absorption at 890 and 1090 cm^{-1}. The first five bands appear intensely in the spectrum of cracked polythenes (molecular weights 500–5,000) while the region between 800 and 1200 cm^{-1} exhibits a number of fairly intense probably unresolved bands which fade out gradually as the molecular weight rises, until only the weak peaks at 890 and 1090 cm^{-1} are left. Two pronounced maxima of absorption at 1640 and 1710 cm^{-1} observed in the compound of lowest molecular weight are equally reduced in intensity in the longer chains. The high-frequency bands

Table 4

Position of band (cm^{-1})	Polarization	Relative intensities
2960	not observed	17
2925	σ	46
2853	σ	31
1710	not observed	0·9
1640	not observed	1·0
1460	σ	100
1380	π	46
1310	not observed	24
1090	not observed	3·5
890	not observed	2·0
725	σ	69

which are associated with the C–H valence vibrations have been investigated in greater detail by Fox and Martin (1940). They found three components at 2960, 2925 and 2853 cm^{-1}; an examination of two different samples of polythene led to identical results for the position and intensity of the bands. The polarization of the bands has been studied by Elliott, Ambrose and Temple (1948, 1949) and by Sutherland and Vallance Jones (1947). All the intense bands are found to absorb more strongly when the electric vector of the incident light is perpendicular to the axis of orientation of the molecule, i.e. the chain axis, with the exception of the 1380 band which shows the reverse effect. The position of the observed bands together with their state of polarization and intensity are given in Table 4 where the term 'relative intensities' refers to the absorption coefficient at the point of maximum absorption.

From a comparison of the observed and calculated states of polarization it is immediately possible to identify 1380 cm^{-1} with ν_2. The assignment of the 1460 band can be decided in the following manner: the choice lies between assigning 1460 to either ν_8 or ν_{14} with 725 as the second alternative. Since a larger force constant Φ (equation (4)) is responsible for the vibration ν_8 as compared with ϕ_{CH} (equation (5)) in the vibration ν_{14}, it seems reasonable to identify ν_8 with 1460. Equally, equations (4) and (5) show that $\nu_7 < \nu_{13}$ so that 2925 may be assigned to ν_{13}, leaving $\nu_7 = 2853$ and $\nu_{14} = 725$ cm^{-1}. If this interpretation is adopted, the following values for the force constants are computed from the equations for the frequencies ν_2, ν_7, ν_8, ν_{13} and ν_{14}: $\phi_{CH} = 0{\cdot}45 \times 10^5$ dyne/cm., $f_H = 4{\cdot}53 \times 10^5$ dyne/cm., $\Phi = 1{\cdot}12 \times 10^5$ dyne/cm., with $a = 1{\cdot}54$ A. and $b = 1{\cdot}08$ A. The values for ϕ_{CH} and Φ lead to a value of $0{\cdot}40 \times 10^5$ dyne/cm. for ϕ_H. With the above values for f_H and ϕ_{CH}, ν_{13} and ν_{14} are calculated to be 2930 and 757 cm^{-1}, as compared with the experimental values 2925 and 725 cm^{-1}.

This interpretation disposes of the active vibrations of the C_nH_{2n} chain; it remains to explain the weak peaks observed in the absorption spectrum. It is well known that the valence frequencies of the C–C linkages lie between the limits 808 and 1140 cm^{-1} (Bartholomé and Teller 1932) so that it seems permissible to identify 890 and 1090 cm^{-1} with the theoretically forbidden bands ν_9 and ν_3 which are caused by the C–C valence force. If ν_9 is assumed to be 890, a value of $3{\cdot}51 \times 10^5$ dyne/cm. obtains for f_C while the assignment $\nu_9 = 1090$ leads to $f_C = 7{\cdot}32 \times 10^5$ dyne/cm., a value which is about 50% higher than that for the C–C linkage in ethane ($4{\cdot}36 \times 10^5$ dyne/cm.). The first interpretation ($\nu_9 = 890$ cm^{-1}) seems therefore more feasible although it results in a very low value for the force constant f_C. There are, however, indications that the C–C valence force in hydrocarbon chains weakens with an increasing number of CH_2-groups. Rasmussen (1948) has shown that the C–C stretching force constant decreases from $4{\cdot}36 \times 10^5$ for ethane to $4{\cdot}15 \times 10^5$ dyne/cm. for iso-butane.

The identification of ν_3 with 1090 leads to a value of $2{\cdot}55 \times 10^5$ dyne/cm. (equation (3)) for F_C, i.e. ϕ_C becomes $= 0{\cdot}54 \times 10^5$ dyne/cm. with $f_C = 3{\cdot}51 \times 10^5$. ν_4 and ν_5 can then be computed and become 2850 and 1555 cm^{-1} while a value of 1660 cm^{-1} is obtained for ν_{10}. Another inactive band, ν_{16}, can be computed from (6) to have the value 1280; it may be identified with the observed band at 1310 cm^{-1}.

An estimate of the magnitude of the constant of twist τ presents the difficulty that all the frequencies involving this force are inactive for the chain C_nH_{2n}. These frequencies have been calculated for a range of values of τ from 0·00 to $0{\cdot}20 \times 10^5$ dyne/cm. and are tabulated in Table 5.

Table 5

τ (10^5 dyne/cm.)	ν_{12} (cm^{-1})	ν_{17} (cm^{-1})	ν_{18} (cm^{-1})
0·00	1280	1127	2950
0·10	1560	1372	2960
0·20	1800	1595	2970

It will be seen from Table 5 that the observed band at 2960 cm^{-1} may be assigned to ν_{18}; since it is mainly caused by the stretching of the C–H valence bonds, it is very insensitive to the value of the force constant τ. The computed values of ν_{17} indicate that the observation of this band is extremely unlikely as it would be completely masked by the intense group between 1300 and 1500 cm^{-1} even if it

were weakly active. If the very faint band at 1710 cm^{-1} is assigned to ν_{12}, τ would assume the value of $0{\cdot}16 \times 10^5$ dyne/cm. which seems rather high.

In Table 6 a survey is given of the observed and calculated frequencies of polythene and a sample of C_nD_{2n+2} (Sheppard and Sutherland 1947), where the same force constants and interatomic distances have been used for the deuterium compound as for the hydrogen compound. The sample of C_nD_{2n+2} does not represent a long chain of CD_2-groups as it was semi-liquid but the frequencies involving movements of the deuterium atoms can be easily picked out as the outstanding bands in the spectrum. The assignment of the bands marked with a question mark must be considered as very tentative only since it is founded on the lattice structure of the long chain.

Table 6

Assignment	Symmetry class	Polythene		C_nD_{2n+2}	
		Calculated	Observed	Calculated	Observed
ν_2	B_u	1380 π	1380 π	1060	1050
ν_3	A_g	1090	1090	1300	1310?
ν_4	A_g	2850	masked by ν_8	2100	not observed
ν_5	A_g	1555	—	897	860?
ν_7	B_u	1460 σ	1460 σ	1065	1100
ν_8	B_u	2853 σ	2853 σ	2080	not observed
ν_9	A_g	890	890	700	710?
ν_{10}	A_g	1660	1640?	1500	not observed
ν_{12}	B_g	1280–1800	?	904–1270	?
ν_{13}	A_u	760 σ	725 σ	543	520
ν_{14}	A_u	2930 σ	2925 σ	2180	not observed
ν_{16}	A_u	1280	1310	904	970?
ν_{17}	B_g	1127–1595	?	954–1336	?
ν_{18}	B_g	2950–2970	2960	2220–2230	not observed

Frequencies are in cm^{-1}.

The C–D valence vibrations were outside the range of the instrument.

The bands 1660 and 1710 have formerly been ascribed to the presence of C=C and C=O groups in polythene since the intensity of these bands increases when the molecule is cracked, i.e. with an increasing degree of oxidation and unsaturation. The C=C linkage is known to possess an eigenfrequency at 1640 and the C=O linkage at 1720. The assignment of the 1640 cm^{-1} band is therefore not certain. It must be emphasized here, however, that the interpretation of the frequency 1380 cm^{-1} seems unambiguous since only one band of parallel polarization has been observed while the theoretical calculations of the C_nH_{2n} spectrum result in the occurrence of only one π-vibration in agreement with experiment. Table 6 shows furthermore that the calculated and observed values of the C_nD_{2n+2} bands deviate no more than 7% from each other.

§ 5. INFLUENCE OF THE CH_3-END GROUPS ON THE POLYTHENE SPECTRUM

It has been shown in the preceding sections that the observed spectrum of polythene can be interpreted as the spectrum of an infinitely long chain of CH_2-groups. The calculations of such a spectrum have shown that the two

C–C valence vibrations of the chain, i.e. ν_3 and ν_9 should be infra-red inactive, provided the dipole moment of the chain is caused by the moments of the C–H linkages. These two bands, however, occur as weak peaks of absorption in the observed spectrum. Since it is generally assumed that the polythene molecule terminates in CH_3-groups like an ordinary hydrocarbon C_nH_{2n+2}, it seems likely that the non-vanishing intensity of ν_3 and ν_9 is connected with the presence of the two additional C–H linkages at the ends of the molecule. In the following, an an investigation is carried out into the vibrations and selection rules of the valence frequencies of a molecule C_nH_{2n+2}. The potential function V is then reduced to the form:

$$2V = f_C \sum_{i=1}^{n-1} l_i^2 + f_H \sum_{i=1}^{n} (l_i'^2 + l_i''^2) + f_H(l_1'''^2 + l_n'''^2),$$

where the symbols have the same meaning as in §2 and l_1''' and l_n''' refer to the stretching of the two additional links at the ends. If the displacements are assumed to oscillate with the angular frequency ω, the frequencies ω are determined by the following system of equations:

$$\left.\begin{aligned}
\omega^2 l_i &= \frac{f_C}{m_C}\{2l_i + \cos\theta(l_{i-1} + l_{i+1})\} + \frac{f_H \cos\theta}{m_C}\{l_i' + l_i'' + l_{i+1}' + l_{i+1}''\},\\
\omega^2 l_i' &= f_H\left\{l_i'\left(\frac{1}{m_H} + \frac{1}{m_C}\right) + \frac{\cos\theta}{m_C} l_i''\right\} + \frac{f_C \cos\theta}{m_C}(l_i + l_{i-1})\\
\omega^2 l_i'' &= f_H\left\{l_i''\left(\frac{1}{m_H} + \frac{1}{m_C}\right) + \frac{\cos\theta}{m_C} l_i'\right\} + \frac{f_C \cos\theta}{m_C}(l_i + l_{i-1}),
\end{aligned}\right\} \quad \ldots\ldots(7)$$

$i = 2, 3, \ldots n-2.$

$$\left.\begin{aligned}
\omega^2 l_1 &= \frac{f_C}{m_C}\{2l_1 + \cos\theta\, l_2\} + \frac{f_H \cos\theta}{m_C}(l_2' + l_2'' + l_1' + l_1'' + l_1'''),\\
\omega^2 l_1' &= f_H\left\{l_1'\left(\frac{1}{m_H} + \frac{1}{m_C}\right) + \frac{\cos\theta}{m_C}(l_1'' + l_1''')\right\} + \frac{f_C \cos\theta}{m_C} l_1,\\
\omega^2 l_1'' &= f_H\left\{l_1''\left(\frac{1}{m_H} + \frac{1}{m_C}\right) + \frac{\cos\theta}{m_C}(l_1' + l_1''')\right\} + \frac{f_C \cos\theta}{m_C} l_1,\\
\omega^2 l_1''' &= f_H\left\{l_1'''\left(\frac{1}{m_H} + \frac{1}{m_C}\right) + \frac{\cos\theta}{m_C}(l_1' + l_1'')\right\} + \frac{f_C \cos\theta}{m_C} l_1.
\end{aligned}\right\} \quad \ldots\ldots(8)$$

$$\left.\begin{aligned}
\omega^2 l_{n-1} &= \frac{f_C}{m_C}\{2l_{n-1} + \cos\theta\, l_{n-2}\} + \frac{f_H \cos\theta}{m_C}(l_{n-1}' + l_{n-1}'' + l_n' + l_n'' + l_n'''),\\
\omega^2 l_n' &= f_H\left\{l_n'\left(\frac{1}{m_H} + \frac{1}{m_C}\right) + \frac{\cos\vartheta}{m_C}(l_n'' + l_n''')\right\} + \frac{f_C \cos\theta}{m_C} l_{n-1},\\
\omega^2 l_n'' &= f_H\left\{l_n''\left(\frac{1}{m_H} + \frac{1}{m_C}\right) + \frac{\cos\theta}{m_C}(l_n' + l_n''')\right\} + \frac{f_C \cos\theta}{m_C} l_{n-1},\\
\omega^2 l_n''' &= f_H\left\{l_n'''\left(\frac{1}{m_H} + \frac{1}{m_C}\right) + \frac{\cos\theta}{m_C}(l_n' + l_n'')\right\} + \frac{f_C \cos\theta}{m_C} l_{n-1}.
\end{aligned}\right\} \quad \ldots(9)$$

With the substitution $f_H l_1'' = f_C l_0^*$ and $f_H l_n'' = f_C l_n^*$, the first three equations of (8) and (9) assume the form of the general equations (7) while the third equations of (8) and (9) become:

$$l_0^*\left\{\omega^2 - f_H\left(\frac{1}{m_H}+\frac{1}{m_C}\right)\right\} = \frac{f_H\cos\theta}{m_C} l_1 + \left\{\frac{2f_H^2\cos^2\theta}{m_C^2}(l_1+l_0^*)\right\}\Big/\left\{\omega^2 - f_H\left(\frac{1}{m_H}+\frac{1+\cos\theta}{m_C}\right)\right\},$$

$$l_n^*\left\{\omega^2 - f_H\left(\frac{1}{m_H}+\frac{1}{m_C}\right)\right\} = \frac{f_H\cos\theta}{m_C} l_{n-1} + \left\{\frac{2f_H^2\cos^2\theta}{m_C^2}(l_{n-1}+l_n^*)\right\}\Big/\left\{\omega^2 - f_H\left(\frac{1}{m_H}+\frac{1+\cos\theta}{m_C}\right)\right\}.$$

The equations can then be solved if we put $l_t = A\sin(i\alpha+\beta)$, where β is determined by

$$\tan\beta = \frac{f_H\cos\theta}{m_C}\sin\alpha\Big/\left\{\omega^2 - f_H\left(\frac{1}{m_H}+\frac{1+2\cos\theta+\cos\theta\cos\alpha}{m_C}\right)\right\},$$

and α is determined by the transcendental equation

$$\left\{\omega^2 - f_H\left(\frac{1}{m_H}+\frac{1+2\cos\theta}{m_C}\right)\right\}^2 \sin(n\alpha) - \frac{2f_H\cos\theta}{m_C}\left\{\omega^2 - f_H\left(\frac{1}{m_H}+\frac{1+2\cos\theta}{m_C}\right)\right\} \times \sin(n-1)\alpha + \frac{\cos^2\theta f_H^2}{m_C^2}\sin(n-2)\alpha = 0.$$

The frequencies ω are obtained from (7):

$$\omega^4 - \omega^2\left\{\frac{2f_C}{m_C}(1+\cos\theta\cos\alpha) + f_H\left(\frac{1}{m_H}+\frac{1+\cos\theta}{m_C}\right)\right\} + \frac{2f_C}{m_C}(1+\cos\theta\cos\alpha)f_H\left(\frac{1}{m_H}+\frac{1+\cos\theta}{m_C}\right) - \frac{4\cos^2\theta f_H f_C}{m_C^2}(1+\cos\alpha) = 0.$$

Since these vibrations are symmetric with respect to the x and y axes

$$l_i' = l_i'' = \left\{\frac{f_C\cos\theta}{m_C}(l_i+l_{i-1})\right\}\Big/\left\{\omega^2 - f_H\left(\frac{1}{m_H}+\frac{1+\cos\theta}{m_C}\right)\right\}$$

The dipole moments associated with the valence vibrations can be calculated as in § 3 and are found to have the following values:

$$M_x = -\frac{e'}{\omega^2}\left(\frac{1}{m_H}+\frac{2}{m_C}\right)\sin\tfrac{1}{2}\theta f_C(l_0^* - l_n^*),$$

$$M_y = \frac{e'}{\omega^2}\left(\frac{1}{m_H}+\frac{2}{m_C}\right)\cos\tfrac{1}{2}\theta f\{l_0^* + (-1)^n l_n^*\},$$

$$M_z = 0.$$

It is seen that the additional two C–H linkages at the ends of the chain are responsible for a weak activity of the valence vibrations. Replacing $l_0^* = A\sin\beta$ and $l_n^* = A\sin(n\alpha+\beta)$, the dipole moments become:

$$M_x = -\frac{e'A}{\omega^2}\left(\frac{1}{m_H}+\frac{2}{m_C}\right)\sin\tfrac{1}{2}\theta f_C\{\sin\beta - \sin(n\alpha+\beta)\},$$

$$M_y = \frac{e'A}{\omega^2}\left(\frac{1}{m_H}+\frac{2}{m_C}\right)\cos\tfrac{1}{2}\theta f_C\{\sin\beta + (-1)^n\sin(n\alpha+\beta)\},$$

where $\sin(n\alpha+\beta)=\pm\sin\beta$, so that the dipole moments become alternately zero and proportional to $2\omega^{-2}\sin\beta$.

In the case of a very long chain, the intensities of the oscillations of the chain are proportional to the square of the product of the dipole moment into the frequency density where the frequency density is proportional to $d\alpha/d\omega$. This product can be calculated from the formulae given above and becomes for $M_x\neq 0$, $M_y\neq 0$:

$$|M_x(d\alpha/d\omega)| = 2e'A\left(\frac{1}{m_H}+\frac{2}{m_C}\right)f_H\left[f_C\omega\left\{\omega^2-f_H\left(\frac{1}{m_H}+\frac{1+2\cos\theta+\cos\theta\cos\alpha}{m_C}\right)\right\}\right.$$
$$\left.\times\left\{1+\frac{(\cos\theta f_H/m_C)\{(f_C/m_C)(1-\cos\theta)-\frac{1}{2}f_H[(1/m_H)+(1+\cos\theta)/m_C]\}}{\{(f_C/m_C)(1+\cos\theta\cos\alpha)-\frac{1}{2}f_H[(1/m_H)+(1+\cos\theta)/m_C]\}^2}\right\}\right]^{-1} \quad \ldots\ldots(10)$$

with a corresponding expression for the y-component where $\sin\beta$ has been replaced by $\tan\beta$ since β is small, and ω, the C–C valence frequencies, are determined by

$$\omega^2=\frac{2f_C}{m_C}(1+\cos\theta\cos\alpha)+\frac{(2\cos^2\theta f_H f_C/m_C{}^2)(1+\cos\alpha)}{(f_C/m_C)(1+\cos\theta\cos\alpha)-\frac{1}{2}f_H[(1/m_H)+(1+\cos\theta)/m_C]}.$$

Expression (10) is a monotonic function of α for the values of f_C and f_H obtained in § 4, thus the polythene molecule should show a weak continuous absorption between 800 and approximately 1200 cm^{-1}. The distinct absorption peaks at 890 and 1090 cm^{-1}, however, are not accounted for if the valence vibrations alone are considered.

It follows from formula (10) that selective absorption will occur at those frequencies for which $d\alpha/d\omega\to\infty$, that is, at frequencies ω where $\omega(\alpha)$ has a maximum or minimum value. Since the valence forces alone are not sufficient to explain the observed selective absorption at 890 and 1090 cm^{-1}, the determinant (1) has been evaluated under omission of the terms containing f_H and ϕ_H. The neglect of these terms is justifiable because the vibrations involving the stretching of the C–H linkages and the bending of the H–C–H angles are relatively independent of the chain vibrations because the displacements of the oscillating hydrogen atoms exceed those of the carbon atoms by a factor of m_C/m_H. As a result, the terms in f_H and ϕ_H in the diagonal elements of determinant (1) are independent of the phase angle α. The following formula is obtained for ω as a function of α:

$$\omega^6-\omega^4\left\{\frac{2f_C}{m_C}(1+\cos\theta\cos\alpha)+\frac{4\phi_C}{m_C}(1+\cos\alpha)(1-\cos\theta\cos\alpha)\right.$$
$$+\frac{a\phi_{CH}}{2b\cos^2\frac{1}{2}\theta}\left(\frac{1}{m_H}+\frac{2}{m_C}\right)+\frac{\phi_{CH}}{am_C}(1-\cos\alpha)[2a+b(1-\cos\theta\cos\alpha)]\Big\}$$
$$+\omega^2\left\{\frac{8\sin^2\alpha}{m_C{}^2}(1+\cos\alpha)f_C\phi_C+\frac{af_C\phi_{CH}}{b\cos^2\frac{1}{2}\theta\, m_C}\left[\frac{1+\cos\theta\cos\alpha}{m_H}\right.\right.$$
$$\left.+\frac{(1+\cos\theta)(1+\cos\alpha)}{m_C}\right]+\frac{2a\phi_C\phi_{CH}}{b\cos^2\frac{1}{2}\theta\, m_C}(1+\cos\alpha)\left[\frac{1-\cos\theta\cos\alpha}{m_H}\right.$$
$$\left.\left.+\frac{(1-\cos\theta)(1+\cos\alpha)}{m_C}\right]+\frac{2\sin^2\alpha}{am_C{}^2}f_C\phi_C[2a+b(1-\cos\alpha)]\right\}$$
$$-\frac{4a\sin^2\alpha(1+\cos\alpha)}{b\cos^2\frac{1}{2}\theta\, m_H m_C{}^2}f_C\phi_C\phi_{CH}=0.$$

The above equation has been evaluated for two cases (the first approximating to the values of the force constants determined in § 4) and it has been found that the branch of the C–C valence vibrations shows the following maxima of the frequency density function: I. $8\phi_{CH}=f_C$, $6\phi_C=f_C$, $d\alpha/d\omega\to\infty$ for $\alpha_1=90°$ and $\alpha_2=143°$: two maxima. II. $10\phi_{CH}=f_C$, $5\phi_C=f_C$, $d\alpha/d\omega\to\infty$ for $\alpha_1=130°$: one maximum. The above values show that the number of maxima, i.e. the number of absorption peaks in the range of the C–C valence vibrations depends on the ratio of the force constants involved. It may be noted here that the absorption spectrum of halothene, a halogen derivative of polythene (Thompson and Torkington 1945) exhibits just one very strongly marked absorption peak in this range at 930 cm^{-1}.

In conclusion, it may be said that the CH_3-groups at the ends of the polythene molecule have the effect of causing absorption in the region of the C–C valence vibrations; the presence of distinct absorption peaks is due to the interplay of valence and angle forces and the number of peaks depends on the ratio of valence to angle force constants.

It seems therefore that the spectrum of polythene can be satisfactorily explained as the spectrum of a very long chain of CH_2-groups with two CH_3-groups at both ends whose presence does not affect the numbers of possible chain vibrations but leads to the infra-red absorption of the otherwise inactive C–C valence vibrations.

REFERENCES

Bartholomé, E., and Teller, E., 1932, *Z. phys. Chem.* B, **19**, 366.

Bunn, C. W., 1939, *Trans. Faraday Soc.*, **35**, 482.

Elliott, E., Ambrose, E. J., and Temple, C. B., 1948, *J. Chem. Phys.*, **16**, 577; 1949, *Proc. Roy. Soc.* A, **199**, 183.

Fox, J. J., and Martin, A. E., 1940, *Proc. Roy. Soc.* A, **175**, 208.

Kellner, L., 1941, *Proc. Roy. Soc.* A, **177**, 456.

Kirkwood, J. G., 1939, *J. Chem. Phys.*, **7**, 506.

Rasmussen, R. S., 1948, *J. Chem. Phys.*, **16**, 712.

Sheppard, N., and Sutherland, G. B. B. M., 1947, *Nature, Lond.*, **159**, 739.

Simanouti, T., and Mizushima, S. I., 1949, *J. Chem. Phys.*, **17**, 1102.

Sutherland, G. B. B. M., and Vallance Jones, A., 1947, *Nature, Lond.*, **160**, 567.

Thompson, H. W., and Torkington, P., 1945, *Proc. Roy. Soc.* A, **184**, 3.

Whitcomb, S. E., Nielsen, H. H., and Thomas, L. H., 1940, *J. Chem. Phys.*, **8**, 143.

Modes of Disintegration of Ionium : an Investigation using β-sensitive Emulsions

By C. Joan D. Jarvis and M. A. S. Ross

Department of Natural Philosophy, University of Edinburgh

Communicated by N. Feather; *MS. received* 16*th November* 1950, *and in amended form* 23*rd February* 1951

ABSTRACT. Kodak NT 4 emulsion has been impregnated in a neutral solution of ammonium ionium oxalate. Observations of α-particle and internal conversion electron tracks are interpreted in terms of excitation levels of the radium nucleus at about 70 kev. (22% intensity) and at about 200 and 270 kev. (combined intensity about 2%). A disintegration scheme is proposed which allocates the known γ-ray of 68 ± 1 kev. to the transition between the two highest levels. The results are reasonably consistent with recent α-ray magnetic analyses and γ-ray absorption measurements.

§ 1. INTRODUCTION

THE γ-radiation from ionium was first observed by Chadwick and Russell (1913), who interpreted it as K, L and M characteristic radiations. An investigation by Ward (1939) indicated the existence of two nuclear γ-radiations of energies 68 ± 1 kev. and 190 ± 20 kev., the energy of the 68 kev. radiation being well established from the marked difference in absorption by tantalum and tungsten, the K-absorption energies of which are 67·2 and 69·2 kev. respectively. Further studies of the γ-radiation by selective absorption have been made by Riou (1949, 1950) and by Curie (1948, 1949), the latter finding evidence for the emission of γ-radiations of energies about 140 and 240 kev., rather than a single radiation of energy 190 kev. as reported by Ward and Riou. The results of these experiments on the γ-radiation are summarized in Table 1.

Table 1. Energies and Intensities of the γ- and L-Radiations of Ionium

Radiation (kev.)	Number of quanta/100 disintegrations		
	Ward	Riou	Curie
L	—	9 ± 2	11
68	~0·1	$0{\cdot}50 \pm 0{\cdot}15$	0·85
140	—	—	0·33
190	~0·1	$0{\cdot}3 \pm 0{\cdot}1$	—
240	—	—	0·05

Feather (1940), discussing Ward's intensities, pointed out that such a weak intensity for an excited state of 68 kev. was difficult to explain unless one assumed a large difference of spin between this state and the ground state of the product nucleus, or assumed that the 68 kev. radiation was highly converted.

Teillac (1948) was the first in recent years to study the β-radiation of ionium. From the distribution of the projected ranges observed in a Wilson chamber, the emission of electrons could be interpreted as due to the internal conversion of a γ-radiation of 68 kev. energy, the conversion electrons appearing, according to Teillac, in 10 to 11% of the disintegrations. More recently a study of the β-radiation has been made by the photographic plate method by Albouy, Faraggi, Riou and Teillac (1949), using Ilford G5 emulsion, 200 μ thick, impregnated in a 5% acetic acid solution of ionium–thorium nitrate. 2,991 α-tracks were measured, of which 276 (or 331 including more doubtful cases) carried a β-track originating from the same point as the α-track. This proportion is very closely the same as the proportion of conversion electrons observed in Teillac's cloud chamber experiments. Both values are very much lower than would be expected from Riou's (1950) work on the L-radiation, from which he deduced that conversion electrons should be emitted in about 24% of the disintegrations.

The results of precise range and energy determinations for the ionium α-radiation are shown in Table 2, in which are included the most recent data, quoted by Curie (1949), for the α-ray fine structure investigated by Rosenblum, Valadares and Vial (1948). Comparing Tables 1 and 2, the γ-ray of energy about 240 kev. (Curie 1949) might be associated with the α-particle group of lowest energy. The fact that the intensity of the γ-ray is quoted as 0·05 quantum per 100 disintegrations, while the corresponding α-group represents 2% of the disintegrations, would then imply that de-excitation of the 260 kev. state takes place mainly by a cascade process or by the emission of hitherto unobserved conversion electrons. The γ-radiation of energy about 190 kev. observed in

other absorption experiments is consistent with the results on the α-ray fine structure, and might belong in part to this cascade, but the supposed 140 kev. radiation presents difficulties of interpretation.

If the 68 kev. γ-radiation of intensity less than 1% is associated with the 24% α-group exciting the 70 kev. state, this radiation must be almost completely converted; conversion electrons should be emitted in about 23%, and characteristic

Table 2. Energies and Intensities of the α-Radiation of Ionium

Author	Range (cm.)	Energy (Mev.)	Lines of fine structure: Energy difference (kev.)	Lines of fine structure: Intensity (%)
Curie and Tsien (1945)	3·110 ± 0·010	(4·62)	—	—
Clark, Spencer Palmer and Woodward (1944)	(3·16 ± 0·02)	4·657 ± 0·011	—	—
Rosenblum, Valadares and Vial (1948)	—	4·682 ± 0·010	—	—
Rosenblum, Valadares and Vial. (Quoted by Curie 1949)	—	—	0	73
	—	—	70	24
	—	—	180	0·7
	—	—	260	2

L-radiation in 10%, of the ionium α-disintegrations. The observed intensity of the characteristic L-radiation confirms this view, but the direct observations mentioned above have failed to find conversion electrons in more than 10% of the disintegrations. In view of this apparent disagreement, a further study of the α-radiation and the associated conversion electrons has been made with electron-sensitive Kodak NT 4 emulsion impregnated with ionium.

§ 2. EXPERIMENTAL METHOD

The ionium was taken from the source previously used by Chadwick and Russell (1913) and Ward (1939); its early history is given in the literature (Boltwood 1911). The percentage of ionium in the ionium–thorium mixture was found by Ward to be (7·8 ± 0·7)%. In addition to the ionium disintegrations (half-life $8{\cdot}3 \times 10^4$ years), the α- and β-disintegrations of the thorium series are also recorded, but owing to the very long half-life of thorium ($1{\cdot}4 \times 10^{10}$ years) the number of such disintegrations is very small compared with the number of ionium disintegrations. Radium α-particles are also present and have a range nearly equal to the ionium α-particle range, but as the solution had recently been purified from radium, not more than six out of 5,000 α-tracks may be attributed to this source.

When the impregnation technique is used, the emulsion layers should be thick in comparison with the particle ranges involved, and the radioactive element should be uniformly distributed in the emulsion. Uniform penetration is difficult to achieve when impregnations are carried out by soaking in simple salt solutions, for ionium, in common with many other heavy elements, tends to be retained in the surface of the emulsion (Yagoda 1949) by ionic combination with gelatine. To avoid this difficulty Messrs. Kodak, Ltd., suggested using a complex salt of ionium, such as ammonium ionium oxalate. The ionium solution, after dilution with nitric acid, was therefore treated with a 0·5% solution of ammonium oxalate, sufficient solution being added to ensure that the soluble

double salt was formed. The resulting solution was heated to boiling point and allowed to cool. Immediately before impregnation, the pH of the ammonium ionium oxalate solution was brought to exactly 7 by the addition of a few drops of saturated ammonium carbonate solution; this ensured standard conditions of impregnation which preserved the full sensitivity of the emulsion (Picciotto 1949) without producing undue swelling and mechanical strain in the gelatine. Small pieces of NT4 plate were then soaked for 30 minutes in the neutral solution. The plates were dried in a stream of slightly warmed nitrogen and were kept at a constant relative humidity of 44% for exposure times of between 47 and 52 hours.

Processing of the plates was carried out by the temperature development method (Dilworth, Occhialini and Payne 1948) using the elon developing solution recommended by Messrs. Kodak, Ltd. Active development was carried out for 35 to 45 minutes at 21°C., the warming-up period being 10 minutes. After processing, the plates were allowed to dry slowly in a horizontal position.

The developed plates were examined by means of a Watson microscope, using a $\frac{1}{12}$inch oil-immersion objective. Projected lengths could be read with an accuracy of about $\frac{1}{10}\mu$ and depth measurements, made by means of the fine focus adjustment, could be read to $\frac{1}{13}\mu$. The depth setting accuracy was about $\frac{1}{4}\mu$. The practical reading increment in measuring α-particle projected ranges may conveniently be taken as the distance between centres of adjacent developed grains (0·3 to 0·4 μ), so that the probable error in length measurements is of the order of 0·2 μ. This is appreciably smaller than the variations due to straggling. The much larger errors involved in measuring the ranges of the strongly scattered electrons are similarly smaller than the natural variations due to straggling. From this it follows that the distribution curves of α-particle and electron ranges are not seriously affected by random errors of observation. The absolute error of calibration may be taken as 1%.

The depth correction factor was determined experimentally by Vigneron's (1949) method, using ThC′ α-particles. If R is the length in microns of any track, x its horizontal projection in microns, and z its vertical projection in arbitrary units (in practice the units of the scale on the fine adjustment control of the microscope), then

$$R^2 = x^2 + S'^2 z^2, \qquad \ldots\ldots(1)$$

where S' is the depth correction factor. Also $S' = Skh$, where S is the ratio of unprocessed emulsion thickness to processed emulsion thickness, k converts depth scale units to microns, and h is the 'apparent depth' correction required if the refractive index of the emulsion differs from that of the immersion oil; h is known to be close to unity, but was not measured.

Measurements of x and z were made on 300 ThC′ α-tracks. The best values of R^2 and S'^2 were computed by the method of least squares and gave $R = 48{\cdot}4 \pm 0{\cdot}2\,\mu$, $S' = Skh = 1{\cdot}73 \pm 0{\cdot}01$ (see Figure 1). Inserting the constant of the microscope depth scale, $k = 10/13$, it follows that $Sh = 2{\cdot}25 \pm 0{\cdot}01$. This result may be compared with Vigneron's (1949) value for C2 emulsion, $S = 2{\cdot}16 \pm 0{\cdot}07$.

In the ionium plates, the x and z values were measured for all observed α-particle tracks having angles of dip less than 40° in the unprocessed emulsion, and originating more than 10 μ from the top or bottom of the emulsion. Ranges were computed in accordance with equation (1) above, using the value of S' previously determined. When the α-particle track had common origin with an

electron track, the range of the latter was also measured by working over the track in short successive portions which could be treated as approximately straight. The x and z values were measured for each such portion and the range calculated as the sum of the lengths of all portions.

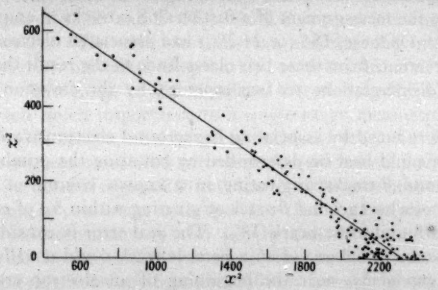

Figure 1. Graph of x^2 against z^2 for determination of shrinkage factor.

Table 3

Angle of dip in unprocessed emulsion (degrees)	0–10	11–20	21–30	31–40
Number of tracks	243	239	197	72
Mean range with standard error (microns)	$18{\cdot}67\pm0{\cdot}04$	$18{\cdot}67\pm0{\cdot}05$	$18{\cdot}86\pm0{\cdot}05$	$19{\cdot}09\pm0{\cdot}11$

The mean ranges of ionium α-tracks lying within definite limits of dip angle were then determined. The results are shown in Table 3. The mean range for angles up to 20° is constant, but beyond this angle, in agreement with the experiments of Rotblat and Tai (1949), an increase in calculated mean range is apparent. If it were desirable to include all tracks in the range measurements, it would, therefore, be necessary to apply an angle of dip correction to the shrinkage factor. In the present work, however, statistics of α-particle ranges have been calculated mainly from tracks with angles of dip less than 30°, and no appreciable error has been introduced by omitting angle of dip correction.

§3. OBSERVATIONS ON INTERNAL CONVERSION ELECTRONS

The first observations were made on plates which had been impregnated in a 2% acetic acid solution. These plates showed some desensitization and it was often doubtful whether an electron track appearing near an α-track should be interpreted as a conversion electron or as a background track. In a total of 1,843 observed disintegrations, 211 (or 11%) conversion electrons were identified. Because of the observational difficulties, it was considered that the proportion of conversion electrons might be too low and that an improved technique of impregnation was necessary. This first result was, however, in agreement with previous cloud chamber and nuclear emulsion work.

Further measurements were made with Kodak NT 4 emulsion, 100μ thick, impregnated in neutral solution as described in §2. These plates showed more uniform penetration by the ionium, and greatly improved electron sensitivity. The average number of grains for the main group of conversion electron tracks

was increased from 15 to 23. The mean distance between the origin of the α-track and the first developed grain of an associated β-track was only $1{\cdot}3\,\mu$ and no difficulty was experienced in the identification of cases of such association.

In one plate 876 α-tracks were measured, of which 208 (or 23·7%) were undoubtedly associated with conversion electrons. Confirmation of this value was obtained by the measurement of a further 768 α-tracks in another plate from the same batch. Of these, 186 (or 24·2%) had associated electron tracks. The combined observations from these two plates leads to the result that at least 24% of the ionium disintegrations are accompanied by the emission of conversion electrons.

The error introduced by associating background electron tracks with ionium α-particle tracks could best be determined by counting the numbers of α-tracks and of background β-tracks originating in a known volume of the emulsion. The probability of a background β-track originating within $5\,\mu$ of either end of an α-track was thus found to be nearly 1%. The real error is considered to be less than this because the initial end of an α-particle track could usually be identified, and because a gap of $5\,\mu$ near the beginning of an electron track was rarely encountered in the later work. The error due to this cause is certainly not greater than 1 per 100 ionium α-tracks.

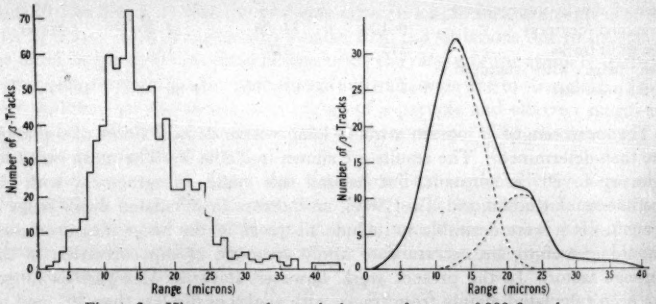

Figure 2. Histogram and smoothed curve of ranges of 803 β-tracks.

Figure 2 shows the histogram of the ranges of 803 β-tracks measured in NT 4 emulsion, the frequencies being plotted for intervals of a micron in range. The smoothed curve is drawn from graduated values obtained by applying the 21-term summation formula of Spencer to the frequencies of the ranges arranged in groups to the nearest $0{\cdot}5\,\mu$. The smoothed curve shows clearly the presence of two prominent groups, the peak ranges, $13{\cdot}2\,\mu$ and $22{\cdot}0\,\mu$, corresponding to energies of 47·5 kev. and 63·5 kev. on the range–energy curve given by Zajac (1949) which is reproduced in Figure 3. The two groups may thus be interpreted as representing the L- and (M + N)-conversion electrons of a γ-radiation of 67 ± 1 kev. energy. An estimate of the areas under the two portions of the curve indicates that the ratio of the intensities of the M- and L-conversion electrons is about 1 to 3. It may be noted that Teillac (1948) gave the value 0·14 for this ratio.

The presence of a small group of conversion electron tracks with a mean range about $35\,\mu$ (energy about 83 kev.) is also indicated from the curve. This

group could be interpreted as electrons arising from the K-conversion of the 190 kev. γ-radiation which, according to Riou (though not according to Curie), is emitted in 0·3% of the disintegrations.

In a small number of the disintegrations, two electron tracks were observed to come undoubtedly from the origin of an α-track. In one such case the electron tracks had ranges of 41·53 and 14·57 μ which correspond to energies of 92 and 50 kev. respectively. The two electrons can therefore be interpreted as the K- and L-conversion electrons, respectively, of γ-radiations of energies about 196 and 69 kev. The range of the associated α-track was 17·53 μ and, although one cannot attach much importance to a single range measurement on account of the straggling of ranges, this range is decidedly less than the mean range, 18·38 μ, of the α-tracks associated with β-tracks (see below) and is in the region expected for α-particles of energy 260 kev. less than the normal energy. The whole observation, then, is consistent with the view that the two electron tracks arise from the internal conversion of two γ-radiations of energies about 190 and 70 kev. which can be emitted in cascade as the result of an α-transition to an excited state differing in energy by about 260 kev. from the ground state.

This particular two-electron event was the only example of its kind observed in over 4,000 α-disintegrations. In 12 other cases, in which there was no doubt as

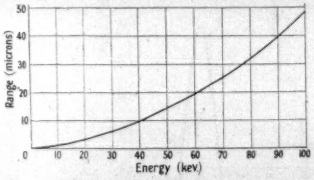

Figure 3. Range–energy curve for β-particles.

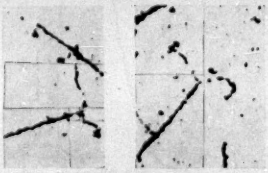

Figure 4.

to the common origin of the three tracks, the two conversion electrons could both be accounted for in terms of the L- or the M-conversion of a γ-radiation of about 70 kev. Photographs of two of these events are shown in Figure 4. The mean range of all these tracks was 14·15 μ and this is the same as the mean range, 14·17 μ, deduced for the main group of 48 kev. L-conversion electrons. The possibility that one of these tracks arises through a K-shell conversion was ruled out on the ground that there was not sufficient evidence from our experiments for a transition of about 150 kev. energy (see below). One must conclude, therefore, that it is possible in the same nucleus to have two transitions each corresponding to an energy difference of about 70 kev. The published α-particle spectrum suggests, as the simplest explanation, that these events may be produced by the de-excitation of the 260 kev. level in triple cascade with successive transitions to the 190 kev., 70 kev. and ground levels. Assuming such a process possible, we conclude that two electrons, each corresponding to the conversion of a 68 or 70 kev. radiation, are emitted, along with a γ-radiation of energy about 120 kev., in roughly 0·3% of all disintegrations.

No evidence was found for the emission of three conversion electrons from one atom, but in 30 cases (0·7% of the disintegrations) a β-track of mean range 14·7 μ was associated with a second β-track, the mean range of which was 4·3 μ (energy 26 kev.). The common origin of the tracks in some of these cases admitted

of some doubt and the identification of the shorter tracks was sometimes difficult, but the occurrence is sufficiently frequent to demand interpretation. There is no Auger transition which could give an electron of 4·3 μ range, nor any evidence from other experiments to support an interpretation of the short track in terms of a conversion in levels above the K-shell. This track can be explained most simply as a K-conversion of a radiation of about 130 kev. energy. The longer of the two tracks corresponds as before to an L- or M-conversion of a 70 kev. radiation. These events may then be ascribed to a portion of the cascade suggested above, but they indicate that the energy difference between the two intermediate levels is nearer to 130 than to 120 kev.

It may be noted that the maximum number of double electron events which can be explained as due to the superposition of a background electron on a single conversion event is not greater than 4 ± 2, and the probability is that these occur mainly in this last group because the background electrons are predominantly short.

§4. OBSERVATIONS ON α-PARTICLES

Figure 5 shows the histogram of the frequency distribution of the ranges of 4,687 α-particles and the smoothed curve obtained by Spencer's method. Only one group of ranges is evident, the two main groups of α-particles with energies of 4·68 and 4·61 MEV., and an expected range difference of about 0·4 μ, not being

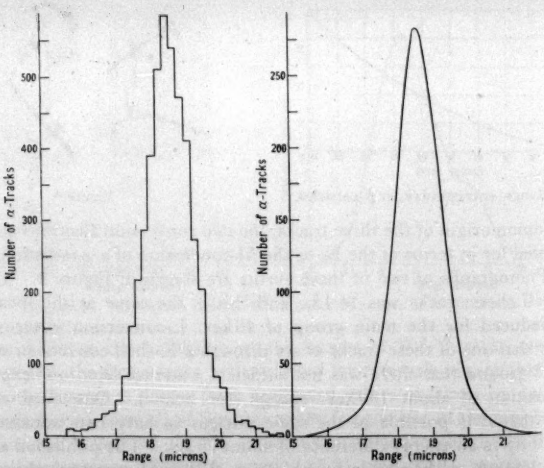

Figure 5. Histogram and smoothed curve of ranges of all α-tracks.

resolved. The mean range of all α-tracks was found to be $18{\cdot}63 \pm 0{\cdot}01\,\mu$ (the error given being the standard error). It is known, however, that all the α-tracks which are associated with conversion electrons must belong to the lower energy group (or possibly to a third group of still lower energy and of very much smaller intensity). The mean range of the 824 α-tracks showing conversion electrons was found to be $18{\cdot}38 \pm 0{\cdot}03\,\mu$. The difference between these two mean ranges cannot be accounted for by random sampling (the Student 't' test of significance gives $t = 8{\cdot}25$!), and $18{\cdot}38 \pm 0{\cdot}03\,\mu$ may therefore be taken as the mean range of the α-particles of 4·61 MEV. energy.

The mean range of the α-particles emitted in the direct transition to ground level was determined from the later measurements in which the expected proportion of conversion electrons was observed. The mean range of 1,232 α-tracks without conversion electrons was found to be $18{\cdot}77 \pm 0{\cdot}02\,\mu$. This is significantly greater than the mean range of all α-tracks and may therefore be taken as the mean range of the 4·68 MEV. α-particles.

The mean ranges given above are about 1% lower than the corresponding ranges deduced from Rotblat's (1950) range–energy curve for α-particles in Ilford C2 emulsion. Rotblat's exposure conditions are not quite comparable with ours, however, as his measurements were made with plates which had been kept *in vacuo* for about two hours before exposure. From Rotblat's curve, the difference between the mean ranges of the two groups of α-particles was found to correspond

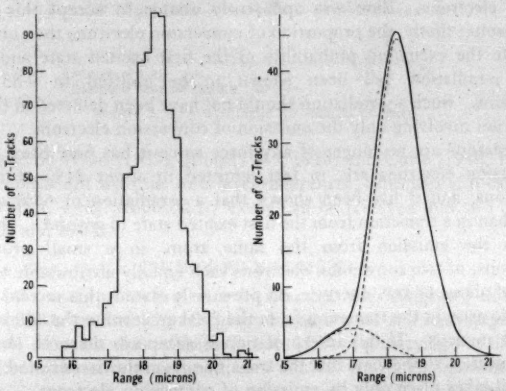

Figure 6. Histogram and smoothed curve of ranges of α-tracks associated with β-tracks.

to an energy difference of 70 ± 4 kev. which is in good agreement with the α-spectrum value and the value deduced above from the energies of the conversion electrons.

Evidence of the existence of α-particle groups of still lower energy has also been obtained. A smoothed curve of the range distribution of the most accurately measured α-tracks, namely those with vertical projection not greater than $2\,\mu$, showed the presence of an imperfectly resolved group of lower range α-particles. This group shows up about four times as strongly in Figure 6 which gives the range distribution of the 24% group of α-particles associated with conversion electrons. The graph shows an attempted resolution of the lowest energy group, which gives the intensity as 8% of the 24% group or 2% of all disintegrations.

§ 5. DISCUSSION

The possible interpretations of the results hitherto obtained for the ionium disintegration have been fully discussed by Riou (1950) who pointed out that, as the intensities of the two main groups of α-ray fine structure indicate that there should be no difference in spin between the ground level of $^{230}_{90}$Io and the first excited state of $^{226}_{88}$Ra, the de-excitation of this level almost certainly involves a transition of the type $0 \rightarrow 0$ and such a transition is strictly forbidden for all types of electromagnetic radiation.

In the case of a 0→0 transition in which the two states have the same parity, atomic electrons can be ejected in a direct transition, the transition probability depending upon the penetration of the atomic electrons in the nucleus. This type of transition mechanism is barred if the two states have different parity and the transition can then occur only as the simultaneous emission of two quanta or of two electrons, or possibly of one quantum and one electron. This latter type of transition was considered by Riou to be the most likely mechanism in the case of the ionium 70 kev. transition. However, from the α-ray selection rule, which states that the parity of the system as a whole must not alter as the result of an α-disintegration, it can at once be deduced that if two levels of the daughter nucleus have zero spin they must also have the same parity. In this case, the most probable type of transition between these levels is undoubtedly the emission of conversion electrons. Riou was apparently unable to accept this conclusion for two reasons: firstly, the proportion of conversion electrons then observed was not equal to the excitation probability of the first excited state and, secondly, a 68 kev. γ-radiation had been shown to be emitted in 0·85% of the disintegrations. Such a γ-radiation should not have been detected in the case of a 0→0 transition involving only the emission of conversion electrons.

These reasons are no longer of any force since it has now been established that conversion electrons are, in fact, emitted in about 24% of the ionium disintegrations, and it has been shown that a γ-radiation of 68 kev. can arise otherwise than in a transition from the first excited state to ground. The evidence for this is the emission from the same atom, in a small proportion of disintegrations, of two conversion electrons each equally attributable to a nuclear transition of about 68 kev. energy. As previously stated, this second possibility is believed to arise in the transition from the 260 kev. level to the 190 kev. level of the product nucleus. If this interpretation is accepted, there no longer seems to be any objection to the view that the transition from the first excited level to the ground level takes place only by emission of conversion electrons.

With this assignment, and taking the intensity of the unconverted 68 kev. γ-radiation as 0·85% and the number of conversion electrons as 0·3% (the number of observed cases of emission of two electrons corresponding to a 68 kev. transition), the value of N_e/N_γ for this line would be 0·35, but a somewhat higher value is probable. The relative intensities of the lines of α-ray fine structure favour a spin difference of +1 between the 260 and 190 kev. levels. Consequently, these two levels probably have different parity and the 68 kev. γ-radiation would be expected to be predominantly electric dipole. This conclusion is supported by the value found for the internal conversion coefficient since the curves of Fisk (1934) indicate a value of N_e/N_γ of about 0·5 for electric dipole radiation converted in the L_I shell.

Obviously every detail of the disintegration is not as yet understood, but the following energy level scheme is put forward as the most satisfactory that can at present be suggested for the daughter (radium) nucleus. In this scheme the de-excitation of the first excited level always takes place by the emission of conversion electrons. An excitation probability for this level of 0·22 is suggested in preference to 0·24, as 8% of the α-particles showing conversion electrons (i.e. 2% of all α-particles) belong to the two lowest energy groups (Figure 7).

The available values for the difference in energy between the first excited state and the ground level are now 70 kev. from α-particle magnetic analysis

(Rosenblum, Valadares and Vial 1948), 70 ± 4 kev. from the present α-particle emulsion ranges, and 67 ± 1 kev. from the emulsion ranges of conversion electrons. The second excited level appears from our K-conversion electron ranges at about 130 kev. above the first excited level, and the difference between the two highest levels is given by the earlier γ-ray work as 68 ± 1 kev. (Ward 1939). The

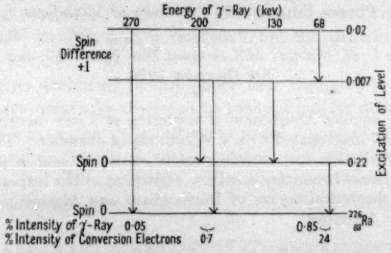

Figure 7. Level scheme for radium nucleus.

γ-ray energies of Ward (1939), Riou (1949, 1950) and Curie (1948, 1949) are all reasonably consistent with the new level differences, especially if it can be shown that the 240 kev. γ-ray proposed by Curie can be resolved into two components at about 200 and 270 kev.

ACKNOWLEDGMENTS

Our thanks are due to Professor N. Feather who suggested that this work should be undertaken and who has given his assistance and encouragement while it proceeded. We also wish to thank Dr. N. Miller for carrying out the extraction of radium from the ionium solution, and Dr. H. O. W. Richardson for helpful discussions.

REFERENCES

Albouy, G., Faraggi, H., Riou, M., and Teillac, J., 1949, *C.R. Acad. Sci., Paris*, **229**, 435.
Boltwood, B. B., 1911, *Proc. Roy. Soc.* A, **85**, 77.
Chadwick, J., and Russell, A. S., 1913, *Proc. Roy. Soc.* A, **88**, 217.
Clark, T. L., Spencer Palmer, H. J., and Woodward, R. N., 1944, *British Atomic Energy Report*, BR 522.
Curie, I., 1948, *C.R. Acad. Sci., Paris*, **227**, 1225; 1949, *J. Phys. Radium*, **10**, 381.
Curie, I., and Tsien, S. T., 1945, *J. Phys. Radium*, **6**, 162.
Dilworth, C. C., Occhialini, G. P. S., and Payne, R. M., 1948, *Nature, Lond.*, **162**, 102.
Feather, N., 1940, *Rep. Prog. Phys.*, **7**, 66 (London : Physical Society).
Fisk, J. B., 1934, *Proc. Roy. Soc.* A, **143**, 674.
Picciotto, E., 1949, *C.R. Acad. Sci., Paris*, **228**, 247.
Riou, M., 1949, *C.R. Acad. Sci., Paris*, **228**, 678; 1950, *J. Phys. Radium*, **11**, 185.
Rosenblum, S., Valadares, M., and Vial, J., 1948, *C.R. Acad. Sci., Paris*, **227**, 1088.
Rotblat, J., 1950, *Nature, Lond.*, **165**, 387.
Rotblat, J., and Tai, C. T., 1949, *Nature, Lond.*, **164**, 835.
Teillac, J., 1948, *C.R. Acad. Sci., Paris*, **227**, 1227.
Vigneron, L., 1949, *J. Phys. Radium*, **10**, 305.
Ward, A. G., 1939, *Proc. Camb. Phil. Soc.*, **35**, 322.
Yagoda, H., 1949, *Radioactive Measurements with Nuclear Emulsions* (London : Chapman and Hall), p. 132.
Zajac, B., 1949, *Thesis*, Edinburgh.
Zajac, B., and Ross, M. A. S., 1949, *Nature, Lond.*, **164**, 311.

The Angular Distribution of 3 MeV. Neutrons scattered by Protons and by Deuterons

By W. F. CAPLEHORN and G. P. RUNDLE *
Physics Department, University of Melbourne

Communicated by L. H. Martin; MS. received 28th June 1950, and in amended form 6th December 1950

ABSTRACT. The angular distribution of scattering of 3 MeV. neutrons by protons and by deuterons has been investigated with a Wilson cloud chamber. The results reveal an almost isotropic distribution for neutron–proton scattering and a strongly anisotropic distribution in the case of neutron–deuteron scattering. The experimental results are compared with the theoretical curves of Buckingham and Massey for the scattering of 2·5 MeV. neutrons by deuterons.

§1. INTRODUCTION

SCATTERING experiments provide one of the most useful sources of information concerning the nature of nuclear forces. The results which are sought are the total cross section for collision, and the angular distribution of scattered particles (the differential cross section). In the case of the scattering of neutrons by protons, theory yields a significant difference in the angular distributions calculated for ordinary and exchange forces only when the energy of the incident neutrons is sufficiently great for the contribution of p-wave scattering to be important. This energy is at least 20 MeV. and no decisive information has been obtained from low energy experiments of this type. Measurements of the angular distribution of neutrons scattered by protons have been made by Dee and Gilbert (1937), Kruger, Shoupp and Stallmann (1937), Bonner (1937) and Coon and Barschall (1946). These results, together with the experiments by Powell and Occhialini (1946 a, b), Laughlin and Kruger (1947) and Barschall and Taschek (1949) indicate that the scattering is essentially isotropic if the neutron energy is less than 15 MeV. although the observations are restricted to angles greater than 70° †. At very high energies (greater than 80 MeV.) however, experiments by Brueckner *et al.* (1949) and Hadley *et al.* (1948, 1949) show that the angular distribution becomes anisotropic, and provide strong evidence for the existence of exchange forces between nucleons.

In this respect the deuteron is a more convenient scattering nucleus since the p-wave contributions are important for much lower energies. The theory of the scattering of fast neutrons by the deuteron has proved a formidable task, but it has been developed at length by Buckingham and Massey (1941, 1947) and Verde (1949) in terms of ordinary and exchange forces. Experimental values of the total cross section plotted against the neutron energy between 1 and 14 MeV. agree generally with the theoretical curve derived on the basis of exchange forces (Rosenfeld 1948). The position is less satisfactory in regard to the angular distribution of 3 MeV. $^2H(d,n)^3He$ neutrons scattered by deuterons. Coon and Barschall (1946), using an ionization chamber, found some agreement with

* Now at University College, London.
† Centre-of-mass system is used.

the theoretical exchange force curve, but Darby and Swan (1948 a, b), using a cloud chamber, reported a distribution which appears to favour the theory of ordinary forces. Kruger *et al.* (1938) who also used a cloud chamber, obtained an angular distribution which does not agree with either of the above experiments but shows more resemblance to the exchange force distribution than the ordinary force distribution predicted by Buckingham and Massey (1941). Darby and Swan (1948 a, b) as well as Kruger *et al.* (1938) found some evidence of a second maximum near 60° to 70°, and a tendency for the distribution to approach zero at 0°.

The experiments described in this paper were designed to study the angular distribution of 3 MeV. neutrons scattered by protons and by deuterons with special reference to the form of the distribution at small angles of scattering. A large Wilson cloud chamber was used with a procedure similar in essentials to that developed by Dee and Gilbert (1937). The experiment was designed to ensure that short tracks were not lost.

§ 2. APPARATUS AND EXPERIMENTAL METHOD

Neutrons of 3 MeV. energy were produced from the reaction $^2H(d, n)^3He$ by a 200 kv. accelerator.

This has been described previously by Martin, Hill and Darby (1947), but it was modified by the introduction of a horizontal acceleration tube with the target at earth potential.

The target was a thin layer of heavy paraffin wax on thin copper sheet. Dry compressed air, after passing through a coil of copper tubing surrounded by dry ice, was directed on the outside of the copper sheet and provided adequate cooling to preserve the target for several hours' intermittent operation. The coil and dry ice were contained in a cylindrical vacuum flask with an aperture in the side to admit the target tube. This cooling system was so arranged that, apart from the copper sheet and the thin walls of one side of the vacuum flask, no scattering material was placed between the target and the cloud chamber. To decrease the intensity of scattered neutrons the target was completely surrounded with paraffin wax blocks, except for a small wedge-shaped aperture between the target and the cloud chamber.

Methane, at a maximum pressure of 2·48 atmospheres was used as the source of proton recoils, and heavy methane, at a maximum pressure of 1·77 atmospheres was the source of deuteron recoils.

In order to produce clear recoil tracks, the relative times of occurrence of the following consecutive events were independently controlled by an electronic timing circuit: (i) the expansion of the cloud chamber, (ii) the admission of a pulse of neutrons, and (iii) the discharge of a condenser through Siemen's photoflash tubes, which were used to illuminate the chamber.

Tracks were photographed stereoscopically with three cameras. The axes of two of the cameras were inclined at 45° to the vertical, and the third camera was placed directly above the chamber. Experience showed that the use of two cameras alone, inclined at 45° to the vertical, led to considerable uncertainty in measuring a short track (length 1·5 cm. or less) when the image was foreshortened because the track was directed towards a camera. The use of the third camera, placed directly over the chamber, overcame this disadvantage since, regardless of the direction of a track, there were at least two images of reasonable length

which could be brought into coincidence on the screen. Moreover, the photographs taken with the third camera were the best in each set, both in the sharpness of tracks and in the freedom from background. The use of three cameras therefore not only improved the accuracy of track measurement but also provided a safeguard against missing short tracks.

The cameras were securely mounted on a portable metal frame so that their positions relative to the cloud chamber were unchanged throughout the experiment. The same cameras, fixed in their same relative positions, were used as projectors.

An inherent shortcoming of the cloud chamber method for angular distribution measurements lies in the difficulty of measuring short tracks and in the possibility of missing some of them altogether. We therefore repeated the experiment using a total stopping power for the chamber gas such that all tracks would be about three times as long as in the initial experiment. This was done by using hydrogen and deuterium in place of methane and heavy methane respectively.

§3. METHOD OF TRACK SELECTION

The track measuring apparatus is shown in Figure 1. It will be seen that the angle of scattering of a recoil particle (relative to the incident neutron direction) could be read directly. No track was measured unless its origin lay in the useful area of the cloud chamber. The criterion for defining this area was that no genuine track originating in it could strike the cylindrical wall of the cloud chamber.

For a track which originated in this area, (*a*) the images were brought into coincidence and the track length and angle of scattering were measured, and

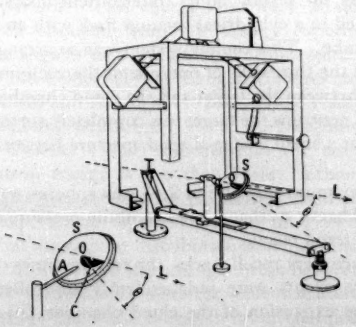

Figure 1. Reprojection apparatus. S movable screen, T position of target, TOL direction of incident neutron, O origin of recoil track, A pointer indicating height of cloud chamber floor, OC recoil track, θ laboratory scattering angle.

(*b*) a polar diagram (giving the calculated range corresponding to the pressure in the cloud chamber after the expansion, for each angle of scattering of the recoil particle) was placed on the screen with its axis along the incident neutron direction, and with its origin at the origin of the track. If any part of the diagram then touched the floor of the chamber when the track was proceeding downwards, or the roof when it was proceeding upwards, the track was rejected. Otherwise it was accepted.

Any other track which was caused by a neutron coming direct from the target, which satisfied the above conditions, which originated from the same point, and which lay in the same half of the polar diagram as the track in question, would also be accepted. There was therefore no discrimination against any angle of scattering, and no azimuthal or length corrections were necessary.

§4. RESULTS

(i) *Neutrons Scattered by Protons*

With the cloud chamber filled with methane (saturated with water vapour) at a pressure of 2·48 atmospheres, a total of 318 expansions were photographed. Altogether 3,131 tracks were measured, excluding those whose origins lay outside the useful area of the cloud chamber described in the previous section. Of the tracks which were measured, only those complying with the selection conditions described above were plotted on the range–angle graphs. Four hundred and seventy-two tracks were rejected in this way; the remaining 2,659 tracks were plotted as points on a series of graphs, with track length as ordinates and laboratory scattering angles of recoil protons as abscissae.

Table 1. Neutrons Scattered by Methane (numbers of recoil protons, measured in equal intervals of cos 2θ in laboratory coordinates)

Interval	cos 2θ	Gross totals	Scattering corrections	Net totals
1	1·0 to 0·8	175	32	143
2	0·8 to 0·6	184	26	158
3	0·6 to 0·4	161	29	132
4	0·4 to 0·2	179	38	141
5	0·2 to 0·0	190	38	152
6	0·0 to −0·2	178	43	135
7	−0·2 to −0·4	202	49	153
8	−0·4 to −0·6	170	27	143

Table 2. Neutrons Scattered by Hydrogen (numbers of recoil protons measured in equal intervals of cos 2θ in laboratory coordinates)

Interval	cos 2θ	Gross totals	Scattering correction	Net totals
7	−0·2 to −0·4	119	30	89
8	−0·4 to −0·6	130	35	95
9	−0·6 to −0·8	119	26	93
10	−0·8 to −1·0	110	28	82

The values of 'atomic stopping powers' quoted by Livingston and Bethe (1937) were used to estimate the theoretical relationship between length of tracks and laboratory recoil angles. Since the neutrons did not all enter the chamber after the expansion, two curves were drawn—one for maximum and one for minimum pressure. These curves were used as the basis for the selection of points which were included in the final results. Allowance was also made for the spread in neutron energy due to the thick target.

Corrections for scattering were made by assuming that the density of points resulting from scattered neutrons in the acceptable zone was the mean of the densities in the regions on either side of, and adjacent to, the zone in which points were accepted.

As was mentioned earlier, the distribution of recoils for small angles was measured by replacing the methane in the expansion chamber with hydrogen at a pressure of 2·81 atmospheres. This pressure was chosen to provide an adequate overlapping with the distribution obtained with methane.

Using the theoretical range–angle curves as before, as a basis for selection of points, the numbers of tracks were counted in equal intervals of $\cos 2\theta$, from

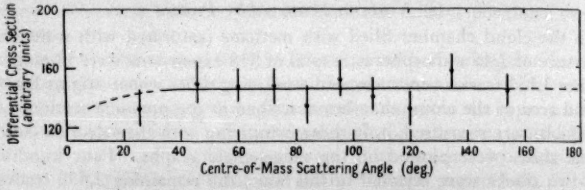

Figure 2. Angular distribution of 3 MeV. neutrons scattered by protons (combined results of high and low stopping power experiments.

$-0{\cdot}2$ to $-1{\cdot}0$. In an attempt to find a value for interval 10, the number of tracks in the interval of $\cos 2\theta$ from $-0{\cdot}8$ to $-0{\cdot}9$ was counted, and doubled.

The results for proton scattering are shown in Tables 1 and 2 and are combined in the graph shown in Figure 2. The uncertainties shown are standard deviations.

(ii) *Neutrons Scattered by Deuterons*

With the same apparatus, a similar set of experiments was performed with the cloud chamber filled with CD_4 to a maximum pressure of 1·77 atmospheres. The gas was saturated with heavy water vapour. Altogether 570 expansions were photographed, from which 3,192 tracks were measured. Of these tracks, 618 failed to satisfy the selection conditions. The remaining 2,574 tracks were plotted on range–angle graphs as before.

To calculate the theoretical range–angle relationship for deuterons in this experiment, we used the known atomic stopping power of carbon and assumed that the stopping power of deuterium was the same as that of hydrogen.

Two inclusion curves were drawn on the range–angle graph, in the same way as was done in the case of scattering by protons. Similar principles were also employed in making scattering corrections in this experiment. In this case, however, it is to be expected that there would be in addition a small number of proton tracks present.

The lengths of proton tracks were estimated as a function of scattering angle for the conditions under which the experiment was performed. The average density of proton tracks was found, as well as the area of the range–angle graph in which a point representing a proton recoil would fall in the acceptable portion of the deuteron graph. By finding the fraction of the acceptable area of the graph which could contain either genuine proton or deuteron tracks, and assuming that the proton distribution is symmetrical, it is possible to estimate the appropriate proton corrections. The results are shown in Table 3.

In the hope of extending the observations beyond interval 7, a low stopping power experiment was performed, in which deuterium at a pressure of

2·12 atmospheres was used as the scattering medium. A further 402 expansions were photographed, from which 743 tracks were measured. These were plotted as points on a range–angle graph as before, after applying the same selection criteria.

Table 3. Neutrons Scattered by Heavy Methane (numbers of recoil deuterons, measured in equal intervals of cos 2θ, in laboratory coordinates)

Interval	cos 2θ	Gross totals	Scattering correction	Proton correction	Net totals
1	1·0 to 0·8	339	39	–	300
2	0·8 to 0·6	192	29	–	163
3	0·6 to 0·4	127	25	–	102
4	0·4 to 0·2	94	17	–	77
5	0·2 to 0·0	97	18	–	79
6	0·0 to −0·2	118	32	–	86
7	−0·2 to −0·4	153	27	2	124
8	−0·4 to −0·6	177	42	4	131

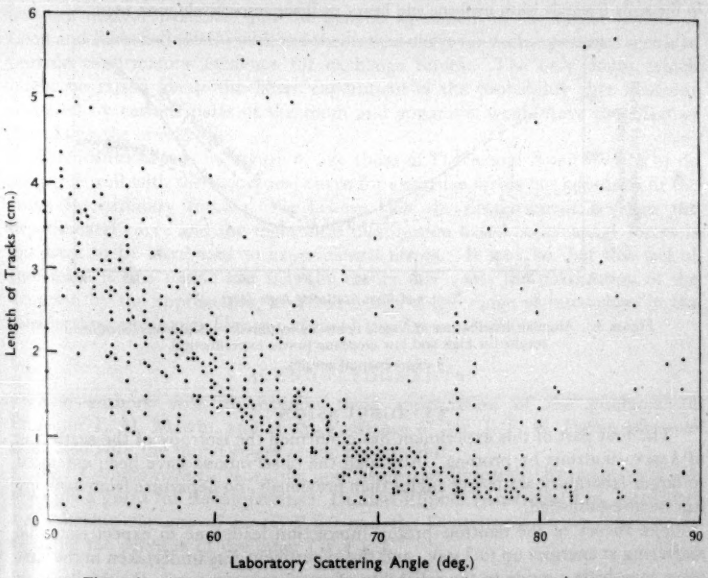

Figure 3. Range–angle plot for low stopping power deuteron experiments.

Table 4 shows the results of this experiment. Figure 3 is included to show a typical range–angle graph. These particular points represent recoil deuterons produced in deuterium gas. The results from Tables 3 and 4 are combined in the graphs shown in Figure 4, in which the corrected values (shown in Table 5) are presented.

Table 4. Neutrons Scattered by Deuterium Gas (numbers of recoil deuterons, measured in equal intervals of cos 2θ, in laboratory coordinates)

Interval	cos 2θ	Gross totals	Scattering coordinates	Proton correction	Net totals
7	−0·2 to −0·4	65	10	1	54
8	−0·4 to −0·6	87	15	3	69
9	−0·6 to −0·8	115	15	5	95
10	−0·8 to −1·0	98	8	6	82

Table 5. The Combined Results of Tables 1 to 4: Neutron–Proton Scattering

Interval	1	2	3	4	5	6	7	8	9	10
Net totals	143	158	132	141	152	135	148	148	150	133

Neutron–Deuteron Scattering

Interval	1	2	3	4	5	6	7	8	9	10
Gross totals	300	163	102	77	79	86	118	136	191	169

Note: The figures for scattering by hydrogen and deuterium were adjusted so that the mean of the numbers in intervals 7 and 8 coincided with the mean of the numbers in the same intervals when methane and heavy methane respectively were used.

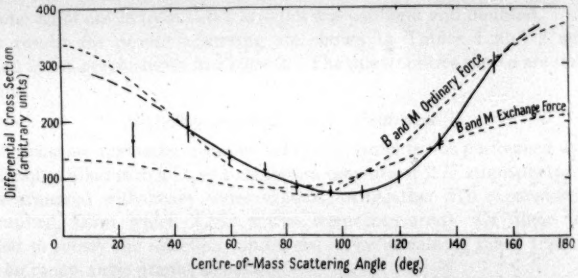

Figure 4. Angular distribution of 3 MeV. neutrons scattered by deuterons (combined results for high and low stopping power experiments).
$\frac{1}{7}$ experimental results.

§ 5. DISCUSSION

The first part of this experiment has confirmed the isotropy of the scattering of 3 MeV. neutrons by protons. Although the observations have been extended to larger laboratory scattering angles than previously, no departure from isotropy has been established.

The theory of the neutron–proton interaction leads one to expect isotropic scattering at energies up to 3 MeV., and the experiment was undertaken in the first place mainly as a guide to the reliability of our measurements. On this basis, a fair degree of confidence in the experiments on the neutron–deuteron scattering is justified, except at the very smallest angles of scattering, i.e. interval 10, where, as will be seen from Figure 4, the same tendency for the curve to drop was observed as in the neutron–proton scattering. It seems reasonable to assume that the differential cross section for deuteron scattering at small angles will be represented by the part of a curve shown dotted in Figure 4. This suggests a maximum at 0° smaller than that at 180°. A comparison of our experimental curves with the

theoretical curves of Buckingham and Massey (1947) is shown in Figure 4, and a comparison of the anisotropy ratios obtained by different workers is made in Table 6. We find no evidence of the maximum at about 60° nor of the steep drop at smaller angles observed by Kruger *et al.* (1938) and by Darby and Swan (1948 a, b).

Table 6

Authors	Method	Angular range covered (deg.)	Anisotropy ratio $d\sigma(180°)/d\sigma(90°)$
Kruger *et al.*	Cloud chamber	22–180	2·9 : 1
Coon and Barschall	Ionization chamber	68–180	2·3 : 1
Darby and Swan	Cloud chamber	36–160	5 : 1
The authors	Cloud chamber	40–160	5 : 1
Buckingham and Massey (theoretical calculations)	Ordinary forces	0–180	5·2 : 1
	Exchange forces	0–180	2·5 : 1

The results of this experiment represent a dilemma in regard to the theory of nuclear forces. The strong backward scattering of very high energy neutrons and protons by protons points unequivocally to the existence of exchange forces between nuclear particles, and the general agreement of the earlier results of Coon and Barschall (1946) with the theoretical curve for exchange forces seems to provide confirmatory evidence for exchange forces. The only doubt which might be raised about the latter experiment is the probability that neutrons scattered by various parts of the room and apparatus would have the effect of decreasing the anisotropy.

Our results shown in Figure 4, like those of Darby and Swan (1948 a, b) do not agree well with the theoretical curve for exchange forces but appear to fit the curve for ordinary forces. We believe that the disagreement between the experimental curve and the theoretical distribution based on exchange forces is too great to be attributed to experimental errors. It may be that this lack of agreement is due to the fact that the theory disregards the polarization of the deuteron by the approaching neutron, uses a single range of interaction in the calculations, and omits higher orders of angular momentum.

ACKNOWLEDGMENTS

The authors wish to express their appreciation of the guidance of Professor L. H. Martin, and of the assistance of Mr. J. F. G. Darby who was associated with the initial stages of the experiment.

The Commonwealth Scientific and Industrial Research Organization made available a grant for the apparatus. Dunlop Rubber (Australia) Ltd., provided a scholarship for one of us (G.P.R.) and the Department of the Army made available the services of the other (W.F.C.).

REFERENCES

Barschall, H. H., and Taschek, R. F., 1949, *Phys. Rev.*, **75**, 1819.

Bonner, T. W., 1937, *Phys. Rev.*, **52**, 685.

Brueckner, K., Hartshough, W., Hayward, E., and Powell, W. M., 1949, *Phys. Rev.*, **75**, 555.

Buckingham, R. A., and Massey, H. S. W., 1941, *Proc. Roy. Soc.* A, **179**, 123 ; 1947, *Phys. Rev.*, **71**, 558.

Coon, J. H., and Barschall, H. H., 1946, *Phys. Rev.*, **70**, 592.

DARBY, J. F., and SWAN, J. B., 1948 a, *Nature, Lond.*, **161**, 22; 1948 b, *Aust. J. Sci. Res.*, **1**, 18.
DEE, P. I., and GILBERT, C. W., 1937, *Proc. Roy. Soc.* A, **163**, 265.
HADLEY, J., KELLEY, E. L., LEITH, C. E., YORK, H. F., WIEGAND, C., and SEGRÈ, E., 1948, *Phys. Rev.*, **73**, 1114; 1949, *Ibid.*, **75**, 351.
KRUGER, P. G., SHOUPP, W. E., and STALLMANN, F. W., 1937, *Phys. Rev.*, **52**, 678.
KRUGER, P. G., SHOUPP, W. E., WATSON, R. E., and STALLMANN, F. W., 1938, *Phys. Rev.*, **53**, 1014.
LAUGHLIN, J. S., and KRUGER, P. G., 1947, *Phys. Rev.*, **71**, 736; 1948, *Ibid.*, **73**, 197.
LIVINGSTON, M. S., and BETHE, H. A., 1937, *Rev. Mod. Phys.*, **9**, 245.
MARTIN, L. H., HILL, R. D., and DARBY, J. F., 1947, *Proc. Roy. Soc. Vic.*, **58**, 135.
POWELL, C. F., and OCCHIALINI, G. P. S., 1946 a, *J. Sci. Instrum.*, **23**, 102; 1946 b, *Report of International Conference on Fundamental Particles* (1946) (London: Physical Society), p. 150.
ROSENFELD, L., 1948, *Nuclear Forces* (Amsterdam: North Holland Publ. Co.), p. 298.
VERDE, M., 1949, *Helv. phys. Acta*, **22**, 339.

Flow of Liquid Helium through Fine Channels

BY G. K. WHITE *
Clarendon Laboratory, Oxford

Communicated by F. E. Simon; *MS. received 9th February* 1951

ABSTRACT. The use of etched copper membranes for studying the flow properties of liquid helium is described. In liquid helium II the velocity of flow is found to be proportional to the nth power of the pressure difference, where the exponent n has the value 0·22 from 1·15° K. to 1·9° K. and increases slightly near the λ-point. Some determinations of the viscosity of liquid helium I give results in general agreement with earlier work, no indication of non-classical or superfluid flow being apparent either immediately above the λ-point or at higher temperatures.

§1. INTRODUCTION

THE unusual transport properties of liquid helium below the λ-point, 2·19° K., have long been a source of interest as indicative of the occurrence of an unusual type of transition at that temperature. In particular the viscocity, which at higher temperatures has an almost constant value, falls markedly between 2·7° K. and 2·19° K. and in the liquid helium II region, i.e. below 2·19° K., it becomes indeterminate by capillary flow methods.

Shortly after it appeared first that the flow of liquid helium II in fine capillaries did not obey the classical laws as regards the dependence of flow velocity on pressure head and capillary radius, Allen and Misener (1939) systematically investigated the flow properties. Using glass capillaries and wire-packed tubes having channels varying in diameter from 438μ to 0·12μ, they found that the flow rate was determined by the relation:

$$\text{Velocity of flow} = \text{constant} \times (\text{pressure head})^n,$$

where the index n approached zero for very fine capillaries ($\sim$0·1μ) at temperatures below about 2° K. However, Johns, Wilhelm and Grayson-Smith (1939), carrying out similar measurements with glass capillaries of approximately 100μ diameter,

* Now at the National Standards Laboratory, Sydney, N.S.W.

reported that the flow could be expressed as a sum of a laminar flow term and a constant term; with a 30μ capillary they found the flow was practically pressure independent.

Thus when some etched copper membrane material was made available to us, it was felt of interest to examine the flow rate of liquid helium II through the 1μ channels in the membrane in order to determine the relation between the flow velocity and pressure head. A knowledge of the flow characteristics of such membranes was also required to decide their suitability for other experiments on the hydrodynamics or superflow properties of liquid helium II. The results of these investigations are described in §3 of this paper.

The flow properties of liquid helium above the λ-point are also of interest as the anomalous decrease in entropy which occurs below 2·6° K. might manifest itself in the transport properties in this region. Bowers and Mendelssohn (1949, 1950 b) investigated the viscosity–temperature relation in liquid helium I using a 40μ glass capillary and found that a marked decrease in viscosity occurred below 2·7° K. In addition they made some observations with finer capillaries, namely wire-packed tubes, which gave generally similar values with no indication of the appearance of non-classical flow. However, the finer channels gave rather scattered values and we have repeated this viscosity determination using a sample of etched copper membrane as a flow channel. This repetition was designed to see whether the flow through a 1μ channel was classical down to the λ-point and whether values of viscosity in agreement with those of Bowers and Mendelssohn would be obtained. In §4 the results of this work are described and discussed.

§2. EXPERIMENTAL METHOD

The results detailed and discussed in the following sections were obtained by suspending the apparatus shown in Figure 1 (*a*) in the experimental space of a

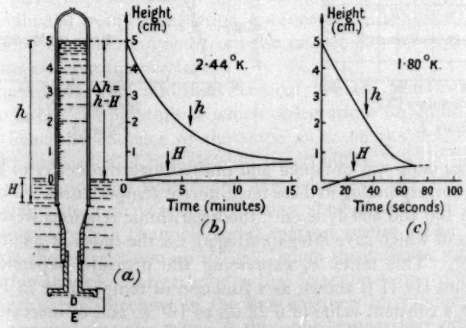

Figure 1.

small Linde helium liquefier, similar to that described by Daunt and Mendelssohn (1948).

The graduated glass vessel had a cross section of about 1 cm², was partially closed at the top to reduce loss by liquid He II film transfer, and was joined by a copper–glass seal and Wood's alloy joint to the brass flange supporting the porous membrane D. The latter was a small circular piece punched from a sheet of

etched copper of thickness about 0·2 mm., and sealed to the flange by soldering round the edge, an effective surface area of about 0·5 cm² being left exposed. In liquid He I bubbles of vapour were prevented from rising and collecting on the undersurface of the membrane by the metal disc E.

The apparatus was supported by cotton fibres from a central sliding rod in the liquefier so that the glass vessel was always partially immersed in liquid helium. Flow could then be initiated by raising or lowering the vessel, the ensuing change in helium levels being recorded as a function of time by observing the graduations on the vessel with an eye-glass.

§ 3. FLOW OF LIQUID HELIUM II

In the observations taken below the λ-point, seventy different curves of level h plotted against time were obtained between 1·16° K. and 2·15° K., a typical graph being shown in Figure 1 (c). The total emptying or filling time was found to vary from 8 minutes near the λ-point to 35 seconds at the lowest temperature.

The slope of each curve was measured at five points corresponding to differences Δh in liquid helium level of 0·5, 1·0, 2·0, 3·0, and 4·0 cm. A table was constructed giving the values of the slope dh/dt for the corresponding pressure heads of 70, 140, 280, 420, and 560 dyne/cm², allowing five curves of dh/dt against temperature to be drawn. From these curves smoothed values of dh/dt for the five pressure heads and for temperatures of 1·2°, 1·3°, 1·4° .... up to 2·1° K. were determined. Thus since the velocity of flow v is proportional to dh/dt, a

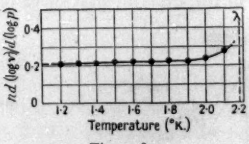

Figure 2.

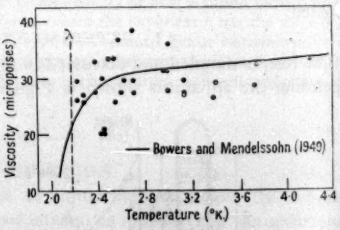

Figure 3.

velocity–pressure table was obtained and plotted logarithmically to give a series of straight lines corresponding to these ten different temperatures. For a pressure head p between 100 and 600 dyne/cm², the logarithmic relations were all straight lines, the slopes of which gave $d(\log v)/d(\log p)$, i.e. the index of p in the equation $v = \text{constant} \times p^n$. This index n, expressing the pressure dependence of the flow rate in liquid He II is shown as a function of temperature in Figure 2; it appears to have a constant value of 0·22 up to 1·9° K. and to increase slightly in approaching the λ-temperature, but nowhere does it reach the classical values ($n = 0{\cdot}5$ for turbulent flow, $n = 1{\cdot}0$ for laminar flow) observed for a normal fluid.

The channels in the membranes used had probably an effective diameter of the order of 1μ, and were very long in comparison with the diameter. The most comparable sized capillaries used by Allen and Misener (1939) were of width 3·9μ and 0·12μ for which values of $n = 0{\cdot}1$ and 0·0 respectively were obtained. These capillaries were however 20 cm. in length and Allen and Misener had observed, notably in the case of a 153μ capillary, that reducing the length increased the value of the index n considerably.

It has been stated that logarithmic plotting of velocity against pressure gave straight lines for pressure heads between 100 and 600 dyne/cm². It should be recorded that at the high temperatures, the slope $d(\log v)/d(\log p)$ was considerably increased at pressure heads below 100 dyne/cm². This shows a close similarity to the observations of Allen and Misener on the flow through 3·9μ capillaries in wire-packed tubes; they found that the flow was represented by $v = kp^n$, where $n = 0{\cdot}1$ for pressure heads greater than 30 dyne/cm², but for smaller pressure heads (at temperatures above 1·7° K.) the index n was increased.

Both from examination of our results and qualitative observation of the helium levels during the experiment it does not seem feasible to represent the flow as a sum of a constant term and a laminar (or turbulent) flow term, i.e. by a relation $v = a + bp^x$, where $x = 1{\cdot}0$ (or 0·5). Johns, Wilhelm and Grayson-Smith (1939) using capillaries about 100μ in diameter and length of the order of 10 cm. reported that the flow could be expressed by an equation of this form; in the case of capillaries of diameter 30μ they reported the flow to be practically pressure independent. However, in their experiments the loss of liquid helium from the inner vessel by film transfer appears to have been comparable in magnitude with the constant term a and may have resulted in a serious error.

§4. VISCOSITY OF LIQUID HELIUM I

Observations of the heights h, H, and time (see Figure 1 (*a*)) were recorded, during both emptying and filling at temperatures from 2·20° K. to 4·20° K. For each set of observations the inner level h was plotted against time, a typical curve being shown in Figure 1 (*b*). Values of the slope of the curve were then determined at from eight to ten points and the slope dh/dt plotted against the height difference $\Delta h = h - H$. In all cases a straight line passing through the origin could be drawn through the points, the average maximum deviation of the points from the straight line being approximately 4%. The values of the viscosity η (Figure 3) were then evaluated from the equation $\eta = \text{constant}(1/\Delta h)(dh/dt)$, the Poiseuille constant having been determined from the rate of flow of oxygen gas through the membrane at room temperature.

The experiments indicate that classical laminar flow persists down to 2·23° K., the lowest temperature at which observations on liquid helium I were made; the linear dependence of the slope dh/dt on the height difference Δh disproves any suggestion of non-classical superfluidity.

Earlier observations by Bowers and Mendelssohn (1949, 1950b) on the flow of liquid helium through wire-packed tubes showed that the viscosity values obtained using very fine channels had a marked scatter. Our determinations of η similarly show variations up to 30%, quite inconsistent with the apparent accuracy within about 4% for each individual determination. This fact probably results from a partial blocking of the fine channels by vapour bubbles. The fact that successive determinations at the same temperature often gave almost identical values of η, whereas slight changes in temperature altered the apparent value of viscosity considerably, supports this suggestion. In the case of liquid helium II, the high thermal conductivity prevents the formation of vapour bubbles and the flow rates are quite reproducible.

Thus although our values are in general agreement with those found by Bowers and Mendelssohn using a glass capillary, as expected it proved impossible to determine the temperature dependence more accurately by using etched membranes.

§ 5. CONCLUSION

The experiments on the flow of liquid helium II support the conclusions of Allen and Misener (1939) that the flow is non-classical and that the dependence of flow rate on pressure head can be expressed by velocity of flow = (pressure head)^n, where the index n is sensibly constant below 2° K.

Our observations indicated the possibility of using the membrane material for other experiments on the properties of superflow in liquid helium II, for example, experiments similar to those of Bowers and Mendelssohn (1950 a) on the pressure distribution along a capillary link between two liquid helium vessels; some such experiments on the hydrodynamics of liquid helium II have already been carried out (Bowers and White 1951).

The flow of liquid helium I through membranes was found to be classical and laminar, the values for viscosity obtained being in general agreement with those of Bowers and Mendelssohn (1950 b). However, as expected from their experiences with wire-packed tubes, such very fine channels (of the order of 1μ in diameter) do not give accurately reproducible flow rates in liquid helium I.

ACKNOWLEDGMENTS

Thanks are due to Professor F. E. Simon and Dr. K. Mendelssohn for their encouragement, and to the Science and Industry Endowment Fund of the Commonwealth of Australia and Carnegie Fund for financial support.

REFERENCES

Allen, J. F., and Misener, A. D., 1939, *Proc. Roy. Soc.* A, **172**, 467.
Bowers, R., and Mendelssohn, K., 1949, *Proc. Phys. Soc.* A, **62**, 394; 1950 a, *Ibid.*, **63**, 178; 1950 b, *Proc. Roy. Soc.* A, **204**, 366.
Bowers, R., and White, G. K., 1951, *Proc. Phys. Soc.* A, **64**, 558.
Daunt, J. G., and Mendelssohn, K., 1948, *J. Sci. Instrum.*, **25**, 318.
Johns, H. E., Wilhelm, J. O., and Grayson-Smith, H., 1939, *Canad. J. Res.*, **17**, 149.

Pressure Gradients in Superflow

By R. Bowers and G. K. White *
Clarendon Laboratory, Oxford

Communicated by F. E. Simon; MS. received 9th February 1951

ABSTRACT. Earlier work on the pressure gradients existing in a narrow channel through which liquid helium II is flowing has been extended by observations on the flow of liquid helium II through porous metallic membranes. Using two membranes of only slightly different flow resistance in series, it has been found that almost all the pressure drop associated with the flow occurs across the membrane of higher resistance, the flow through the membrane of lower resistance taking place under almost zero pressure gradient. The phenomenon is compared with a similar effect in film flow and is interpreted in terms of a critical flow rate in liquid helium II.

§ 1. INTRODUCTION

In two earlier communications (Bowers and Mendelssohn 1950, Bowers, Chandrasekhar and Mendelssohn 1950), brief descriptions were given of a series of experiments on the pressure and temperature gradients which exist in a channel through which liquid helium II is flowing. One of the most

* Now at the National Standards Laboratory, Sydney, N.S.W.

interesting results of this investigation was the fact that when helium II flowed through the narrow channel between two optically polished plates, the fall in pressure along it was not given by the homogeneous gradient expected from classical considerations. It was found that almost all of the pressure drop across the channel occurs at one part of the channel and the flow through the remainder takes place under a very small, if not zero, pressure gradient. The principle of this type of experiment can be seen by reference to Figure 1. Helium is allowed

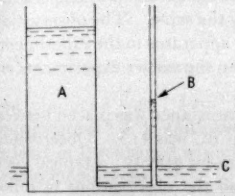

Figure 1.

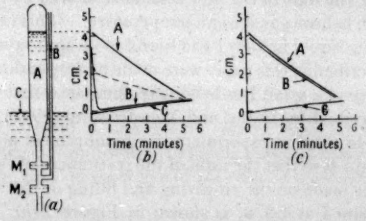

Figure 2 (*a*). Flow apparatus. Figure 2 (*b*) and (*c*). The flow of liquid helium out of reservoir under gravity.

to flow from a reservoir A into the surrounding bath C through the narrow channel connecting them. The pressure at the entry and the exit of the channel may be obtained directly from the levels of the liquid in the reservoir and outer bath respectively. The pressure at some intermediate point in the channel is observed by attaching a small manometer tube B to the channel as shown in the diagram. The existence of the sudden pressure drop in one section of the channel was easily observed with this apparatus since, when helium was allowed to flow through it under gravity, the liquid in the side tube B always maintained approximately the same level as the liquid in the outer bath, showing that the flow in the channel between B and C was taking place under a very small pressure gradient. In the experiments cited above, the ratio of the resistance A to B to that between B and C was found to be of the order of 4 : 1, so that for a 5 cm. pressure head across AC the level in B should have stood about 1 cm. above the level in the outer bath, if the flow had been the normal viscous type. With liquid helium II, however, it was never more than $1\frac{1}{2}$ mm. above the bath level, which is of the same order as the normal capillary rise.

In order to extend and check these experiments, we have repeated the observations described above using a method which allowed us to bring the ratio of the flow resistances closer to unity. In these experiments the deviation of the laws of flow of helium from those to be expected classically are even more marked, and it has been possible to demonstrate positively that the rapid fall in pressure occurs across the narrowest section of the channel. These experiments have been carried out using porous diffusion membranes as flow resistances (White 1951). These membranes are made of etched copper and contain channels that are tortuous, having probably an effective diameter of the order of 1 micron and occupying a small fraction of the total surface area.

§ 2. METHOD

The flow apparatus used in this experiment is shown in Figure 2 (*a*). It consisted of a cylindrical graduated glass vessel with a cross section of about 1 cm^2. It was joined through a copper glass seal to a brass box which supported

two of the membranes M_1 and M_2. The membranes had a surface area of a few square millimetres and were sealed into the brass box by soldering round the edge. Thus helium contained in A must flow through both membranes into the outer bath, and the pressure in the space between the two membranes could be observed, as in all the previous experiments, by the attachment of a small side-arm B. The membranes were both cut from the same material and were carefully chosen so that the ratio of the resistances of M_1 and M_2 for laminar flow was approximately 4 : 3, the ratio of the flow resistance offered by the two membranes being measured with helium gas at room temperature. This ratio was checked at low temperatures using liquid helium I and found to be approximately the same. The observations described in this paper were made by suspending the apparatus in the experimental space of a small Linde liquefier similar to that used in the earlier experiments and described by Daunt and Mendelssohn (1948).

In the first experiment the membrane of higher resistance was placed between A and B so that the ratio of the resistances of AB and BC was 4 : 3. Observations were made on the emptying and filling of the tube under gravity; a typical curve obtained at 1·8° K. is shown in Figure 2(*b*). In all the observations of inflow and outflow the side level B remained within 1 mm. of the bath level throughout, indicating that practically the entire pressure drop occurs across the membrane of higher resistance. In Figure 2(*b*) the dotted line shows the course which the side level would take according to classical considerations.

For the second experiment the membranes were reversed so that the membranes M_2 and M_1 now occupied the position between A and B and B and C respectively. The gravitational flow properties are recorded in Figure 2(*c*). During all observations B remained within 1½ mm. of the level A, showing that the pressure drop again occurred across the higher resistance membrane even though its position had been reversed.

In the Table we have recorded the average positions of the side level B with respect to C in experiment 1 or with respect to A in experiment 2. The capillary

Experiment	T (° K.)	Position of B	
		Emptying	Filling
No. 1	2·01	0·6 mm. above level C	0·3 mm. below level C
No. 1	1·80	0·6 mm. ,, ,, C	0·2 mm. ,, ,, C
No. 1	1·17	0·4 mm. ,, ,, C	0·2 mm. above ,, C
No. 2	2·02	1·1 mm. below ,, A	1·4 mm. ,, ,, A
No. 2	1·75	0·4 mm. ,, ,, A	1·0 mm. ,, ,, A
No. 2	1·27	0·2 mm. above ,, A	0·5 mm. ,, ,, A

rise in B due to surface tension is approximately ½ mm. The inaccuracy in observation amounts to at least ±0·1 mm., but it is nevertheless possible to observe several regularities in the Table which will be discussed in the next section.

It was found possible to represent the flow through the double membrane channel by a power law of the type $v = KP^n$, where v = velocity of flow, P = total pressure difference across the two membranes, and K is a constant. The variation of the index n with temperature is shown in Figure 3. The character of the flow through the double membrane seems to be the same as that observed by White (1951) for the single membrane. The numerical value of n, however, does not seem to be exactly the same in the two cases.

Observations were also made on the fountain effect but, due to the metallic construction of the apparatus, most of the heat supplied by a heating coil in the reservoir tube flowed directly into the bath through the copper base, with the result that very small fountain heads were produced. The maximum fountain

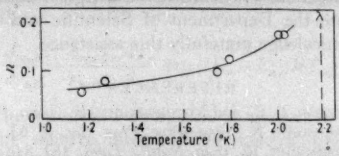

Figure 3. Variation of index n with temperature.

head produced was 1·4 cm. (i.e. the level A was 1·4 cm. above level C) at a temperature of 1·4° K. and a heat input of 27 milliwatts. During these experiments the level in B remained within $\frac{1}{2}$ mm. of C irrespective of the relative positions of the two membranes.

§ 3. DISCUSSION

The experiments described above show that even if the ratio of flow resistances is much closer to unity than in the earlier experiments, B still takes up a position close to the level of the reservoir, to which it is connected by the membrane of lower flow resistance. If the flow were of the normal viscous type, B would have taken up a position (dotted in Figure 2(*b*)) about midway between C and A. The Table illustrates the tendency shown by the side level B in aligning itself with the respective level of A or C. It is noticeable, however, that B does not remain exactly $\frac{1}{2}$ mm. above C in experiment 1 nor exactly $\frac{1}{2}$ mm. above A in experiment 2, at all temperatures, as would be the case for zero pressure drop across one membrane, including the capillary rise. B shows a slight tendency to take up an intermediate position between A and C, the tendency decreasing with the temperature. It seems probable that this very small effect should be associated with a small degree of viscous flow of the normal component of helium II. This is supported by the fact that the effect decreases sharply with temperature; such an influence of the normal component would become very small below about 1·5° K., and any modification of the level B due to it would be masked by the capillary rise of $\frac{1}{2}$ mm.

Apart from this small effect, we are clearly faced with a flow in which the entire pressure drop occurs across the membrane of higher resistance, so that flow through the lower resistance takes place under effectively zero pressure gradient (cf. Mendelssohn 1945). Thus the earlier experiments with a higher ratio of flow resistances are confirmed, and the present experiments emphasize that the effect is analogous to the double beaker experiment of Daunt and Mendelssohn (1946). They were able to show that flow through the film would take place under zero pressure gradient, providing the flow rate was less than the critical value. The evidence of the present work suggests that a similar critical flow rate exists not only in the film but also in the bulk liquid. As a result of this, the membrane of higher resistance probably limits the total flow, there being a critical flow rate for the fine channels through it. The actual flow rate through the channels of the lower resistance would then be less than this critical value, so that no pressure gradient would be produced across it.

ACKNOWLEDGMENTS

The authors wish to thank Professor F. E. Simon and Dr. K. Mendelssohn for their advice and for their interest in this work. During the work G. K. White has received financial support from the Science and Industry Fund of the Commonwealth of Australia and from the Carnegie Fund, and R. Bowers has received support from the Department of Scientific and Industrial Research, and they wish to acknowledge gratefully this assistance.

REFERENCES

BOWERS, R., CHANDRASEKHAR, B. S., and MENDELSSOHN, K., 1950, *Phys. Rev.*, **80**, 856.
BOWERS, R., and MENDELSSOHN, K., 1950, *Proc. Phys. Soc.* A, **63**, 178.
DAUNT, J. G., and MENDELSSOHN, K., 1946, *Nature, Lond.*, **157**, 839; 1948, *J. Sci. Instrum.*, **25**, 318.
MENDELSSOHN, K., 1945, *Proc. Phys. Soc.*, **57**, 371.
WHITE, G. K., 1951, *Proc. Phys. Soc.* A, **64**, 554.

Excitation Temperatures of Hydrogen Arcs

BY H. EDELS AND J. D. CRAGGS
Department of Electrical Engineering, University of Liverpool

MS. received 27th December 1950

ABSTRACT. Measurements of the relative intensities of the first three Balmer series lines (H_α, H_β and H_γ) excited in low current (up to 10 amp.) D.C. arcs in hydrogen are described. The pressure range was from 1–2 atmospheres. The results after correction for self-absorption show that the populations of the appropriate excited states are not those given by a Boltzmann distribution, that is, the data obtained cannot be described in terms of a single excitation temperature. Possible causes of this effect are briefly considered.

§1. INTRODUCTION

THE measurements described in this paper were undertaken as part of a larger programme of work on the D.C. hydrogen arc which is partly intended to show by means of measurements of excitation, electron, and gas temperatures on the same type of arc how nearly the state of thermal equilibrium is approached. The data are also of interest because excitation processes in high pressure discharges have seldom been studied in detail.

It is necessary for the purpose of clarity to define these temperatures. The electron temperature T_e of a discharge is related to the mean electron energy $3\boldsymbol{k}T_e/2$, where $\boldsymbol{k}$ is Boltzmann's constant, the gas temperature is the ordinarily understood kinetic temperature of the unexcited and un-ionized gaseous atoms or molecules in the discharge, and the excitation temperature T_{ex} (defined more fully by Edels (1950) see also Williams, Craggs and Hopwood (1949)) and references there cited) refers to the distribution of excited atoms amongst the various possible levels. Thus the population of excited atoms in state n is

$$N_n = N_0(g_n/g_0)\exp\{-E_n/\boldsymbol{k}T_{ex}\} \qquad \ldots\ldots(1)$$

where N_0 is the concentration of atoms in the ground state, E_n is the excitation energy for state n, g_n and g_0 are the statistical weights of state n and the ground state respectively.

Equation (1) applies only for a Maxwell–Boltzmann distribution and T_{ex} is defined on this basis, as is also T_e above.

If m, n and r denote the various excited states and r can conveniently be the state above which the m and n levels have excitation energies E_m and E_n respectively, the intensities of two spectral lines $J_{n,r}$ and $J_{m,r}$ with frequencies $\nu_{n,r}$ and $\nu_{m,r}$ are related thus:

$$\frac{J_{n,r}}{J_{m,r}} = \frac{\nu_{n,r} g_n A_{n,r}}{\nu_{m,r} g_m A_{m,r}} \exp\{(E_m - E_n)/\boldsymbol{k} T_{ex}\}. \qquad \ldots\ldots(2)$$

$A_{n,r}$ and $A_{m,r}$ are the respective spontaneous transition probabilities. Thus, measurements of the relative intensities of spectral lines together with the necessary knowledge of the g and A coefficients enable T_{ex} to be determined. This paper deals with such measurements for the simple case of the atomic hydrogen Balmer lines H_α, H_β and H_γ. In what follows $T_{\alpha\beta}$ and $T_{\beta\gamma}$ will designate excitation temperatures derived from equation (2) for the lines H_α and H_β and H_β and H_γ respectively. $T_{\alpha\beta}$ should equal $T_{\beta\gamma}$ if the excited state populations for $n=3$, 4 and 5 (H atom) obey a Boltzmann distribution.

Despite the technical importance of the hydrogen arc (in which dissociation of the hydrogen molecules is virtually complete) and its suitability for fundamental study (since collision processes occurring in atomic hydrogen are better known and in general easier to investigate theoretically than in heavier atoms), there appear to be only two published investigations on excitation temperatures of atmospheric pressure hydrogen arcs, namely by Ornstein, Eymers and Wouda (1931) and by Vijverberg (1937). The former carried out preliminary measurements of excitation temperatures from the observations of line intensities of H_α, H_β and H_γ and concluded that the excited state populations followed a Maxwell distribution and gave excitation temperatures of 5,000° K. for currents of 4–8 amperes. Vijverberg's work was more extensive but was with A.C. arcs. His results, referred to in §4, indicated that $T_{\alpha\beta}$ differed markedly from $T_{\beta\gamma}$ at pressures appreciably less than one atmosphere for currents up to 10 amp., but that the differences between $T_{\alpha\beta}$ and $T_{\beta\gamma}$ decreased with increasing pressure. Similar work on low pressure ($<0{\cdot}1$ mm. Hg) hydrogen discharges is due to Ornstein and Lindeman (1930, 1931) with criticism by Kopfermann and Ladenburg (1930), and work on hydrogen sparks at 1 atmosphere is due to Craggs *et al.* (1948) (see §4) who found that no single excitation temperature apparently existed but that $T_{\alpha\beta} < T_{\beta\gamma}$ in contrast with the results given here for appreciably different discharge conditions. A detailed review of published work on the temperatures of gaseous discharges has been made by one of us (Edels 1950).

The present paper therefore presents the results of measurements of the excitation temperatures $T_{\alpha\beta}$ and $T_{\beta\gamma}$ in hydrogen arcs at about 1 to 2 atmospheres pressure and carrying currents varying from about 3 to 10 amperes. It appears that for these ranges of pressures and currents $T_{\alpha\beta}$ differs appreciably from and is greater than $T_{\beta\gamma}$.

§2. EXPERIMENTAL METHODS

In order to obtain maximum arc stability it was found necessary to use horizontal discharges. The arcs were struck between fixed horizontal tungsten electrodes (0·32 cm. diameter) mounted 0·47 cm. apart in a water-cooled metal chamber, and the initiation was obtained by the application of a high-voltage

impulse to the arc gap. Details of the circuit used in arc initiation are given by Edels (1951 a).

Gas of cylinder grade (containing about 0·5–1% oxygen) was used. A typical arc is shown in Figure 1.

The arc image was focused (as shown in Figure 2(*a*)) on to a vertical slit 0·5 mm. in width and the radiation from this central portion of the arc was allowed to fall on the spectrograph slit. The optical arrangement used for obtaining plate calibrations with a standard lamp was that shown in Figure 2(*b*).

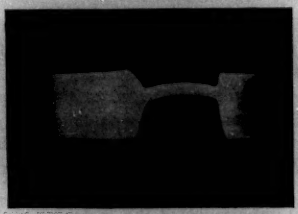

Figure 1. Typical arc in hydrogen between 0·32 cm. diameter tungsten electrodes.

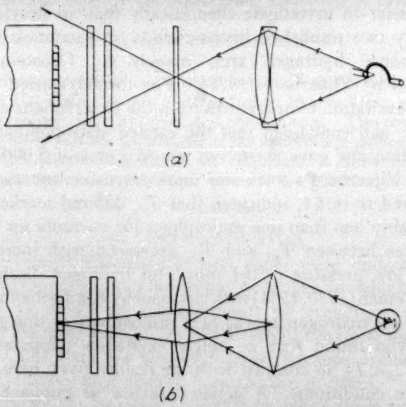

Figure 2. Optical systems used in the experiments.

The spectra were recorded on Ilford H.P.3 plates, using a Hilger step filter mounted on the spectrometer (Hilger constant deviation type) and illuminated uniformly.

Since (see Table) the I_α/I_β ratios were so large, the intensity calibrations were often difficult to make with the step filter alone in such a way that sufficient overlap of the plate calibrations (Figure 3) was obtained. In these cases I_α was reduced by the use of a Wratten filter (No. K78AA) placed in the optical system in an appropriate position (see Figure 2).

The spectral response of the plates was obtained by the use of the standard tungsten filament lamp and filter (as shown in Figure 2), with wavelength

calibrations provided by photographing suitable lines from a small mercury lamp, superimposed on the lamp continua. A typical plate is shown in Figure 4 (*a*) Great care was taken to ensure uniformity of plate development and much

Total Intensity Ratios for the Balmer Hydrogen Lines H_α, H_β and H_γ

Pressure 86 cm. Hg				Pressure 110 cm. Hg				Pressure 153 cm. Hg			
Arc No.	Current (amp.)	I_α/I_β	I_β/I_γ	Arc No.	Current (amp.)	I_α/I_β	I_β/I_γ	Arc No.	Current (amp.)	I_α/I_β	I_β/I_γ
1	5·6	6·20	3·66	6	3·34	10·1	4·59	13	3·54	5·83	3·67
	5·7	6·23	—		3·34	9·95	4·59		3·70	5·85	3·67
	5·7	6·38	3·83		3·36	9·80	4·44		3·86	5·90	3·84
2	5·9	5·55	3·99	7	3·50	9·55	4·58	14	4·04	5·35	3·62
	6·0	5·90	—		3·54	10·3	4·58		4·05	5·30	3·54
	6·2	—	3·88		3·56	9·90	4·58				
3	6·5	5·55	—	8	5·1	6·00	3·78	15	5·0	4·87	3·67
	7·7	5·04	3·61		5·2	6·06	3·65		5·1	4·90	3·65
	7·7	5·02	3·55		5·2	5·86	3·76		5·2	5·05	3·68
4	8·8	4·68	3·54	9	5·4	5·85	3·40	16	5·8	4·54	3·50
	9·4	4·58	—		5·4	5·85	3·54		5·8	4·42	3·45
	10·0	4·24	3·50						6·0	4·59	3·37
5	9·0	4·77	—	10	8·6	4·10	—	17	5·9	4·45	3·38
	9·4	4·58	3·26		8·66	4·35	3·50		6·0	4·53	3·35
	10·4	4·30	3·32						6·0	4·54	3·20
				11	8·68	4·14	3·46	18	8·2	3·68	3·51
									8·4	3·80	3·40
				12	8·80	—	3·26	19	8·6	3·52	3·73
									9·1	3·54	3·60

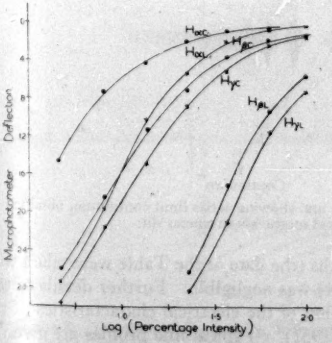

Figure 3. Typical plate calibrations.

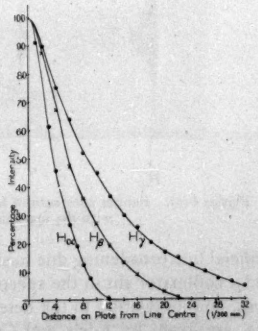

Figure 5. Typical line profiles of a hydrogen arc.

preliminary work was carried out before the experimental conditions were finally accepted.

Typical plate calibrations are given in Figure 3 where $H_{\alpha L}$ and $H_{\alpha C}$ represent the data for the hydrogen line spectrum and the lamp continuum respectively.

The data of Figure 3 were taken with a Hilger microphotometer for the centres of the Stark broadened lines (see Figure 5). The line profiles were also measured at the same time, preliminary experiments having been made to ensure that

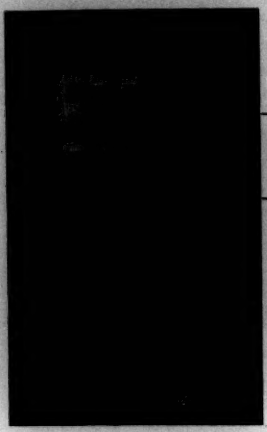

Figure 4 (*a*). Typical plate showing Balmer series, with standard lamp and Hg line calibrations, taken with uniform illumination of the spectrometer slit.

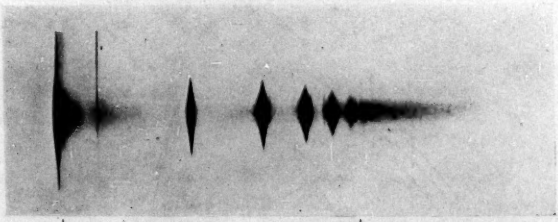

Figure 4 (*b*). Balmer spectrum of hydrogen arc, showing series limit continuum, obtained with the arc image focused on the spectrometer slit.

artificial line broadening due to slit widths (the data of the Table were taken with a 13 μ collimator slit in the spectrometer) was negligible. Further details of this work, and its relation to the determination of the electrical characteristics of the arcs, are given by Edels and Craggs (1951). Typical line profiles are given in Figure 5.

§ 3. EXPERIMENTAL RESULTS

The most important values of line intensity ratios (integrated line intensities are invariably taken of course since the lines are so wide and vary in width through the series) for the Balmer H_α, H_β and H_γ lines are given in the Table. The reproducibility of the results may be deduced from the data given for various plates.

From these data, the excitation temperatures may be readily determined, if self-absorption corrections are negligible, from the curves of Figures 6 and 7 in which the variations of I_α/I_β and I_β/I_γ with temperature for the case of simple thermal excitation are given. A detailed examination of the self-absorption correction (Edels 1951 b *) showed that allowance must be made in the case of H_α at the higher pressures, and the final corrected excitation temperatures are given in Figure 8. It must be emphasized that these results give the mean temperatures

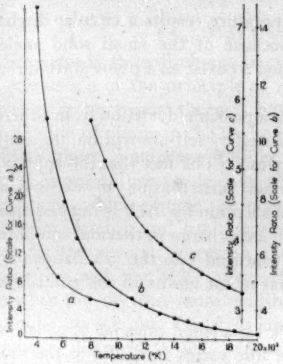

Figure 6. Variation of the ratio I_α/I_β with temperature.

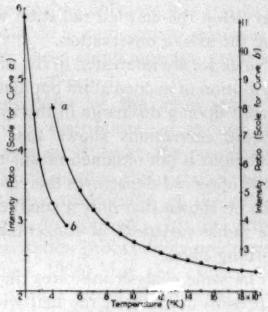

Figure 7. Variation of the ratio I_β/I_γ with temperature.

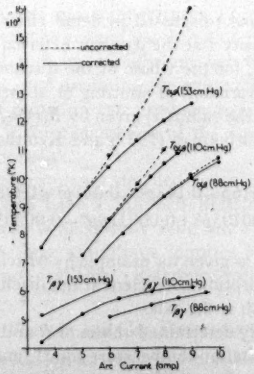

Figure 8. Variation of $T_{\alpha\beta}$ and $T_{\beta\gamma}$ with arc current, with and without correction for self-absorption. The arc pressures are shown on the curves.

(or at least the mean intensity ratios) for the whole observed part of the discharge, since the optical system was arranged to give uniform illumination of the spectrometer collimator slit by the chosen central part of the arc (see § 2).

Self-absorption problems are discussed, for example, briefly by Mitchell and Zemansky (1934) and in more detail by Cowan and Dieke (1948), Bartels

* Paper to be published.

(1948, 1949, 1950) and Edels (1951 b *). A brief summary of the procedure used in correcting for self-absorption is as follows.

It should first be realized that the amount of self-absorption for a given spectral line emitted by a discharge depends on the total concentrations and spectral energy distributions of the excited atoms in the emitting and absorbing states, and upon the spatial variation of these quantities in the discharge. Because a general solution of the problem presents difficulties certain simplifying assumptions have to be made.

For the correction of the excitation temperature results a circular discharge with radial symmetry was assumed and because of the small solid angle of observation the emitted radiation was assumed to exist as a plane wave directed along the axis of observation.

Since we are interested in the first place in a possible deviation from a thermal distribution of excited atom populations produced by self-absorption, the analysis is based upon a discharge in thermal equilibrium. The fact that the application of these corrections shows that a Boltzmann distribution of excited state populations is not obtained means that self-absorption by itself is not responsible for the observed departures therefrom. With a discharge in thermal equilibrium it can be shown that only a small error is introduced into the calculations if the same radial variations of concentration are taken for atoms in the emitting and absorbing states.

The same analysis indicates that for Stark broadened lines (as obtained with the present discharges) the half-width of the line varies (radially) as the square root of the concentration variation. It was shown also that the observed (whole discharge) Stark profile can be replaced with sufficient accuracy by a triangular profile.

With these assumptions (discussed in detail elsewhere, Edels 1951 b *) the ratio of the received intensity I at the detector external to the discharge column, to the emitted intensity I_e for the whole of the discharge section with radius R may be found. A radial variation of emitting or absorbing atom concentrations (N_0 at the axis and N_r at the radius r) given by $F(r)=N_r/N_0=[1-(r/R)^2]$ which is justified by results of Brinkman (1937) and Kruithof (1943) is assumed and this leads to

$$\frac{I}{I_e} = \begin{matrix} 1-0{\cdot}416p+0{\cdot}143p^2-0{\cdot}041p^3+0{\cdot}00954p^4 \\ -0{\cdot}00195p^5+0{\cdot}000316p^6-0{\cdot}0000532p^7+\ldots. \end{matrix} \qquad \ldots\ldots(3)$$

Here $p=RK_0/\Delta\nu_0$ and K_0, as given for example by Mitchell and Zemansky (1934), is the total integrated absorption coefficient at the discharge axis. $\Delta\nu_0$ is the total triangular profile line width at the axis.

With the experimentally determined values of R and $\Delta\nu$ it is possible to obtain the variation I/I_e with excitation temperature for H_α and H_β and so to determine the correct I_α/I_β ratios free from self-absorption from which $T_{\alpha\beta}$ and $T_{\beta\gamma}$ can be determined. At the pressures used in the present experiments, self-absorption is only appreciable for H_α and even then only at the high currents. Figure 8 gives the excitation temperatures corrected for self-absorption in this manner.

The results obtained after correction for self-absorption are mean excitation temperatures. It should be noted that even for a discharge in thermal equilibrium, different mean excitation temperatures will be found for different pairs of levels because the radial variations of intensity would not be the same for all lines.

* Paper to be published.

The radial variations of temperature are however relatively small (Brinkman 1937, Kruithof 1943) and an analysis of this problem using different arbitrary radial temperature variations shows that the anomalous excitation temperatures described here are not the result of mean temperature determinations.

In conclusion therefore it is apparent from the results of Figure 8 that the excited state populations in the hydrogen arcs studied do not follow the simple Boltzmann distribution given in § 1.

§ 4. DISCUSSION OF RESULTS

For a steady state discharge in complete thermal equilibrium it is known that the postulation of the principle of detailed balance is sufficient to maintain the discharge in its steady thermal state. Under these conditions the population (distribution of atoms in the excited states) is also thermal.

With these conditions the relative magnitudes of the atom–atom and electron–atom collisions do not affect the final distribution of excited atom populations, which remain thermal. If however we consider the possibility of a different electron and gas temperature, and still assume that detailed balance holds for the several processes, then the relative magnitudes of the collision frequencies will markedly affect the resultant distribution. In the extreme case when the electron–atom collisions and excitation probabilities predominate it can be shown (cf. Ornstein and Brinkman 1934) that the excited atom population distribution will still be thermal with a temperature equal to that of the electrons, as shown by Ladenburg's results (1933) on a neon discharge. Similarly with atom–atom collisions predominating the distribution will indicate the gas temperature. Therefore in the following a discussion will be given of the difference in electron and gas temperatures $(T_e - T_g)$ and of the relative magnitudes of the various excitation and de-excitation processes.

It will be appreciated that an equilibrium between radiation and matter cannot exist in a discharge, and assuming the existence of an otherwise thermal discharge the emission of radiation can produce a non-thermal distribution of excited atom populations if the radiation is of the same order of magnitude as the other de-excitation processes.

In the above we have postulated detailed balance and assumed implicitly that the electrons and atoms have a Maxwell–Boltzmann energy distribution. Neither of these assumptions is necessarily valid but a calculation of the excited atom populations without these conditions requires a considerable amount of data which are at present not available. Reference will be made to this problem later.

(*a*) *The Value of the Electron and Gas Temperature Difference,* $T_e - T_g$

$T_e - T_g$ may be deduced for an electrical discharge by Townsend's early method (Townsend 1925) for the case when $T_g \ll T_e$, i.e. for low pressure, low current, discharges. Norinder and Karsten (1949) and others however have applied the method to the case of a high pressure discharge where $T_g \sim T_e$. Thus if the electron mean free path for elastic collisions is assumed independent of energy, which is certainly only an approximation as the work of Ramsauer and others has shown, so that a mean free path corresponding to the mean electron energy is taken, and if the only mode of energy loss is through elastic collisions, then $T_e - T_g$ may be simply found for a steady state discharge. This quantity is obtained by equating the gain of electron energy from the field X per

mean time τ between elastic collisions, which is $Xe v\tau$, to the average energy loss at such a collision which is (Cravath 1930)

$$\frac{1}{2}mu^2\frac{8}{3}\frac{mM}{(m+M)^2}\left(\frac{T_e-T_g}{T_e}\right). \qquad \ldots\ldots(4)$$

Here v is the drift velocity of the electrons (mass m, charge e) whose mean kinetic energy of translation is $\frac{1}{2}mu^2$. M is the atomic or molecular mass, in the present case 1,840 m. Now Loeb (1939, pp. 182–188) gives

$$v=0{\cdot}815\,e\lambda X/mu, \qquad \ldots\ldots(5)$$

$$\tau=\lambda/u_1, \qquad \ldots\ldots(6)$$

and

$$\tfrac{1}{2}mu^2=3kT_e/2. \qquad \ldots\ldots(7)$$

In this u and u_1 are respectively the average and r.m.s. velocities of the electron. Further since $u_1=0{\cdot}922u$ for a Maxwellian distribution we shall put $u_1=u$ so that $\tau=\lambda/u$ and the factor 0·815 will be omitted since the treatment is only approximate. Then finally

$$(T_e-T_g)=\frac{X^2e^2\lambda^2}{12k^2T_e}\frac{M}{m}=\frac{v^2M}{4k} \qquad \ldots\ldots(8)$$

which is simpler to use.

The values of v may be obtained, with a knowledge of X, from the data of electron mobility in hydrogen as tabulated by Healey and Reed (1941) from Townsend's results. These data however need alteration in several respects before being used for the hydrogen arcs, because (i) $T_g\sim T_e$ for arcs whilst $T_g\ll T_e$ for the Townsend case, (ii) M is now 1 instead of 2 because dissociation is virtually complete, (iii) the value of the mobility will be different since the total collision cross section will be less in H than in H_2 since excitation of vibrational and rotational states is possible in the latter case (Loeb 1939, p. 191).

An analytical expression for the mobility can be obtained however (Loeb 1939), and is

$$k_e=\frac{271\times10^3(273/T_g)^{1/2}L_{1,0}}{[1+\{1+1{\cdot}106\times10^6ML_{1,0}(X/p)^2\}^{1/2}]^{1/2}}, \qquad \ldots\ldots(9)$$

where $L_{1,0}$ is the electron mean free path at 1 mm. Hg, 273° K. for elastic collisions, since at sufficiently low values of X/p the inelastic collisions may be ignored. X is the electric field in v/cm. and p is the pressure in mm. Hg.

It will be seen from the mobility expression that since the X/p term in the denominator is negligible the M factor may in practice be ignored. The mobility for H will be nearly equal to that for H_2 if the latter is calculated for elastic collisions only (Bradbury and Nielsen 1936 and Loeb 1939, Figure 78), because $L_{1,0}$ differs little for the two cases. This is shown by the calculated data for Ramsauer cross sections in H (kindly supplied by Professor Massey), and the experimental data for H_2.

Thus it is possible, assuming elastic collisions only, to calculate the drift velocity from the mobility expression. The difficulty is clear since we have to know both T_g and T_e before the calculation can be made. T_g can, however, be taken as 5,000° K. without undue error since $T_g^{1/2}$ is involved and the Ramsauer cross section does not vary unduly in the region of energies corresponding to the expected mean electron energies in the discharge. The lack of a precise knowledge of the electron energy distribution is also an objection, but (Druyvesteyn and Penning 1940) at the high arc gas densities and low X/p it is unlikely that the distribution will depart much from Maxwellian. Reference should be made here to work by Jones (1944) which gives a detailed treatment of electron mobilities

in helium, for an appreciation of the difficulties. See also Davydov (1935) who deals with the relevant case of $T_g \sim T_e$ and the comprehensive work of Smit (1937).

If however we take a mean electron energy of 1 ev. ($T_e = 7{,}700°$ K.) the Ramsauer mean free path in atomic hydrogen is $1/84 \times 760$ cm. at 1 atmosphere pressure with variation between 0·5 and 1·5 ev. of 50%, and $X/p = 100/760 = 0{\cdot}13$ v/cm/mm. Hg. The term $(273/T_g)^{1/2}$ corrects for density changes, and calculation gives $v = k_e X = 1{\cdot}7 \times 10^6$ cm/sec. It is further necessary to correct k_e for the effect of positive ion scattering (Gabor 1933, Gvosdover 1937, 1938, Schulz 1947) and this approximately halves the mean free path for the above conditions. Details of the calculation are more appropriately given elsewhere (Edels and Craggs 1951, Craig and Craggs 1951 *). We may therefore put $v \sim 8{\cdot}5 \times 10^5$ cm/sec. and, with the reservations clearly stated above that until $L_{1,0}$ is known accurately, the result can only be taken as an approximation, we find that $T_e - T_g \sim 2{,}200°$ K. However by more complete calculation for a range of values of T_e and T_g (Edels and Craggs 1951, Table 2), we find that this value of v is consistent with $T_e - T_g$ varying from 0–5,000° K. for a fixed value of T_e, since v is found to be relatively insensitive to variations in T_g. Variations in T_e are more important. It should be noted that the experimental value obtained for v is $3{\cdot}6 \times 10^5$ cm/sec. (Edels and Craggs 1951) and this value also is consistent with a large range of values of $T_e - T_g$.

It seems possible therefore that $T_e - T_g$ may be appreciable even in an arc at atmospheric pressure. It is important however to repeat that no accurate evaluation of $T_e - T_g$ may be made in this way and indeed because of the many difficulties connected with the electron energy distribution, electron scattering cross sections, and other matters, the best procedure is if possible to measure T_e and T_g directly for the same discharge. This work is in hand in this laboratory. Further discussion of the electron mobility in hydrogen is given elsewhere (Edels and Craggs 1951).

(*b*) *The Relative Magnitudes of Atom–Atom and Electron–Atom Excitations*

Since we have found that an appreciable difference in the electron and gas temperatures appears possible, it is of interest to determine whether in the hydrogen arc discharge any one of the collision processes predominates. Whereas for a system in a condition of detailed balance the ratio of the probabilities of collision of the first and second kind at a given energy may be obtained, a knowledge of the excitation probability variation with energy is required if a calculation of the number of these collisions is to be made. For the electron–atom collision process it is possible to carry out this calculation from known results but for the atom–atom process no data are known which allow a comparable calculation (see Massey 1949). Thus a rigorous calculation of the relative magnitudes of these processes or of the resulting excited atom populations for different values of T_e and T_g is not possible.

If however the excitation cross sections are assumed to be constant with energy of the existing particle, and taken as the gas kinetic values, then approximate calculations may be made such as those given by Ornstein and Brinkman (1934) and von Engel and Steenbeck (1934). Application of this type of analysis to the hydrogen arc with electron concentrations of 10^{16}/cm^3 (Edels and Craggs 1951) indicates that the atom–atom and electron–atom excitations are of the same order of magnitude, account being taken of the positive ion scattering effect.

* Paper to be published.

With this condition, then, and different values of T_e and T_g we may expect a non-thermal distribution of excited atom populations, and in this case also the form of the electron energy distribution may be of importance.

A comparison of the rate of reduction of the excited states by radiation with the reduction rate given by collisions of the second kind for both electrons and atoms, calculated with the kinetic cross sections, indicates that for H_α this form of radiation disturbance may be of importance. It seems possible also, since this effect is less marked for H_β, H_γ, etc., that the disturbance may be producing the anomalous excitation temperatures since the effect would in practice reduce the population of the $n=3$ state, and thus produce a high value of $T_{\alpha\beta}$. The uncertainties in the cross section values however make a firm conclusion impossible.

(*c*) *Miscellaneous Effects*

A strengthening of the higher members of a spectral series may sometimes be caused by cumulative excitation as shown for example by Fabrikant and Zirg (1937) for certain mercury vapour discharges. The latter authors suggest that the effect may be important in high density plasmas; if it is operative in the present case it would tend to give a relatively high value of $T_{\alpha\beta}$ with respect to $T_{\beta\gamma}$.

It is of interest in this connection to note that the cross sections for excitation by electron impact from the 2p level to the $n=3$ shell, which have been kindly communicated to us by Dr. Burhop, are surprisingly high. Thus for 2 ev. electrons the cross sections for 2p–3s, 2p–3p and 2p–3d (transitions which may be important in high pressure discharges if cumulative excitation is occurring) are respectively about 5, 6 and 27 πa_0^2, whilst for comparison the excitation from 1s to the $n=3$ shell has a cross section of the order of $0{\cdot}1\ \pi a_0^2$. Similar information for transitions from the $n=2$ and $n=3$ to the $n=4$ shell would be of value but if, as has been suggested above, electron excitation is appreciable for the discharges under consideration, then the complementary collisions of the second kind might be such that detailed balancing will not be obtained. The extent to which this effect is of importance cannot be decided until more information on cross sections for collisions of the first and second kind is available. It seems likely also that departures from a Maxwellian distribution for the electron energies, due to the rapidly increasing Ramsauer cross sections at low electron energies in atomic hydrogen, might be appreciable for the present low field discharges ($X/p \sim 0{\cdot}1$ v/cm/mm. Hg). This disturbance of the distribution might affect the relative amounts of quenching of H_α and H_β through collisions of the second kind.

Measurements of electron energy distributions are not easy for high pressure discharges but it is possible that large departures from a Maxwellian distribution may show in the measurements of intensity variations in the recombination continuum (see Figure 4(*b*)) which will be made shortly. Until these results and those of experiments on the determination of gas temperatures are available it does not seem profitable to take the discussion further.

The results obtained by Vijverberg (1937) for A.C. arcs seem to be the only data comparable with those of the present paper, and his results may be briefly summarized as follows. Pressures varied from 9 to 76 cm. Hg with currents varying from 1 to 40 amp. Down to 20 cm. Hg the values for $T_{\alpha\beta}$ and $T_{\beta\gamma}$ are roughly equal but with a very large scatter so that often $|T_{\alpha\beta} - T_{\beta\gamma}| \sim 1{,}000$ or 2,000° K. At $p=76$ cm. Hg, 7 amp., Vijverberg's $T_{\alpha\beta}=8{,}100°$, and $T_{\beta\gamma}=11{,}000°$, whilst at 9 amp. his results are 7,400° and 8,400° K. The results given by our

work for the same conditions are $T_{\alpha\beta}=8{,}500°$ and $T_{\beta\gamma}=5{,}400°$ K. and 10,000° and 5,000° K. respectively. The only conclusion to be drawn from a comparison of the two sets of data is that the excitation temperatures are very roughly the same in both cases, but since Vijverberg worked with A.C. arcs further discussion seems inadvisable. His results are not internally consistent.

§5. CONCLUSIONS

It should be emphasized that the tentative discussion given in §4 requires a great deal of further data before confirmation of any one explanation is possible. The experimental data presented here relating to the relative intensities of H_α, H_β and H_γ, show that no single excitation temperature for the Balmer levels was found in our experiments, and further discussion awaits further measurements of T_g and other quantities. The excitation temperatures vary from 5,000–12,000° K. for the range of variables quoted.

ACKNOWLEDGMENTS

The authors are indebted to Professor J. M. Meek and Professor F. J. Teago, for their encouragement and sustained interest and to Mr. W. Hopwood for much invaluable advice and help in the optical work. One of us (H. E.) is indebted to University of Liverpool for the award of a Fellowship and to the Electrical Research Association for generous financial assistance and for permission to publish this work.

REFERENCES

Bartels, H., 1948, *Z. Phys.*, **125**, 597; 1949, *Ibid.*, **126**, 108; 1950, *Ibid.*, **127**, 243.
Bradbury, N. E., and Nielsen, R. A., 1936, *Phys. Rev.*, **49**, 388.
Brinkman, H., 1937, *Dissertation*, Utrecht.
Cowan, R. D., and Dieke, G. H., 1948, *Rev. Mod. Phys.*, **20**, 418.
Craggs, J. D., Williams, C. G., and Hopwood, W., 1948, *Phil. Mag.*, **39**, 329.
Cravath, A. M., 1930, *Phys. Rev.*, **36**, 248.
Davydov, B., 1935, *Phys. Z. Sowjet*, **8**, 59.
Druyvesteyn, M. J., and Penning, F. M., 1940, *Rev. Mod. Phys.*, **12**, 87.
Edels, H., 1950, *E.R.A. Report*, No. L/T230.
Edels, H., and Craggs, J. D., 1951, *Proc. Phys. Soc.* A, **64**, 574.
von Engel, A., and Steenbeck, M., 1934, *Elecktrische Gasentladungen*, Vol. 1 (Berlin: Springer), para. 31.
Fabrikant, W., and Zirg, J., 1937, *Phys. Z. Sowjet*, **12**, 324.
Gabor, D., 1933, *Z. Phys.*, **84**, 474.
Gvosdover, S. D., 1937, *Phys. Z. Sowjet*, **12**, 164; 1938, *Ibid.*, **13**, 133.
Healey, R. H., and Reed, J. W., 1941, *The Behaviour of Slow Electrons in Gases* (Sydney: Amalgamated Wireless (Australia) Ltd.).
Jones, F. Ll., 1944, *Proc. Phys. Soc.*, **56**, 239.
Kopfermann, H., and Ladenburg, R., 1930, *Z. Phys.*, **65**, 187.
Kruithof, A. M., 1943, *Physica*, **10**, 493.
Ladenburg, R., 1933, *Rev. Mod. Phys.*, **5**, 243.
Loeb, L. B., 1939, *Fundamental Processes of Electrical Discharge in Gases* (New York: Wiley)
Massey, H. S. W., 1949, *Rep. Prog. Phys.*, **12**, 248 (London: Physical Society).
Mitchell, A. C. G., and Zemansky, M. W., 1934, *Resonance Radiation and Excited Atoms* (Cambridge: University Press).
Norinder, H., and Karsten, O., 1949, *Ark. Mat. Astr. Fys.*, **36A**, Part 4.
Ornstein, L. S., and Brinkman, H., 1934, *Physica*, **1**, 797.
Ornstein, L. S., Eymers, J. G., and Wouda, J., 1931, *Proc. K. Akad. wet. Amst.*, **34**, 4.
Ornstein, L. S., and Lindeman, H., 1930, *Z. Phys.*, **63**, 8; 1931, *Ibid.*, **67**, 1.
Schulz, P., 1947, *Ann. Phys., Lpz.*, **1**, 318.
Smit, J. A., 1937, *Physica*, **3**, 543.
Townsend, J. S., 1925, *J. Franklin Inst.*, **200**, 563.
Vijverberg, W. R., 1937, *Dissertation*, Utrecht.
Williams, C. G., Craggs, J. D., and Hopwood, W., 1949, *Proc. Phys. Soc.* B, **62**, 49.

Balmer Line Widths in Hydrogen Arcs

By H. EDELS and J. D. CRAGGS
Department of Electrical Engineering, University of Liverpool

MS. received 22nd December 1950

ABSTRACT. The paper describes measurements of the widths of the Balmer lines H_α, H_β and H_γ in D.C. hydrogen arcs (1–2 atmospheres pressure), for currents up to 10 amp. The results are used to deduce ion concentrations, and their bearing on the physical properties of the discharges is discussed.

§ 1. INTRODUCTION

As part of a study of the physical characteristics of high pressure gaseous discharges, it was considered of interest to investigate, more completely than before, the relatively simple case of the hydrogen arc. Since the emission spectra of atomic hydrogen are simple and have been studied theoretically in an exhaustive manner, partly for their fundamental importance and partly for their bearing on other, e.g. astrophysical, problems, it seemed likely that spectroscopic and other experiments on continuous discharges such as arcs might give interesting results. The data might then be of use in the elucidation of the more difficult case of transient (e.g. spark) discharges in hydrogen (Craig and Craggs 1951 *, and references there cited).

Despite the technical and scientific importance of hydrogen arcs the published work on them appears to be scanty (see Edels and Craggs 1951). Thus, excitation temperatures have been measured by Carst and Ladenburg (1928), Ladenburg (1928), Ornstein and Lindeman (1930, 1931) (see Kopfermann and Ladenburg 1930, Jackson 1934, 1936) for low-pressure hydrogen discharges. Atmospheric pressure arcs have been similarly studied by Ornstein *et al.* (1931) in a short paper, by Vijverberg (1937) for A.C. arcs and by Edels and Craggs (1951, to be referred to as I) in detail for D.C. arcs. The electrical measurements of Suits (1939 a, b) on hydrogen arcs, over a wide pressure range are well known, and will later be referred to in more detail.

Apart from the early approximate measurements of Rossi (1911), de Groot (1931) and Reman (1937) the present experiments appear to be the first made with any accuracy on ion concentrations in hydrogen arcs, although similar work has been carried out on hydrogen sparks, where the ion concentrations are higher by a factor of the order of 10 to 40, by Craggs and Hopwood (1947, and references given there to earlier work), see also Grimley and Saxe (1951 *) and Hopwood, Craig and Craggs (1951 *). Preliminary work on glow discharges, also qualitative, has been carried out by Frisch and Kagan (1943). The importance of accurate measurements of ion concentrations (although the present data do not represent the most accurate data that can be obtained, as we hope to show in the near future) lies in the use of such data in Saha's equation, relating the degree of ionization and the temperature for a state of thermal equilibrium, and in studies of the drift current equation. In the latter, considered further in § 5, values of electron concentration may be used to determine electron mobilities, a matter

* Papers to be published.

of considerable interest in high density discharges (Druyvesteyn and Penning 1940).

The theory of Stark line broadening in inhomogeneous fields, such as the ion–ion and electron–ion fields encountered in gaseous discharges, was first studied by Holtsmark (1919) and was later extended to include the effects of fine structure by Verweij (1936), Unsöld (1938 a), Craggs and Hopwood (1947 and references there cited) and van Dien (1949). This statistical theory has been replaced by the nearest neighbour approximation by Grimley and Saxe (1951 *) with limitations discussed by Hopwood, Craig and Craggs (1951 *); the latter authors also discuss other possible limitations to the above method of deducing ion concentrations from line widths (first order Stark effect).

§ 2. EXPERIMENTAL METHODS

The D.C. hydrogen arcs studied in the present work carried currents up to 10 amp. at pressures of about 1 to 2 atmospheres and were struck between $\frac{1}{8}$ in. tungsten rods by means of a high voltage impulse (see Edels 1951 a *). Excitation temperatures were measured in the same arcs (see I) and some technical details are described by Edels (1951 a *). The optical techniques are normal and are briefly described by Edels and Craggs (1951). The photographic plates were given careful intensity and wavelength sensitivity calibrations in the usual fashion although for the present purpose the latter data are virtually unnecessary (see below) since measurements were studied only of profile widths, that is over a small wavelength range centred round each line (H_α H_β and H_γ of the Balmer series). Care was taken to ensure that the profiles obtained were not affected by the spectrometer slit size; thus, after exploratory work had been carried out with fine lined spectra, such as those obtained with iron–air arcs, data were obtained for H_α for spectrometer collimator slits 7, 13, 22 and 30 microns wide, with a hydrogen arc operated at 8 amp. and a pressure of approximately 110 cm. Hg. It was found that below 13 microns slit width the observed line profile alters only slightly and this is in fair agreement with the 'limiting slit width' (van Cittert 1930, Sawyer 1944) for the instrument used, viz. 13 microns, calculated from the geometry of the spectrometer.

Care was also taken to check that the spectral variations in plate sensitivity near H_α and H_β were negligible. This ensures that the line profiles are not distorted, that is, that they are symmetrical about the mean wavelength line.

A typical plate is that shown in Figure 4 (*a*) of I. The widened Balmer lines are to be noted, also the mercury comparison spectrum for wavelength calibration and the continuum from the standard lamp for intensity calibrations over the spectral range required. The spectra were taken through a Hilger step filter in the usual manner. The hydrogen gas used was of cylinder grade and contained, according to the suppliers, 0·5–1% of oxygen.

§ 3. EXPERIMENTAL RESULTS

Preliminary experiments showed that the reproducibility of line widths was satisfactory. Typical line widths for H_α H_β and H_γ at 88 cm. Hg pressure and for currents varying from 5·8–9·2 amp. are given in Figures 1, 2 and 3. H_β profiles for 8 amp. current are given in Figure 4 for pressures varying from 88 to 230 cm. Hg and Figure 5 gives profiles for H_α, H_β, H_γ and H_δ at 153 cm. Hg pressure and 8 amp.

* Papers to be published.

Although the profiles obtained in any discharge for H_α, H_β and H_γ will be different in shape since the fine structures are different (see the results plotted by Craggs and Hopwood 1947), the extent of the difference will depend on the discharge, and will be more apparent for the line widths obtained in sparks (where the electron concentration N_e may be of the order of 10^{17} per cm^3) which

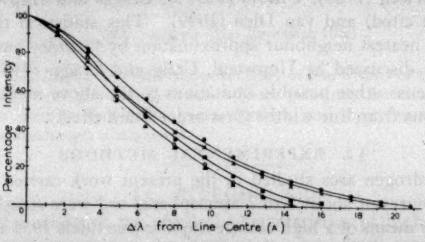

Figure 1. Balmer line profiles of H_α at 88 cm. Hg pressure and various currents. ○ 5·8 amp. ▲ 6·6 amp. ■ 7·7 amp. × 8·8 amp. ● 9·2 amp.

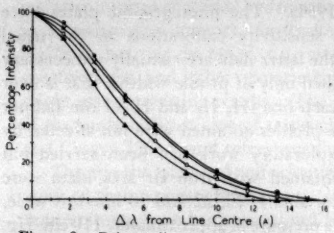

Figure 2. Balmer line profiles of H_β at 88 cm. Hg pressure and various currents. ▲ 6·6 amp. ○ 7·7 amp. × 8·8 amp. ● 9·2 amp.

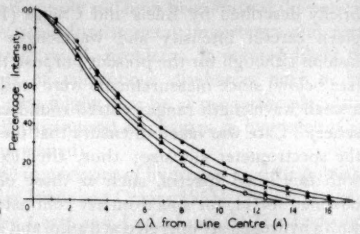

Figure 3. Balmer line profiles of H_γ at 88 cm. Hg pressure and various currents. ○ 5·8 amp. ▲ 6·6 amp. × 8·8 amp. ● 9·2 amp.

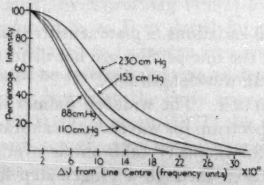

Figure 4. Balmer line profiles of H_β at 8 amp. D.C. and various pressures.

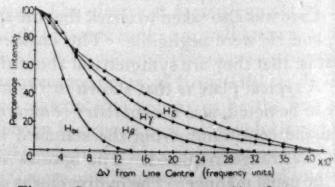

Figure 5. Balmer line profiles for arc at 153 cm. Hg pressure and 8 amp. current.

are generally wider than those obtained in the present arcs ($N_e \sim 10^{16}$/cm^3). Thus when the profiles for H_α, H_β and H_γ (88 cm. Hg pressure, but for all currents) were normalized for intensity, and the intensities plotted as a function of the half width, it was found that H_α and H_β lay together, but that H_γ showed a distinctly different line profile shape. These results have little fundamental significance but have been used by one of us (Edels 1951 a *) in a study of self-absorption problems in discharges.

* Paper to be published.

§4. DEDUCTION OF ELECTRON CONCENTRATIONS FROM LINE PROFILES

It is first necessary to justify the use of Stark broadening analysis with the arc line profiles, that is, to show that the main process leading to such line broadenings will be the interatomic (inhomogeneous field) Stark effect. For the conditions of the present discharges reference to standard works on spectroscopy (White 1934, Margenau and Watson 1936, Tolansky 1947) show that the broadening due to Stark effect predominates. There is also indirect support of the use of Stark theory in that the line profile shapes are in general agreement with those deduced from the fine structure and that electron concentrations deduced from different lines, on Stark theory for inhomogeneous fields, agree quite closely (see below, Craggs and Hopwood 1947, Hopwood, Craig and Craggs 1951 *).

It will be shown later in this paper that a knowledge of the longitudinal voltage gradient X in the discharge and the current density is necessary. The latter was determined from microphotometer measurements of the arc core and a mean value of current density obtained. The metal vapour flame surrounding the channel complicates the problem considerably for horizontal arcs of the type studied. The values taken for current densities at 88, 110 and 153 cm. Hg

Table 1

Pressure (cm. Hg)	88	88	88	153	153	153
Current (amp.)	5	7	9	5	7	9
$N_e \times 10^{-16}$ from H_α	0·9	1·2	1·4	1·4	1·7	2·1
$N_e \times 10^{-16}$ from H_β	0·7	0·8	0·9	1·2	1·4	1·6

pressure respectively were 580, 608 and 670 amp/cm^2. Since accuracy in measurements does not justify the use of three significant figures the values 600, 600 and 670 amp/cm^2 will be used. Suits (1939 a, b) working with hydrogen at 1 atmosphere pressure, for 2–10 amp. current found in a similar fashion a current density of 565 amp/cm^2.

Similar difficulties of measurements, now due largely to the uncertainty of the total arc length, render the determination of X inaccurate. For the purpose of calculations $X = 100$ v/cm. will be taken since this gives a close approach to the value obtained at 88 cm. Hg pressure for 8–10 amp. current (where $N_e(H_\beta) \simeq 10^{16}$/cm^3—see Table 1). At this pressure X changes from about 160 v/cm. at 5 amp. to about 105 v/cm. at 10 amp. and at 153 cm. Hg pressure for currents of 5–10 amp., X varies from 230 to 160 v/cm. These values are consistent with the electrode voltage drops measured by Craig (1951 *) for hydrogen sparks, and agree satisfactorily with Vijverberg's (1937) gradients which were, for a hydrogen arc between tungsten electrodes at 76 cm. Hg pressure, approximately 125 and 100 v/cm. at currents of 5 and 10 amp. respectively. Suits (1939 a, b), also at 1 atmosphere pressure, measured gradients for the above conditions of 160 and 90 v/cm. which agree closely with our measurements.

The analysis of the data provided by Figures 1–5 can proceed either (*a*) by arbitrarily taking the discharge to be a region of constant electron concentration or (*b*) by taking a more practical case and allowing for the radial changes in electron concentration which unquestionably occur in discharges.

* Papers to be published.

For the present paper, we propose to use the approximate procedure (*a*). The line profile for any line, e.g. H_β, and for any value of electron concentration, e.g. $N_e = 10^{16}/cm^3$, may be found by using the procedure given by Verweij (1936), Unsöld and others, and based on the work of Holtsmark (1919) ; Figure 6 shows a typical result for H_α. Although the centre of the discharge H_α profile is not filled in by a theoretical profile, the fit indicates that the mean electron concentration in the discharge will be fairly close to that given by the interionic

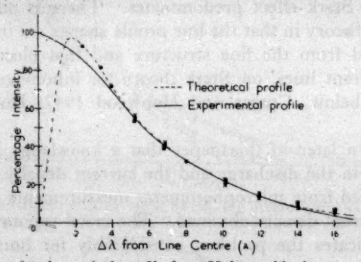

Figure 6. An example of a theoretical profile from Holtsmark's theory, using Unsöld's (1938) fine structure data, fitted to an experimental profile at $\Delta\lambda = 8$ A.

field calculated for the theoretical profile given in Figure 6. Later and more exact analyses will be made when other data on the arc discharges are available. Using the fitting method of Figure 6 the data of Table 1 were derived.

Reman (1937) working with an 8·5 amp. arc between tungsten electrodes in hydrogen at 76 cm. Hg pressure found $N_e = 4 \times 10^{15}/cm^3$ from observations of Stark broadened lines. His line profiles were slightly narrower than ours.

The above analysis assumes that the concentration of tungsten positive ions is such as to have a negligible effect on the line broadening.

§ 5. THE DRIFT CURRENT EQUATION

If the positive ion drift current in the discharge is negligible in comparison with the electron drift current, as can be shown, then the current density is

$$I = N_e \epsilon v \qquad \ldots\ldots(1)$$

where N_e is the electron concentration; ϵ and v are respectively the electron charge and drift velocity. Thus if I is known from measurements of the arc current and diameter (see below for further discussion of the latter) and if v is found from a knowledge of the electron mobility in the arc conditions and the measured voltage gradient X in the discharge, then N_e may be calculated and compared with the Stark value of N_e. Conversely, the Stark value of N_e may be used in equation (1) with I to give v for comparison with the value of v deduced from X etc. It should be clearly stated that, at the present, no accurate data for I, N_e or v are available, and the following comments on these quantities should be made.

(*a*) The current density I is known only to the extent that the arc diameter and the radial variations of current density within that diameter are known. Although preliminary measurements of radial variations of light intensity, from which radial variations of N_e can be found from the line profile data of Figures 1–5 have been made, we prefer for the present to use crude current densities deduced from the apparent visible diameters. Since the radial variation of electron

concentration falls off less rapidly than the radial variation of light emission (Edels 1951 c) the true mean current density will be less than the values deduced as above. Later experiments will be made to increase the accuracy of the measurements of current densities, and radial variations in N_e etc.

(*b*) The values of N_e given in Table 1 are the most accurate known to us for hydrogen arcs but are clearly not as satisfactory as true mean N_e values would be. Further discussions are given by Grimley and Saxe (1951*) and Hopwood *et al.* (1951*). It will be noticed that the fit obtained, see Figure 7, between the the experimental or 'total arc' profile and the profile for a discharge of uniform N_e is considerably better even than that previously obtained for sparks (Craggs and Hopwood 1947). If N_e and the discharge pressure are known, the use of Saha's equation enables the temperature to be calculated on the assumption of thermal equilibrium (see below).

(*c*) The quantity v, the electron drift velocity, is difficult to determine, for a knowledge of N_e and the discharge gas temperature T_g are required.

We have, from the classical mobility expression for discharges with low ion (or electron) concentration (Loeb 1939)

$$v = k_e X = \frac{X \times 271 \times 10^3 (273/T_g)^{1/2} L_{1,0}}{[1+\{1+1{\cdot}1 \times 10^6 M L_{1,0}{}^2 (X/p)^2\}^{1/2}]^{1/2}},$$

where M is the atomic or molecular weight, $L_{1,0}$ is the electron mean free path, for elastic collisions, at 1 mm. Hg pressure and 273° K., X is in v/cm. and p is in mm. Hg. For monatomic gases (the present arcs show virtually complete dissociation into atomic hydrogen) the inelastic collision energy losses are negligible at low X/p (see Smit (1937) for He, and Loeb 1939). For the greatest accuracy the calculation of v should allow for the variations of $L_{1,0}$ with electron energy (see, for example, Jones 1944 and references there cited) and also for the effect of the high gas temperature. The most appropriate treatment is that of Davydov (1935) who calculated electron mobilities and mean electron energies for this case, $T_g \sim T_e$, but who did not allow for variations of $L_{1,0}$ with electron energy. A general discussion of these matters with references is given in the review paper by Druyvesteyn and Penning (1940).

A very important effect, namely the increased electron scattering by the positive ions, appears for discharges in which N_e is high. This problem has been treated by Gabor (1933) and Gvosdover (1937) and the latter's treatment is usually used (Schulz 1947, Elenbaas 1949, Druyvesteyn and Penning 1940, and others). In the presence of positive ions the electron mean free path becomes $L_{1,0} = 1/(NQ + N_+Q_+)$ where NQ and N_+Q_+ are respectively the total atom and ion cross sections for the particles in 1 cm^3; N and N_+ are the particle concentrations. Gvosdover finds that

$$N_+Q_+ = \frac{\pi}{2} \log \left(\frac{1{\cdot}5 \boldsymbol{k} T_e}{\boldsymbol{e}^2 N_+{}^{1/3}} \right) \cdot \frac{\boldsymbol{e}^4}{\boldsymbol{k}^2 T_e{}^2} N_+.$$

§ 6. DISCUSSION OF ARC CONDITIONS

Table 2 gives the results of calculations of v assuming $N_e = 10^{16}$/cm$^3 = N_+$ for the calculation of N_+Q_+, and $X = 100$ v/cm.

The value of $L_{1,0}$ for the k_e formula is taken at the mean electron energy for the various values of T_e in Table 2 on the assumption of a Maxwellian distribution

* Papers to be published.

of electron velocities. Ramsauer cross sections calculated for atomic hydrogen have been kindly supplied to us by Professor Massey. It must be emphasized that this value of $L_{1,0}$ is only approximate since the weighted mean $L_{1,0}$ for the whole energy distribution, using the energy variations of Ramsauer free paths, should be taken. In the present state of knowledge of the high pressure, high current density plasmas, it does not seem advisable to proceed further at the present. The values of $L_{1,0}$ so obtained are then reduced in proportion to the total elastic collision and ion scattering cross sections and give the final value of v. It will be noticed that X/p affects k_e negligibly (I) but, of course, v varies directly as X. The Gvosdover term is especially important at low values of T_e, and becomes increasingly so as N_e increases (see Craig and Craggs 1951 * for details of experiments on hydrogen spark channels where $N_e \sim 10^{17}/\text{cm}^3$). Table 2 shows that variations in T_g over a fairly wide range, for given T_e, affect v relatively little.

Table 2. Drift Velocities v (cm/sec.) for Electrons in Hydrogen Arcs

$N_e = 10^{16}/\text{cm}^3$, and $X = 100$ v/cm., $p = 1$ atmosphere. σ_{el} and σ_{Gv} are the atom and ion scattering cross sections per cm^3 of gas (see text) in the usual units.

T_g (° K.)	5,000	10,000	15,000
$T_e = 5{,}000°$ K.	$\sigma_{el} = 4{\cdot}0 \times 10^3$ $\sigma_{Gv} = 5{\cdot}4 \times 10^3$ $v = 0{\cdot}46 \times 10^6$		
$T_e = 10{,}000°$ K.	$\sigma_{el} = 3{\cdot}0 \times 10^3$ $\sigma_{Gv} = 1{\cdot}7 \times 10^3$ $v = 0{\cdot}93 \times 10^6$	$\sigma_{el} = 1{\cdot}5 \times 10^3$ $\sigma_{Gv} = 1{\cdot}7 \times 10^3$ $v = 0{\cdot}96 \times 10^6$	
$T_e = 15{,}000°$ K.	$\sigma_{el} = 2{\cdot}6 \times 10^3$ $\sigma_{Gv} = 0{\cdot}68 \times 10^3$ $v = 1{\cdot}3 \times 10^6$	$\sigma_{el} = 1{\cdot}3 \times 10^3$ $\sigma_{Gv} = 0{\cdot}68 \times 10^3$ $v = 1{\cdot}55 \times 10^6$	$\sigma_{el} = 0{\cdot}88 \times 10^3$ $\sigma_{Gv} = 0{\cdot}68 \times 10^3$ $v = 1{\cdot}7 \times 10^6$

For $T_g = T_e = 3{,}000°$ K., $\sigma_{el} = 8{\cdot}6 \times 10^3$, $\sigma_{Gv} = 13 \times 10^3$ and $v = 0{\cdot}07 \times 10^6$.

From the drift current equation, for a pressure of 88 cm. Hg

$$v = I/N_e \boldsymbol{e} = 580/N_e \boldsymbol{e} = 3{\cdot}64 \times 10^{21}/N_e = 3{\cdot}6 \times 10^5 \text{ cm/sec. for } N_e = 10^{16}/\text{cm}^3.$$

Thus the mobility data suggest that the arc temperature, and by this we mean primarily T_e, since Table 2 cannot give T_g so sensitively, is about 5,000° K. This agrees reasonably well with the excitation temperature $T_{\beta\gamma}$ (see I) which was found to be 5,100–5,900° K. for 6–9·5 amp. at 1 atmosphere pressure, but not with $T_{\alpha\beta}$ which was, in the above conditions, 9,500–12,500° K.

Gabor's (1933) theory of the plasma in which the mutual influence of electrons and positive ions is discussed (see Ornstein and Brinkman 1934) gives $k_e = 8{\cdot}3 \times 10^{14} T_e^{1/2}/N_e^{2/3}$ and the drift velocities derived therefrom for $N_e = 10^{16}/\text{cm}^3$ and for $X = 100$ v/cm. (note that the above formula is in C.G.S. units) and for $T_e = 5{,}000$, 10,000 and 15,000° K. respectively are $0{\cdot}41 \times 10^6$, $0{\cdot}60 \times 10^6$ and $0{\cdot}73 \times 10^6$ cm/sec. The agreement with the data of Table 2 is perhaps as good as could be expected.

Suits (1939 a, b) and many other workers (see Edels 1950 for references) have used Saha's equation to determine arc temperatures, using N_e values derived from the drift current equation and not, as in the present work, by

* Paper to be published.

direct measurement. The determination of the electron mobility has sometimes been made without due regard to the effect of high gas temperatures (see I for further discussion) or to the fact that the arc gas is atomic hydrogen. Sometimes the positive ion scattering has been neglected and (Table 2) this can introduce appreciable error. It is necessary to assume that thermal equilibrium is attained, and though there is much, but somewhat incomplete, evidence in favour of this (Edels 1950) it is not entirely a justifiable assumption in all cases (see Vijverberg 1937 and Edels and Craggs 1951). Indeed one of the aims of our present programme of experimental work is to measure T_e, T_g and the excitation temperature for the same arc discharges. Further, as Professor K. G. Emeléus kindly reminded us, the precise value of the ionization potential V_i to be used for example in Saha's equation for discharges of high ion or electron densities is not easy to determine, because of level smearing (treated by Unsöld 1938 b and Borchert 1950 and mentioned by Craggs and Meek 1946). The true value of V_i will be less than the value for single atoms, but by not more than 0·2 ev. since H_ξ (see Figure 4 (*b*) of I) is just resolved. This photograph was obtained with the arc focused on the spectrometer slit and was taken with the purpose of showing the presence of the Balmer recombination continuum; spectra taken in the manner described by Edels and Craggs (see I) and exemplified by Figure 4 (*a*) of I do not show the continuum so clearly. Saha relates the degree of ionization x to the pressure p (in atmospheres) for given V_i and absolute arc temperature T with the equation

$$\log \frac{px^2}{1-x^2} = \frac{-5{,}040V_i}{T} + 2{\cdot}5 \log T - 6{\cdot}5.$$

Putting $V_i = 13{\cdot}5$ ev., $N_e = 10^{16}/\text{cm}^3$, and $p = 1$ and noting that $p = N\boldsymbol{k}T = N_a\boldsymbol{k}T_a$ where N and N_a are the atom concentrations at the arc temperature and the room temperature T_a respectively, and $\boldsymbol{k}$ is Boltzmann's constant, we find $T = 9{,}200°$ K. This value, which differs widely from $T_{\beta\gamma}$ or the temperature deduced indirectly from Table 2, will be an upper limit since V_i in practice could be less than 13·5 ev. by virtue of the effect mentioned above or through the presence of electrode vapour (tungsten) in the arc. The latter effect cannot be accurately assessed since the partial pressure of tungsten vapour in the arc is unknown and is very difficult to estimate. Little or no tungsten radiation is observed in the emission spectrum of the central part of the arc flame above the red column; we believe this to be due to a small partial pressure rather than to 'complete' ionization since air arcs usually show excitation with metals of lower ionization potential than tungsten. Taking $V_i = 8{\cdot}1$ volts for tungsten and $T = 5{,}000°$ K. it is found that a tungsten atom concentration of about $1 \times 10^{19}/\text{cm}^3$ is required to give $N_e = 10^{16}/\text{cm}^3$ (reduced to room temperature) so that $p_W \sim \frac{1}{3}$ atm., which seems appreciably higher than could reasonably be expected for a refractory metal. It is difficult to take the argument further unless an estimate of the tungsten vapour pressure is made. However, it is found that a partial pressure of tungsten vapour of 4×10^{-6} times the hydrogen pressure will give equal contributions from tungsten and hydrogen to the total electron population.

Suits (1939 a, b) derives Saha's temperatures of 6,500–7,400° K. for 1-atmosphere hydrogen arcs carrying 1 to 10 amp., but using N_e values derived from the drift current equation.

§ 7. CONCLUSIONS

Preliminary measurements of ion concentrations deduced from the Stark broadened lines emitted by hydrogen arcs suggest that the arc electron temperature may be about 5,000° K. from considerations of the drift current equation. The arc gas temperature should not be very far from this value which agrees with the excitation temperature $T_{\beta\gamma}$ measured from the relative intensities of the Balmer lines H_β and H_γ but not with T measured from H_α and H_β. The Saha temperature, namely about 9,000° K., falls between $T_{\alpha\beta}$ and $T_{\beta\gamma}$. Further experimental work is proceeding.

ACKNOWLEDGMENTS

The authors wish to acknowledge the interest shown by Professor J. M. Meek and Professor F. J. Teago in this work. They wish also to thank Professor K. G. Emeléus, Dr. A. von Engel and Mr. W. Hopwood for many valuable discussions, and the Electrical Research Association for financial support given to one of them (H. E.), who also wishes to make acknowledgment to the University of Liverpool for the award of a Fellowship.

REFERENCES

Borchert, A., 1950, *Ann. Phys., Lpz.*, **7**, 321.
Carst, A., and Ladenburg, R., 1928, *Z. Phys.*, **48**, 192.
van Cittert, P. H., 1930, *Z. Phys.*, **66**, 547.
Craggs, J. D., and Hopwood, W., 1947, *Proc. Phys. Soc.*, **59**, 755.
Craggs, J. D., and Meek, J. M., 1946, *Proc. Roy. Soc.* A, **186**, 241.
Davydov, B., 1935, *Phys. Z. Sowjet*, **8**, 59.
van Dien, E., 1949, *Astrophys. J.*, **109**, 452.
Druyvesteyn, M. J., and Penning, F. M., 1940, *Rev. Mod. Phys.*, **12**, 87.
Edels, H., 1950, *E.R.A. Report* L/T230; 1951 c, *Proc. Phys. Soc.* B, **64**, 354.
Edels, H., and Craggs, J. D., 1951, *Proc. Phys. Soc.* A, **64**, 562.
Elenbaas, W., 1949, *Philips Res. Rep.*, **4**, 221.
Frisch, S., and Kagan, J., 1943, *J. Phys. U.S.S.R.*, **7**, 208.
Gabor, D., 1933, *Z. Phys.*, **84**, 474.
de Groot, W., 1931, *Physica*, **11**, 307.
Gvosdover, S. D., 1937, *Phys. Z. Sowjet*, **12**, 164.
Holtsmark, J., 1919, *Ann. Phys., Lpz.*, **58**, 577.
Jackson, W. W., 1934, *Phil. Mag.*, **17**, 33; 1936, *Ibid.*, **22**, 633.
Jones, F. Ll., 1944, *Proc. Phys. Soc.*, **56**, 239.
Kopfermann, H., and Ladenburg, R., 1930, *Z. Phys.*, **65**, 187.
Ladenburg, R., 1928, *Z. Phys.*, **48**, 15.
Loeb, L. B., 1939, *Fundamental Processes of Electrical Discharge in Gases* (New York : John Wiley), p. 228.
Margenau, H., and Watson, W. W., 1936, *Rev. Mod. Phys.*, **8**, 22.
Ornstein, L. S., and Brinkman, H., 1934, *Physica*, **1**, 797.
Ornstein, L. S., Eymers, J. G., and Wouda, J., 1931, *Proc. K. Akad. wet. Amst.*, **34**, 505.
Ornstein, L. S., and Lindeman, H., 1930, *Z. Phys.*, **63**, 8; 1931, *Ibid.*, **67**, 1.
Reman, G. H., 1937, *Dissertation*, Utrecht.
Rossi, R., 1911, *Astrophys. J.*, **34**, 299.
Sawyer, R. A., 1944, *Experimental Spectroscopy* (New York : Prentice Hall).
Schulz, P., 1947, *Ann. Phys., Lpz.*, **1**, 95.
Smit, J. A., 1937, *Physica*, **3**, 543.
Suits, C. G., 1939 a, *J. Appl. Phys.*, **10**, 203, 728, 730; 1939 b, *Phys. Rev.*, **55**, 561.
Tolansky, S., 1947, *High Resolution Spectroscopy* (London : Methuen).
Unsöld, A., 1938 a, *Physik der Sternatmosphären* (Berlin : Springer), pp. 180–184; 1938 b, *Ann. Phys., Lpz.*, **33**, 607.
Verweij, S., 1936, *Publ. Astr. Inst. Amst.*, No. 5.
Vijverberg, W. R., 1937, *Dissertation*, Utrecht.
White, M. E., 1934, *Introduction to Atomic Spectra* (New York : McGraw-Hill).

LETTERS TO THE EDITOR

Paramagnetic Resonance in Nickel Ammonium Sulphate

The paramagnetic resonance from the Ni^{++} ions in nickel ammonium sulphate has been investigated at room temperature for wavelengths between 0·85 cm. and 1·79 cm., by the method of observing the power transmitted through a loaded cavity resonator as described by Bagguley and Griffiths (1950). The results are consistent with the assumption that each of the two ions in unit cell is subjected to a crystalline electric field of rhombic symmetry. The splittings between adjacent levels of the ground state spin triplet ($S=1$) are found to be 1·85 and 0·77 cm^{-1}, and the g value, assumed isotropic, is 2·25.

Resonances in nickel salts used in powder form (including $Ni(NH_4)_2(SO_4)_2 . 6H_2O$) have previously been found by Bagguley *et al.* (1948), but the only crystal that has been investigated in detail by the paramagnetic resonance method is $NiSiF_6 . 6H_2O$ (Penrose and Stevens 1950). Here it was found that the non-cubic part of the crystalline field acting on the nickel ions was of trigonal symmetry, and that the ground state spin triplet was split into a singlet and a doubly degenerate level.

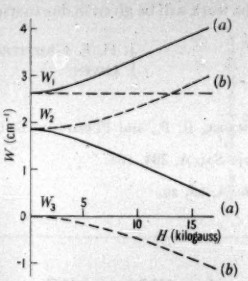

Figure 1.

(*a*) $H \parallel z$ axis; (*b*) $H \parallel y$ axis.

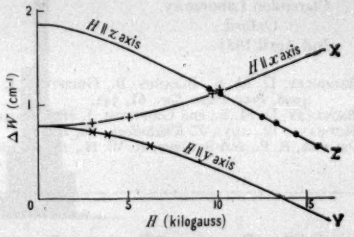

Figure 2.

To account for the results in $Ni(NH_4)_2(SO_4)_2 . 6H_2O$ it is necessary for the non-cubic part of the electric field to be of rhombic symmetry, and there is then no degeneracy in the ground state spin levels. The spin triplet is described by the Hamiltonian $\mathcal{H}=DS_z^2+E(S_x^2-S_y^2)+g\beta HS$ leading to an expression for the energy levels W:

$$-W^3+2DW^2+W(E^2-D^2+g^2\beta^2H^2)-g^2\beta^2H^2\{D(l^2+m^2)-E(l^2-m^2)\}=0, \quad \ldots\ldots (1)$$

where (l, m, n) are the direction cosines of the applied magnetic field H, referred to the axes (x, y, z) of the rhombic field, β is the Bohr magneton, g the gyromagnetic ratio (assumed isotropic), and D and E constants of the rhombic field. (These equations were kindly derived for us by K. W. H. Stevens.) For $Ni(NH_4)_2(SO_4)_2 . 6H_2O$ it is found that $g=2·25$, $D=2·24$ cm^{-1}, $E=0·38_7$ cm^{-1}, the splitting between adjacent levels when $H=0$ being $D-E=1·85$ cm^{-1}, and $2E=0·77$ cm^{-1}.

The Tutton salts, whose crystallography has been investigated by Hofmann (1931), have two ions per unit cell. For $Ni(NH_4)_2(SO_4)_2 . 6H_2O$ the directions of the rhombic axes of the crystalline field for each of these two ions are found from the present measurements to be as follows: the z axes of both ions, z_1 and z_2, are very nearly parallel to each other, and to K_1 the principal axis of susceptibility; the direction cosines referred to the crystal axes (a, b, c) are approximately $(-0·50, 0, 0·97)$. The axes x_1 and y_2 are very nearly parallel to each other, and make an angle of 45° with the other susceptibility axes K_2 and K_3; the direction cosines are approximately (0·61, 0·71, 0·17).

Figure 1 shows how the energy levels of the spin triplet, W_1, W_2, W_3 vary with the external magnetic field H, (*a*) with H parallel to a z axis, and (*b*) with H parallel to a y axis. These levels are calculated using equation (1) with the values of D, E, and g as given above. For the wavelengths used (0·85 to 1·79 cm^{-1}) transitions can be observed between W_2 and W_3 when H is parallel to z, and between W_1 and W_2 when H is parallel to x or y. In Figure 2 the curve X shows the calculated variation of W_1-W_2 when H is parallel to x, and the crosses are the experimentally observed transitions ; curve Y shows the variation of W_1-W_2 when H is parallel to y, with the crosses the experimental points ; the curve Z shows the variation of W_2-W_3 when H is parallel to z, with the circles the experimental points. For other directions of H the agreement between theory and experiment is also good.

Additional evidence for the form of crystalline field proposed is provided by the transition probabilities, which vary rapidly both with the direction of the external magnetic field and with the direction of the oscillating magnetic field. The theoretical and observed intensities show good qualitative agreement, but an exact comparison between theory and experiment is difficult for various experimental reasons which will not be detailed here.

From preliminary measurements the absorption line widths seem to be greater than would be expected if only dipolar interaction were present.

Measurements on other nickel Tutton salts are being continued, and the results on the potassium and thallium sulphates, and on ammonium selenate, can be interpreted in a similar way to those for ammonium sulphate. A full account of the work will be given in due course.

Clarendon Laboratory,
Oxford.
2nd April 1951.

J. H. E. Griffiths.
J. Owen.

Bagguley, D. M. S., Bleaney, B., Griffiths, J. H. E., Penrose, R. P., and Plumpton, B. I., 1948, *Proc. Phys. Soc.*, **61**, 542.
Bagguley, D. M. S., and Griffiths, J. H. E., 1950, *Proc. Roy. Soc.* A, **204**, 188.
Hofmann, W., 1931, *Z. Kristallogr.*, **78**, 279.
Penrose, R. P., and Stevens, K. W. H., 1950, *Proc. Phys. Soc.* A, **63**, 29.

The Range of Protons from the Reaction $^{14}N(n, p)^{14}C$ in Ilford C2 Photographic Emulsion

The object of this note is to report an accurate determination of a point on the range–energy curve for protons of low energy in Ilford C2 photographic emulsion. For this purpose the reaction ^{14}N (n, p) ^{14}C, induced by the action of thermal neutrons on nitrogen present in the emulsion, has been employed. The importance of this reaction was first pointed out by Cornog, Franzen and Stephens (1948), who measured the range in air of the emitted proton. The results of such measurements, together with measurements on the disintegration of ^3He and ^6Li by thermal neutrons, enabled Bethe (1950) to publish an accurate range–energy curve for slow protons in air. For similar investigations with photographic emulsion the first reaction is the most suitable, since nitrogen is a normal constituent of the emulsion* and there is no need to impregnate the emulsion with some foreign material. The energy of the protons from this reaction is given by Bethe (1950) as $0{\cdot}584 \pm 0{\cdot}003$ Mev.

The problem was first approached by Cuer (1947), who used neutrons from the ^2H (d, n) reaction, moderated with paraffin. However, he found it necessary to impregnate the emulsion with sodium azide to increase the nitrogen content. Recently Nerson and Reines (1950) have reported measurements on plates exposed to the thermal neutrons from a chain reacting pile. Both these measurements suffer from a background of recoil protons in the emulsion.

* The only other known reaction which might occur is ^{17}O (n, α) ^{14}C (May and Hincks 1947), but this is very improbable owing to the small amount of ^{17}O which is present in the emulsion and to the small cross section of this reaction.

In the present measurements use was made of a graphite column with dimensions $340 \times 195 \times 190$ cm. placed with its front face 400 cm. from the beryllium target of the Liverpool cyclotron. The bombarding particles were 8 MeV. deuterons. Two Ilford C2 nuclear research plates having emulsion of 100 μ thickness, were wrapped in black paper and placed at a distance of 190 cm. from the front face of the column. At this position it is known that the flux of neutrons consists almost entirely of thermal neutrons. The flux of these neutrons was measured with a BF_3 chamber and was found to be 5×10^4 n/cm^2/sec. The time of exposure was 90 minutes.

The plates were examined with a binocular microscope for nuclear research built by Cooke, Troughton and Simms with a 95× oil immersion objective and a 10× eyepiece. The scale was carefully calibrated using a special micrometer gauge and it was found that one scale division was equivalent to 0·416 μ. Measurements were made only on those tracks which lay nearly parallel to the surface of the emulsion in order to avoid correction for emulsion shrinkage during processing. The criterion for selection was that the track should lie wholly within the depth of focus of the microscope ($\sim 0{\cdot}5$ μ).

The lengths of a thousand tracks were estimated to half a scale division and were plotted as shown in the Figure. The range distribution can be fitted with a Gaussian type curve,

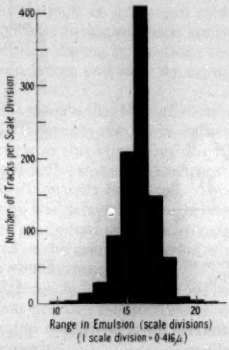

having a half width at half maximum of 0·42 μ. This half width is mainly due to range-straggling in the emulsion. The mean range was calculated to be $6{\cdot}55 \pm 0{\cdot}01$ μ. This range includes the track of the recoil ^{14}C nucleus.

The range of the recoil nucleus ^{14}C is about 0·03 cm. of air as estimated by Cornog *et al.* (1948). Taking the range of the proton as $0{\cdot}995 \pm 0{\cdot}01$ cm. of air, as given by Bethe (1950), and assuming that the stopping power in the emulsion for the ^{14}C recoil is the same as that for these protons, the range of the recoil nucleus in the emulsion was estimated to be 0·19 μ. Thus the range of the proton of energy $0{\cdot}584 \pm 0{\cdot}003$ MeV. can be stated as $6{\cdot}36 \pm 0{\cdot}05$ μ.

The author wishes to express his thanks to Dr. J. R. Holt for helpful discussion and valuable assistance and to the Egyptian Government for financial aid during the period in which this work was done.

George Holt Physics Laboratories,
University of Liverpool.
13th March 1951.

F. A. El-Bedewi.

Bethe, H. A., 1950, *Rev. Mod. Phys.*, **22**, 213.
Cornog, I. C., Franzen, W., and Stephens, W. E., 1948, *Phys. Rev.*, **74**, 1.
Cuer, P., 1947, *J. Phys. Radium*, **8**, 83.
May, A. N., and Hincks, E. P., 1947, *J. Canad. Res.* A, **25**, 77.
Nerson, N., and Reines, F., 1950, *Rev. Sci. Instrum.*, **21**, 534.

Soft Radiations from ^{239}Pu

Absorption measurements by Ghiorso (1944) first revealed the presence of soft radiations from ^{239}Pu. More recently, Rosenblum, Valadares and Goldschmidt (1950) have reported a low energy group of alpha-particles which differ in energy by about 50 kev. from the main group. The present work was undertaken to look for gamma-radiation in the 50 kev. region which would be expected to accompany the low energy group of alpha-particles.

A Maze type proportional counter, of diameter 5 cm. and active length 34 cm., fitted with a thin mica window (thickness 0·0038 cm.) was used. It was filled with krypton (48·6 cm. Hg pressure) and pure methane (7·4 cm. Hg pressure). The plutonium source (66 micrograms) was deposited on an aluminium disc. The majority of the radiation detected was L x-radiation. Figure 1 shows the pulse-size distribution due to this radiation

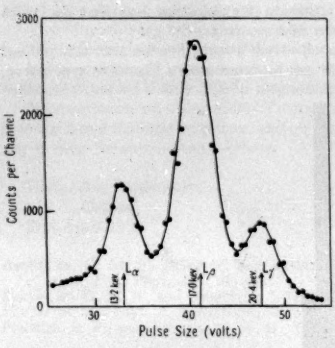

Figure 1. Pulse-size distribution of the L x-radiation from ^{239}Pu.

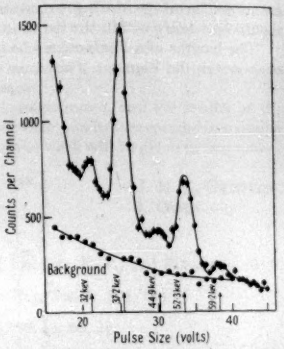

Figure 2. Pulse-size distribution of weak electromagnetic radiations from a ^{239}Pu source.

which was measured with a 30-channel pulse analyser. The energies of the three groups of L rays were determined by calibrating the counter with 20·2 kev. x-rays, from a ^{103}Pd K capture source. The Table gives the experimental values together with the energies of the L x-rays of plutonium and uranium.

Experimental values (kev.)	13·2±0·3	17·0±0·2	20·4±0·2
Energies of uranium L x-rays (kev.)	13·6	16·9	20·2
Energies of plutonium L x-rays (estimated) (kev.)	14·2	17·9	21·4

It is evident that the radiation is the L x-radiation of uranium. An estimate of its intensity was obtained by measuring the counting rate for each group of L rays when the counter was exposed to a collimated beam of the radiation. The efficiency of the counter was estimated from the geometry and the known absorption coefficients of krypton for the individual radiations. The measured intensity was 4×10^{-2} L rays per alpha-particle with an estimated uncertainty of $\pm1\times10^{-2}$.

The fact that the radiation is uranium L x-radiation rules out the possibility that it is produced by the bombardment of plutonium atoms by alpha-particles from other plutonium atoms. The possibility that it is due to the excitation of the electronic structure of its parent atom by an alpha-particle is excluded on intensity grounds, since the emission of L x-rays with such a high intensity is not a universal property of alpha-emitters. Since orbital electron capture is impossible with ^{239}Pu (^{239}Np is β^--active) the L radiation can only arise as a result of the internal conversion of a gamma-ray which follows alpha-particle emission. The presence of conversion electrons has been reported very recently by Albouy and Teillac (1951) who find 0·16 conversion electron per alpha-particle with an energy of about 30 kev. corresponding to the L conversion of a gamma-ray of about 50 kev.

A search for soft gamma-radiation was made using much stronger sources than were necessary for investigating the L rays. Only very weak radiations were found; their pulse-size distribution is shown in Figure 2. It should be noted that a monokinetic gamma-radiation gives rise to two peaks in a krypton-filled proportional counter: one at the full energy, and a second (the escape peak) of about equal intensity at the full energy minus 12·7 kev. (West and Rothwell 1950). From the distribution in Figure 2 it is evident that radiations of energies 59·2, 52·3, 37·2 and 32 kev. are present. The escape peak from the 59·2 kev. radiation lies at 46·5 kev. and probably accounts for the peak at 44·9 kev. The escape peak from the 52·3 kev. radiation lies at 39·6 kev. and accounts for about half the intensity of the peak at 37·2 kev. The intensities of the radiations estimated from the calculated efficiencies of the counter are:

Energy of γ-radiation (kev.)	$59{\cdot}2\pm0{\cdot}5$	$52{\cdot}3\pm0{\cdot}4$	$37{\cdot}2\pm0{\cdot}5$	$32{\cdot}0\pm1{\cdot}0$
Estimated intensity per α-particle	10^{-5}	7×10^{-5}	3×10^{-5}	10^{-5}

Some of these radiations may arise from residual fission products present in the plutonium source. Their energies correspond to those of K x-rays from elements in the fission product region. They were however still present with approximately the same intensities after the plutonium sample had been put through an additional cycle of repurification specifically designed to remove preferentially those fission products known to be the most probable ones to have remained with the plutonium during its previous treatments. The ratio of fission products present in the plutonium before and after the repurification was expected to be at least 10 : 1.

In spite of this it is not possible to state that the radiations are definitely due to plutonium and not to fission products. At all events the above figures give an upper limit of about 10^{-4} gamma-rays per alpha-particle in this energy region. Taken in conjunction with the much higher intensities of L rays and conversion electrons observed, this means that the gamma-ray involved is very highly internally converted. In view of this an experiment was performed to find if the L radiation was delayed. A separation of the uranium daughter was made from samples of the same plutonium solution by means of solvent extraction. No L radiation was however detected in the uranium fraction which enabled the half-life of the transition to be set at less than two minutes.

The authors wish to acknowledge helpful discussions with Dr. B. Pontecorvo in the early stages of the work. Thanks are also due to Miss R. M. Elliott for assistance in the purification of the plutonium and to the Director, Atomic Energy Research Establishment, for permission to publish these results.

Atomic Energy Research Establishment,
Harwell, Didcot, Berks.
13th March 1951.

D. West.
J. K. Dawson.

Albouy, G., and Teillac, J., 1951, *C.R. Acad. Sci., Paris*, **232**, 326.
Ghiorso, A., 1944, *Plutonium Project Report* CK 1511.
Rosenblum, S., Valadares, M., and Goldschmidt, B., 1950, *C.R. Acad. Sci., Paris*, **230**, 638.
West, D., and Rothwell, P., 1950, *Phil. Mag.*, **41**, 873.

The Distribution of Electron Energies in a Discharge constricted by its Self-Magnetic Field

It is well known that the self-magnetic field associated with a high current arc tends to cause a constriction of the discharge (Tonks 1937, 1939, Alfvén 1950, Thonemann and Cowhig 1950, 1951, Cousins and Ware 1951). In addition to this 'pinch' effect, the magnetic field affects the distribution of electron velocities and hence a distribution differing considerably from the Maxwellian may be discovered in some high current discharges.

In a discharge where the electrons collide mainly with atoms in elastic impacts the velocity distribution is almost spherically symmetrical, because only a small fraction of the electron

energy is lost in such collisions. Hence the first two terms of the expansion of the distribution function in spherical harmonics suffice, in general, to represent this function to a high degree of accuracy : thus

$$f(\mathbf{p})=f_0(p)+f_1(p)\cos\theta, \qquad \ldots\ldots(1)$$

where θ is the angle between the momentum $\mathbf{p}=m\mathbf{v}$ and the direction of current flow The function can also be written in the form

$$f(\mathbf{p})=f_0(p)+\frac{1}{p}\mathbf{p}\,.\,\mathbf{f}_1(p) \qquad \ldots\ldots(2)$$

or, in terms of the momentum, irrespective of direction in space, as

$$p^2dp\int f\,d\omega=4\pi f_0(p)p^2dp\,. \qquad \ldots\ldots(3)$$

Davydov (1937), by consideration of only the elastic collisions between electrons and atoms, has derived, from the kinetic equation of Boltzmann, the following vector equation :

$$\frac{\partial\mathbf{f}_1}{\partial t}+v\,\mathrm{grad}\,f_0+e\mathbf{E}\frac{\partial f_0}{\partial p}+\frac{e}{mc}(\mathbf{H}\wedge\mathbf{f}_1)\frac{v}{l}\mathbf{f}_1=0. \qquad \ldots\ldots(4)$$

l is the mean free path defined by $l=1/Nq(p)$, where N is the concentration of atoms and $q(p)$ is the atomic cross section for the transfer of momentum.

Equation (4) can be applied to the positive column of a high current arc as an extension of Davydov's work. In cylindrical coordinates, putting $\partial f/\partial t=0$, $\partial f/\partial\eta=0$ and neglecting the small radial flow of electrons the following pair of equations is obtained :

$$\frac{p}{m}\frac{\partial f_0}{\partial r}+eE_r\frac{\partial f_0}{\partial p}+\frac{e}{mc}Hf_{1z}=0, \qquad \ldots\ldots(5);$$

$$eE_z\frac{\partial f_0}{\partial p}+\frac{p}{ml}f_{1z}=0, \qquad \ldots\ldots(6)$$

where E_z and E_r are the longitudinal and radial electric fields respectively and H is the self-magnetic field of the discharge; e is the charge of an electron and is, therefore, intrinsically negative. Elimination of f_{1z} between (5) and (6) gives

$$\frac{p}{m}\frac{\partial f_0}{\partial r}+eE_r\frac{\partial f_0}{\partial p}+\frac{1}{p}\frac{\partial f_0}{\partial p}R(r)=0, \qquad \ldots\ldots(7)$$

where $R(r)=-le^2E_zH/c$ assuming that l is a constant.

Only the case where E_r is negligible will be considered here, because in this case the magnetic field alone prevents the electrons from rapidly diffusing outward, i.e. the 'pinch

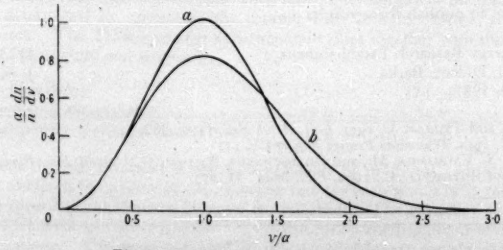

Electron velocity distribution functions.

Curve *a*. Distribution existing in certain magnetically constricted discharges.
Curve *b*. Maxwellian distribution.

effect' is definitely operative. For such a discharge the quantity $[\overline{Heur}_0/c]$ must be of the same order of magnitude as the mean electron energy, where u is the drift velocity and r_0 is the radius of the discharge. The recent measurements of Thonemann and Cowhig (1950) for a low pressure mercury arc show that E_r may be negligible over a wide range of currents.

The solution of equation (7) when E_r is negligible is

$$f_0=C\mu(r)\exp(-p^3/p_0^3), \quad \text{where} \quad \mu(r)=\exp\left[\frac{3m}{p_0^3}\int_0^r R(r)\,dr\right]$$

and C and p_0 are constants. The distribution in terms of the momentum may be written as $4\pi C\mu(r)p^2 \exp(-p^3/p_0^3)dp$ from equation (3), or in the form $dn=(2n/\alpha^3)v^2 \exp(-2v^3/3\alpha^3)dv$, where n is the electron concentration and α is the most probable velocity. The concentration n increases towards the axis of the discharge. The above analysis has been extended to allow for the variation of atomic cross section with electron velocity.

The Figure shows the form of the distribution for the case where l is constant. This distribution differs considerably from the Maxwellian, the percentage of fast moving particles being much smaller.

This analysis holds only for the case where the degree of ionization is small so that the mutual interaction between electrons can be neglected. When the degree of ionization is sufficiently high to cause equation (4) to depart from a correct description of the discharge, i.e. when $nq_e \sim Nq$, where q_0 is the effective cross section for collisions between electrons, the electron interaction establishes a distribution more like the Maxwellian (Davydov 1937, Cahn 1949). Even in this case, however, the magnetic field still tends to reduce the number of high velocity electrons.

Department of Electrical Engineering, J. E. Allen.
University of Liverpool.
28th March 1951.

Alfvén, H., 1950, *Cosmical Electrodynamics* (Oxford : Clarendon Press).
Cahn, J. H., 1949, *Phys. Rev.*, **75**, 293.
Cousins, S. W., and Ware, A. A., 1951, *Proc. Phys. Soc.* B, **64**, 159.
Davydov, B., 1937, *Phys. Z. Sowjet.*, **12**, 269.
Thonemann, P. C., and Cowhig, W. T., 1950, *Nature, Lond.*, **166**, 903; 1951, *Proc. Phys. Soc.* B, **64**, 345.
Tonks, L., 1937, *Trans. Electrochem. Soc.*, **72**, 167; 1939, *Phys. Rev.*, **56**, 360.

The Electrical Conductivity of Simple p-Type Semiconductors

In particle theories of simple semiconductors the case of an empty conduction band and a single donor level below is the only one considered in detail. The case of a p-type semiconductor where conductivity takes place in the nearly filled band and the acceptor level lies above the top of this band is usually referred to as completely analogous to the n-type case. Statements are made that results obtained from consideration of electronic conduction are applicable to cases where the carriers of electricity are holes (Shifrin 1944, Hutner *et al.* 1950). This requires some qualification although the processes involved may be in perfect ' mirror image ' relation.

The electronic conductivity of a non-ionic lattice is (Shifrin 1944)

$$\sigma=\sigma_0 \ln(1+A), \qquad \ldots\ldots (1)$$

where A is related to the thermodynamic potential (Fermi level) ζ by $A=e^{\zeta/kT}$. A discussion of this formula for a simple n-type semiconductor is given by Ehrenberg (1950).

In the case of a p-type semiconductor the corresponding formula will be

$$\sigma'=\sigma_0' \ln(1+B), \qquad \ldots\ldots (2)$$

where $B=e^{-\zeta-\Delta E/kT}$, and $-\Delta E$ is the position of the top of the nearly full band below the bottom of the conduction band which is being taken as the zero of energy.

Formula (2) is derived in a manner analogous to (1) from the general expression (Seitz 1940)

$$\sigma=\frac{e^2}{3}\int vl\frac{\partial f_0}{\partial E}d\omega, \qquad \ldots\ldots (3)$$

where e is the electronic charge, l the mean free path of carriers, f_0 the electron distribution function $(A^{-1}e^{E/kT}+1)^{-1}$ and $d\omega$ the number of states in the energy integral dE per unit volume.

When carriers of electricity are holes we must replace f_0 by the corresponding distribution function $f_0'=1-f_0$. The density of states $d\omega$ at the bottom of the conduction band must be replaced by $d\omega'$ valid for the top of the nearly full band which in the present notation is $d\omega'=(4\pi/h^3)(2m_h)^{3/2}(-E-\Delta E)^{1/2}\,dE$, and the integration is to be carried between $-\infty$ and $-\Delta E$.

To determine B we set up the equilibrium equation : density of free holes in nearly full band = density of bound electrons on acceptor levels,

$$\int_{-\infty}^{-\Delta E} f_0'(E)\, d\omega' = N_a/(A^{-1}e^{-\Delta\epsilon/kT}+1).$$

After simple transformation we obtain

$$C(kT)^{3/2}F(B) = N_a/(Be^{\Delta E-\Delta\epsilon/kT}+1), \qquad \ldots\ldots (4)$$

where $F(B)=\int_0^\infty \frac{x^{1/2}dx}{B^{-1}e^x+1}$ and $C=\frac{4\pi}{h^3}(2m_h)^{3/2}$.

$-\Delta\epsilon$ is the position of the acceptor level below the zero of energy and N_a is the concentration of acceptors. Equation (4) may be solved for B using approximate expressions for $F(B)$ appropriate to the problem (Ehrenberg 1950).

It is found that in a general case B and with it σ' increases with temperature, passes through a maximum and then decreases for large temperatures. Thus a complete analogy with the n-type case is established (which is of course in agreement with experiment) provided the correct formula for hole conductivity is used.

Research Laboratory, A. Lempicki.
Electronic Tubes Ltd.,
High Wycombe, Bucks.
15th March 1951.

Ehrenberg, W., 1950, *Proc. Phys. Soc.* A, **63**, 75.
Hutner, R. A., Rittner, E. S., and de Pré, F. K., 1950, *Philips Res. Rep.*, **5**, 188.
Seitz, F., 1940, *The Modern Theory of Solids* (New York : McGraw-Hill), p. 175.
Shifrin, K., 1944, *J. Phys. U.S.S.R.*, **8**, 242.

Photoconductivity in the Elements

Although the first photoconductive material known was the element selenium, little work has yet been carried out on photoconductivity in other elements. Prior to the end of the recent war, only two other elements were investigated at all fully, namely sulphur, and carbon in the form of diamond. As the outcome of work on crystal detectors, results on silicon were published soon after the end of the war. These were the only elementary photoconductors on which data had been published when the present work began.

It was postulated at the outset that all elements which were not metals, and which had a high refractive index (i.e. greater than about two) would be photoconductive. This classification covers the ten elements boron, carbon (as diamond), silicon, germanium, phosphorus, arsenic, sulphur, selenium and iodine (further remarks on the non-metallic gray tin will be made later). Measurements have been carried out on tellurium, phosphorus, iodine, arsenic, and boron; and since other workers have now published results on germanium, the original postulate has been confirmed by the measurement of photoconductivity in all the specified elements.

One of the main interests in the work was the comparison of optical and thermal activation energies, the former obtained from spectral measurements of photoconductivity, and the latter from resistance–temperature or Hall effect–temperature measurements. For various reasons (Moss 1950) it was decided that the optical activation energy was given by the quantum energy at the wavelength where the spectral sensitivity had fallen to half its maximum value or, when there was no well-defined maximum, by half the value of the flat region preceding the rapid long-wavelength fall in sensitivity. The collected results, obtained by the author or other workers, are given in Table 1. In addition to the values found from photoconductive and resistance–temperature measurements, there are given approximate values calculated from the specific resistance (when this is sufficiently high for the results to be fairly accurate) and from the photo-emissive measurements of Apker and his co-workers. The last column gives results for the temperature shift of the activation energy.

It will be seen that the optical and thermal activation energies given in the first two columns of the Table agree closely, showing that for all the photoconductive elements the

two activation energies are substantially the same. No difference in energy values should result in consequence of the Franck–Condon principle provided the dielectric constants at high and low frequencies are the same, as of course they should be for monatomic solids.

An attempt was made to correlate the threshold wavelengths of the photoconductive effect with the refractive indices of the materials, the data being summarized in Table 2.

It appears from the Table that the more highly refractive elements are photoconductive at longer wavelengths, the only definite discrepancy being the last on the list, viz. diamond.

For germanium, silicon and diamond, a more specific relation appears to hold, namely $En^4 =$ constant.

Table 1. Activation Energies (in ev.)

Element	Photo-conductivity	Resist./ Temp.	Spec. resist.	Photo-emissive	Shift (ev/°c.)
Tellurium	0·37	0·37	—	0·36	$+1{\cdot}9\times10^{-4}$
Phosphorus	1·40–1·56	1·51–1·64	—	—	—
Iodine	1·30	1·24	1·35	—	—
Arsenic	1·2	1·2	1·1	1·0	−5
Boron	0·96–1·27	0·88–1·28	1·0	1·0	−3 to −4
Selenium (red)	1·6	1·7–1·8	—	—	$-4{\cdot}5\pm1$
Sulphur	2·5	2·65	2·5	—	−15
Diamond	5·35	$5{\cdot}2\pm0{\cdot}3$	5·5–6·0	—	−2
Silicon	1·15	1·13	—	—	-4 ± 1
Germanium	0·73	0·75	—	0·66	−1·0

Table 2

Element	Te	Ge	B	Si	As	I	P	Se	S	C
$\lambda_{1/2}(\mu)$	3·3	1·7	1·1	1·08	1·03	0·96	0·85	0·8	0·5	0·23
n_∞	4·8	4·00	>3	3·43	3·35	~3	2·6	2·5	2·0	2·38

For the three elements the value of the 'constant' lies within $\pm 8\%$ of 174. Also for silicon carbide which, although a compound, is clearly similar to the above elements, the En^4 value lies in the same range. We may thus conclude that, in general, there is a qualitative relation between the refractive index and the photoconductive 'threshold' wavelength, the relation becoming specific when applied only to materials with the same crystal structure.

It was announced at the Semiconductor Conference held at Reading University in 1950 that gray tin has been shown to be a semiconductor with an activation energy of about 0·1 ev. In view of the good agreement of optical and thermal activation energies found for the other elements, gray tin should be photoconductive at wavelengths as great as 12μ. Assuming the $En^4 = 174$ relation to hold for gray tin, the refractive index would have the extremely high value of 6·5.

The above work, which was carried out at the Department of Colloid Science, Cambridge University, will be published more fully in the future.

Acknowledgment is due to the Chief Scientist, Ministry of Supply, for the opportunity of carrying out the research at Cambridge University, and for permission to publish this letter.

Telecommunications Research Establishment,
Ministry of Supply,
Great Malvern, Worcs.
12th March 1951.

T. S. Moss.

Moss, T. S., 1950, *Dissertation* (Cambridge).

Ultra-Violet Absorption Spectra of Tin Vapour in Atmospheres of Helium and Hydrogen

In a recent note (Garton 1950), the observation of new atomic absorption lines of tin in the vacuum ultra-violet, has been reported. Improved plates have since been obtained, resulting in the discovery of further lines, the total being some forty-five lines in the range 1600–1800 A., with an additional strong triplet in the 1300–1400 A. region. The analysis of this extension of the Sn I spectrum is in progress.

Work on tin vapour has also been extended into the near ultra-violet. Metallic tin was vaporized, in the usual way, in a King-type furnace, into which was introduced either helium, purified over copper oxide and charcoal, or hydrogen purified over charcoal. With the hydrogen continuum as background, exposures were made with a Hilger medium-quartz spectrograph, at furnace temperatures from 1,400° to 1,800° C., one of the above gases being present at a pressure of some 100 mm.

A large number of Sn I absorption lines, which start on the levels of the $^3P_{012}$ ground state, are present on the spectrograms, and check well with Megger's (1940) analysis of the arc spectrum. In addition certain new bands have been obtained. The most prominent of these is a double-headed, red-degraded, apparently diffuse feature, with heads at 2259·5 and 2255·3 A., which occurs strongly in the hydrogen atmosphere but is absent in helium. This is shown at X in the reproduction. There is a suggestion of a similar structure at Y,

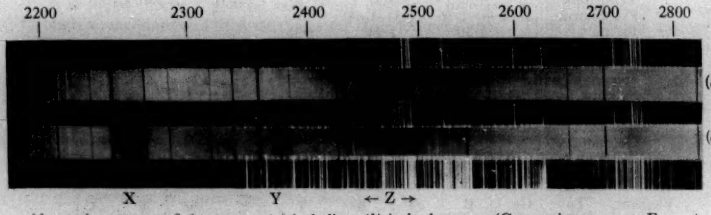

Absorption spectra of tin vapour, (*a*) in helium (*b*) in hydrogen. (Comparison spectra Fe arc.)

but examination of the plates seems to indicate that this consists of a faint doublet of aluminium (present as impurity), one member of which develops a shading to the red in the presence of hydrogen. A more definite extra feature, which may not show well on the reproduction, is a headless patch of diffuse absorption centred at 2750 A., which again occurs only with hydrogen in the furnace. In both hydrogen and helium atmospheres, occur several narrow diffuse bands in the 2450–2500 A. region, shown at Z.

The interpretation of these bands is not obvious without further work. That they are definitely associated with tin is indicated by the paucity of impurity lines, and the absence of the bands from plates taken under similar conditions, but with tin absent. The feature X and the diffuse patch at 2750 A. also require the presence of hydrogen, suggesting a hydride. The bands Z may be due to molecular tin or a carbide.

Details of further work on these spectra will appear later.

Department of Astrophysics,
Imperial College, London S.W.7.
28th February 1951.

W. R. S. GARTON.

GARTON, W. R. S., 1950, *Nature, Lond.*, **166**, 690.
MEGGERS, W. F., 1940, *Bur. Stand. J. Res., Wash.*, **24**, 153.

On a Band System ascribed to the CH Molecule*

In 1927 McDonald observed two bands at 2264 A. and 2367 A. in discharges through hydrocarbons. These were ascribed by him to the molecule CH. More recently these bands were re-investigated by Gerö and Schmid (1941 a, b) using ordinary and deuterated hydrocarbons. In addition to the two bands observed by McDonald they observed several other bands. The wavelengths of these bands (head measurements) and the vibrational assignments proposed by Gerö and Schmid are listed in the Table. These authors concluded that the isotope shift supported the assignment to a diatomic CH molecule and they considered the ion CH^+ as the most likely emitter. Douglas and Herzberg (1942) obtained bands in the near ultra-violet which they have conclusively shown to be due to CH^+. The Gerö–Schmid bands did not appear on their spectrograms and they were led to

* Contribution No. N.R.C. 2428 from the National Research Council.

doubt the assignment of the bands to CH^+. They tentatively suggested CH^{++} as a possible emitter. Whilst preparing experiments to make a fuller examination of these bands their wavelengths were checked with the list prepared by Pearse and Gaydon (1950) and several coincidences with wavelengths of HgH^+ band heads were noted. A complete comparison is given in the Table. The data on HgH^+ are taken from the work of Mrozowski and Szulc (1937) and those on HgD^+ from the work of Mrozowski (1935). There can be little doubt that the two sets of bands are identical. The HgH^+ and HgD^+ bands have been extensively investigated and their assignment appears certain. We are thus led to the conclusion that the bands of McDonald and of Gerö and Schmid were caused by mercury impurity in their vacuum systems. It is of interest to note that Jezewski (1928), in an early paper on the HgH^+ spectrum, commented on the coincidence of two of his bands with those observed by McDonald but considered this to be accidental.

'CH'	HgH^+	'CD'	HgD^+
2264·0 (0,0)	2263·7 (0,0)	2262·4 (0,0)	2262·4 (0,0)
2367·0 (0,1)	2267·3 (0,1)	2336·1 (0,1)	2336·0 (0,1)
2474·8 (0,2)	2474·7 (0,2)	2412·4 (0,2)	2411·9 (0,2)
2388·0 (1,2)	2387·9 (1,2)	2350·4 (1,2)	2350·3 (1,2)
2492·9 (1,3)	2492·9 (1,3)	2425·0 (1,3)	2424·8 (1,3)
	2286·8 (1,1)	2366·4 (2,3)	2366·3 (2,3)
	2413·3 (2,3)	2439·8 (2,4)	2439·5 (2,4)
		2385·3 (3,4)	2385·0 (3,4)
		2457·0 (3,5)	2457·0 (3,5)
		2479·5 (4,6)	(2482·4) (4,6)

Notes on Table. All the bands are degraded to the red. All the HgH^+ and HgD^+ bands measured by Mrozowski and Szulc are listed. The (4,6) HgD^+ band has not been measured A calculated wavelength for its head is quoted. The (1,1) and (2,3) HgH^+ bands are weak and their absence in the ' CH ' spectrum is not surprising.

M. W. Feast†.

Division of Physics,
National Research Council,
Ottawa, Canada.
4th April 1951.

† National Research Laboratories Postdoctorate Fellow.

Douglas, A. E., and Herzberg, G., 1942, *Canad. J. Res.* A, **20**, 71.
Gerö, L., and Schmid, R. F., 1941 a, *Phys. Rev.*, **60**, 363; 1941 b, *Naturwissenschaften*, **29**, 504.
Jezewski, H., 1928, *J. Phys. Radium*, **9**, 278.
McDonald, F. C., 1927, *Phys. Rev.*, **29**, 212 (A).
Mrozowski, S., 1935, *Acta Phys. Polon.*, **4**, 405.
Mrozowski, S., and Szulc, M., 1937, *Acta Phys. Polon.*, **6**, 44.
Pearse, R. W. B., and Gaydon, A. G., 1950, *The Identification of Molecular Spectra* (London: Chapman and Hall).

REVIEWS OF BOOKS

Cosmical Electrodynamics, by H. Alfvén. Pp. viii + 237. 1st Edition. (London: Oxford University Press, 1950.) 25*s*.

H. Alfvén's book is of particular interest at a time when electrodynamical problems seem to be the major stumbling blocks in astrophysics. The great problems of the origin of cosmic rays, the causes of the terrestrial and stellar magnetic fields, of sunspots and solar activity and of cosmic radio noise clearly belong to this province ; one may well feel that the absence of a solution here again spreads uncertainty to those parts of astrophysics which have seemed more settled.

In the first part of the book Alfvén gives a variety of extremely valuable considerations which enable the reader to develop an insight into electrodynamical processes which may be of relevance to astronomical problems. The classical books on electrodynamics, though more rigorous and perhaps more accurate, do not assemble just these considerations,

being more concerned with topics related to possible laboratory experiments, and in this subject a substantial change of scale frequently alters the character of the processes which occur.

Alfvén's magneto-hydrodynamic waves are a phenomenon which occurs on a large scale only, and they are described in considerable detail. But a treatment of conducting fluids in motion requires more than the addition of a particular electrodynamic process to hydrodynamics, and it is there that the author does not give much guidance. It is true that the complete combination of the two subjects leads to prohibitive mathematical difficulties, and that progress there must depend on the correct choice of approximations. In this respect Alfvén's treatment is not always quite convincing.

The subject which is most fully discussed in the book is solar physics. The major part of the chapter on that subject is, as the author admits, quite speculative. This is not a weakness, but in many cases even the starting point of a speculation cannot be claimed to be more than the author's private opinion, and the arguments which are then advanced are not always adequate. It is not clear why only circular magneto-hydrodynamic whirls (whose appearance would explain bipolar spot pairs) should be emitted by the turbulent solar interior. Why do the waves not bring an image of the turbulence to the surface? How does such order spring from chaos?

There has been much discussion of mechanisms for setting up such strong magnetic fields as occur in sunspots. Alfvén leaves the reader to assume that it is an easy job for magneto-hydrodynamic waves to produce a 200-fold increase of the local field strength. It would have been valuable to know the displacement amplitudes that go with so huge a disturbance, so as to ascertain whether their effects would remain undetectable.

In several places in the book the simplicity of the engineer's approach is a great asset, but a treatment resulting from a mixture of Maxwell's equations and equivalent circuits also has its dangers, for the concepts appertaining to each must be kept separate from the other. If the concept of inductance is used in a discussion which starts with Maxwell's equations, then the confusion of the reader is the most likely result.

Magnetic storms, aurorae, and cosmic rays are the other topics which are discussed with considerable clarity of exposition. The speculations on the origin of cosmic rays unfortunately lack the quantitative discussion of the mean energy, which is so commonly the stumbling block of theories which can account for the individual particle energies. The author does not enter into the discussion of the origin of stellar and terrestrial magnetic fields.

The book is certainly stimulating, and it shows clearly how wide a field there is in which speculation has to be replaced by careful analysis. Whether such analysis will then lead on in the directions which Alfvén outlines cannot at present be predicted.

T. GOLD.

Two Lectures, by W. HEISENBERG. Pp. 51. 1st Edition. (Cambridge: University Press, 1949.) 3*s*. 6*d*.

As the title indicates, this little book consists of the text of two lectures delivered in Cambridge in 1948, with little or no modification. In them Professor Heisenberg sets out his views on two very different topics.

The first lecture gives a challenging survey of fundamental problems associated with the interaction and creation of elementary particles. His approach is primarily physical, and he emphasizes the need for being aware of the full scope of the phenomena which have to be brought in to any satisfactory theory. He sets forth the essential problems which must eventually be solved, and makes many penetrating comments on them. In particular he is sceptical of the value of Hamiltonian mechanics as the foundation of the mathematical theory, and gives some cogent reasons why one should attempt to break away from it. Although time may show that these particular criticisms are not relevant, the lecture will remain a masterpiece of clarity and stimulating thought.

The second lecture is quite different in matter, approach and achievement. It is an account of the author's attempt at a deduction of the phenomenon of superconductivity from the basic laws of atomic behaviour. It is a theory which does not by any means command universal agreement, and can be criticized on many grounds. It is indeed little more than a sketch of what might result from a systematic investigation of the problem if one

possessed mathematical methods powerful enough to treat it adequately. It has many logical gaps bridged only by optimism. Its basis is an attempt to show that the electrical interactions between electrons may, under certain circumstances, result in setting up persistent filaments of electric current, rather similar to the domains of persistent magnetism in a ferromagnetic. A plausible enough explanation of the specific heat of superconductors results—though the same result follows from many different lines of thought—but the deduction of the electrical and magnetic properties is scarcely convincing. It is indeed doubtful whether the filament idea can really provide a satisfactory description of superconductivity. In justice, however, it must be said that Professor Heisenberg is well aware of the unsatisfactory nature of much of the theory, and is at pains to point out that it aims more at reconciling previous attempts of others to give a systematic description of the phenomenon, than at being a complete solution of one of the most puzzling problems of 'classical' quantum mechanics. M. H. L. PRYCE.

Elementary Pile Theory, by H. SOODAK and E. C. CAMPBELL. Pp. ix+71. 1st Edition. (New York: John Wiley and Sons, Inc.; London: Chapman and Hall, Ltd., 1950.) 20*s*.

The treatment of elementary pile theory in this book is not so comprehensive as that in the *Science and Engineering of Nuclear Power*, Vol. 1, and the approach to the theory is more formal; but in many respects this is an advantage, and this book gives a very good introduction to the subject. The basic ideas are expressed clearly, and the many complications which arise in practice are only indicated here and do not obscure the simple treatment.

The first half of the book (Chapters 1 to 9) is devoted to the theory of slowing down for fast neutrons and to diffusion theory for thermal neutrons, and the required formulae are derived from well-known physical ideas, while the mathematical treatment is kept as simple as possible.

In the next section (Chapters 10 to 12) the application of these results to the design of a pile is discussed, and the formulae for the dimensions of a critical pile deduced. Refinements of the simple theory, such as the use of a reflector and of multi-group theories, are introduced in the next two chapters and, although lack of space prevents any detailed treatment of these subjects, the basic principles are well set out. Finally, in the last section (Chapters 15 to 17) the problems of the control of a pile and its time-dependent behaviour are briefly discussed.

In a small volume such as this it is clearly impossible to discuss in any detail all the problems involved in pile theory, and here a good choice has been made between what should be inserted or omitted. It would, however, have been an advantage to have included a short bibliography of the literature already published in scientific journals which deals in detail with many of the subjects mentioned in this book. C. A. RENNIE.

Atomic Physics, by W. FINKELNBURG. Pp. x+498. (London: McGraw-Hill Book Co., Inc., 1950.) 55*s*. 6*d*.

Dr. Finkelnburg is well known to students of spectroscopy as an investigator and writer. In his latest book, which is translated from the German, he turns to a wider field and undertakes the difficult task of writing an up-to-date survey of the whole of modern physics. The book is addressed to experimentalists—it contains very little mathematics—and is intended to display both the fundamental concepts and the present position in all the fields where quantum ideas have been applied: the physics of nuclei, atoms, molecules and crystals.

The book begins with a summary of the evidence for the atomic nature of matter, then deals with atomic spectra and their interpretation in terms of the Bohr theory and the later quantum mechanics. The experimental side is treated in some detail. Following this comes a chapter on nuclear physics, which is sufficiently up to date to include references to the new accelerators, pile physics, and thermonuclear reactions. The next chapter is concerned with molecular physics, special emphasis being given to the spectra of diatomic molecules and to the applications of the Franck–Condon principle. In the final chapter

the properties of crystals and metals are discussed; lattice properties, the theory of metallic conduction, lattice defects, and semiconductors are dealt with at length, and there are references to ferromagnetism, latent image theory, germanium rectifiers, and luminescence.

The inclusion of so many topics in a book of less than 500 pages inevitably results in an elementary treatment, but the book may prove of interest to the trained physicist who wishes to extend his general knowledge. Unfortunately it cannot be recommended to students. The treatment of the basic concepts is clouded by a tortuous development of the argument, omissions of essential derivations, and a looseness in expression that can only confuse the beginner. These criticisms apply particularly to the treatment of the quantization of angular momentum: there are frequent references forward to later results, the formula for the Landé g-factor is quoted without any sort of derivation, and there is no explicit mention of the difference between the gyromagnetic ratios of the orbital and spin motions of the electron. Indeed, it is suggested that the spin and magnetic moment of the electron are explicable in terms of a charged rotating sphere, and the formula for the Bohr magneton is said to be based on a classical model.

Elsewhere in the book, similar obscurities in expression, omissions of units from formulae etc., mar the presentation but do not have such serious consequences for the reader. Few, for instance, will take the following sentence literally: " A nuclear isomer differs from an excited nucleus in that it does not revert to a normal state by emitting γ-radiation " (p. 269). Some odd verbal expressions (' the beginning student ', ' the earth alkalies ') reveal that the book is a translation. The appearance of ' long wave ' for ' short wave ' (p. 122), ' magnetic ' for ' electric ' (p. 259), ' diffraction maximum ' for ' diffraction minimum ' (p. 199), etc., will not mislead the alert reader, nor will the curious convention which assigns negative binding energies to stable systems (p. 87). The graph of the nuclear binding energies (Figure 152) makes the italicized statement (p. 319) that *the α-particle is the most stable nuclear structure* appear rather odd. Some errors of fact noted in the nuclear physics section include the following: the half-life of ^{24}Na is 15 hours, not 15 minutes (p. 310); Van de Graaff accelerators have not yet been used at 15 MeV. (p. 255); cadmium will not detect neutrons by induced radioactivity (p. 292); and the fission of ^{235}U is usually stated to release 2–3 free neutrons, not 3–4 (p. 300). There is also an error of fact in the treatment of isotope separation by thermal diffusion: the lighter atoms do not necessarily diffuse in the direction of the higher temperature; this depends upon the power law of the attractive forces between the atoms.

It will not be difficult to remedy many of these defects in a future edition, but the earlier chapters appear to need extensive revision if they are to be of service to students making their first approach to atomic physics. For the present, such students would be well advised to read first a book such as Born's *Atomic Physics*; they could then turn to the present work for interesting information about recent developments in many different branches of atomic physics.

H. R. ALLAN.

Physical Chemistry of Electrolyte Solutions, by H. S. HARNED and B. B. OWEN. Pp. xxvi+645. 2nd Edition. (New York: Reinhold Publishing Corp.; London: Messrs. Chapman and Hall, 1950.) 80*s*.

The title of this book is misleading. The book contains an exhaustive description of Debye's theory of the thermodynamic properties of electrolyte solutions, of Onsager's theory of electrical conductivity and other irreversible phenomena in such solutions, of the various extensions and modifications of these theories, of the experimental data of all kinds having a direct bearing on these theories, and of experimental measurements of the same quantities at higher concentrations. The reviewer did not detect any serious omissions in any of these theoretical topics but he noticed some glaring omissions of important experimental results. The numerous accurate solubility measurements made by Brönsted and his pupils are scarcely mentioned. In particular the measurements of Brönsted and La Mer, which afford incomparably the best available test of Debye's theory as applied to mixtures, are dismissed in a few words without a single diagram or table. The supremely fine measurements of conductivities in anhydrous hydrocyanic acid made by Coates have also been ignored. It is inconceivable that the authors should be ignorant of the existence of this work. On the other hand the book does not deal with the following aspects of the physical

chemistry of electrolytic solutions: chemical equilibria, indicators, optical properties, reaction rates, ampholytes, colloidal electrolytes, electrode processes. Thus the book covers a well-defined field, but the field is narrower than is suggested by the title.

This edition differs from the previous (1943) edition by the inclusion of Appendix B which contains revisions of the tables of the theoretical functions (occasioned by Birge's revision in 1941 of the 'best' values of the fundamental constants), extensions of some of the tables of data and discussions of a few recent experimental and theoretical contributions. The amendment of formulae whenever a better value becomes available for a physical constant would be appreciably simpler if the formulae were quoted in a less clumsy form. Although there are several textbooks on electrolytes, including the one under review, written by well-known research workers, not one of these authors has troubled to write Onsager's formula for conductivity in a compact and memorizable form. For a symmetrical electrolyte one such form, never found in textbooks, is

$$\Lambda=\Lambda_0-\frac{|\ln\gamma|}{3(1+\sqrt{2/2})}\left(\Lambda_0+\frac{(2+\sqrt{2})D\epsilon_0\boldsymbol{R}T}{\pi\eta}\right),$$

where Λ denotes molar conductivity, Λ_0 the value of Λ at infinite dilution, γ the mean activity coefficient according to Debye's limiting law, D the dielectric constant of the solvent, ϵ_0 the permittivity of free space equal to $1{\cdot}113\times10^{-12}$ coulomb/volt cm., $\boldsymbol{R}$ the gas constant, T the absolute temperature and η the viscosity. It is easy to check that this formula is dimensionally correct and nothing is gained by inserting numerical values for ϵ_0, $\boldsymbol{R}$, π until one is ready to assign numerical values to the remaining quantities inside the bracket.

This book will be invaluable to anyone doing or intending to do research in the field covered. It will be found too overloaded with details for use in teaching. E. A. G.

Practical Spectroscopy, by G. R. HARRISON, R. C. LORD and J. R. LOOFBOUROW. Pp. xiv+650. 1st Edition. (London: Blackie and Son, 1950.) 35*s*.

For many years there has been a need for a modern laboratory handbook on the practical technique of spectroscopy which would serve the requirements of both the industrial and the academic spectroscopist. The book under review fills this need in a very admirable fashion indeed. It condenses within a moderate-sized volume the essence of the years of experience of its three authors, who are outstanding scientists interested in spectroscopy from three different aspects, namely, the physical, the chemical and the biological. For several decades Professor Harrison has been director of the spectroscopic laboratory of the Massachusetts Institute of Technology, which is possibly the best-equipped spectroscopic laboratory in the world. For much of that time he has been editor of the *Journal of the Optical Society of America*, and he has also organized at the M.I.T. a long series of summer conferences on applied spectroscopy. There could be no better background for the writing of such a book as this.

In view of the widespread use of spectroscopy in all branches of science and its increasing importance in the analytical control of many industrial processes, a manual giving the technical details essential to obtain the best results is more than welcome. The book not only gives an account of the normal everyday 'tricks of the trade', but indicates the lines of development that are going on at the present time. The historical approach to the subject has been discarded in favour of a more logical and practical one, and this makes the arrangement of the subject matter more orderly and easy of reference. It should be stressed that only a brief introduction to the interpretative side of the ultra-violet, infra-red and Raman spectra is given. It has been wisely decided to leave this aspect of applied spectroscopy, which is in itself a vast and rapidly growing subject, to be dealt with in specialized handbooks and articles.

The inclusion of two short chapters, one on the spectroscopy of the vacuum ultra-violet and the other on interferometric spectroscopy, is valuable, as both these fields are finding increasing practical applications in academic and technical work.

As might be expected in view of the rapidity with which spectroscopic equipment is being developed, several new instruments have been reported since the book was written. However, the fundamental treatment of this book will enable all of them to be easily

understood and their special advantages more readily appreciated. Finally, it should be said that the book, which is printed in the United States of America, conforms to the high standard of the Prentice-Hall Physics series. It is profusely illustrated and the price is quite modest in relation to the vast amount of sound and valuable information which it contains. W. C. PRICE.

Mechanics, by M. SCOTT. Pp. xi + 394. (New York: McGraw-Hill Book Co., Inc., 1949). 38*s*. 6*d*.

This book on mechanics by Merit Scott follows conventional lines and is divided into approximately two equal sections on statics and dynamics respectively. No mathematics higher than the calculus is employed, and the book should provide a sound basic course for a first year physics honours undergraduate.

The author includes both the long form notation and the vector notation, with simple vector operations which are explained in Chapters I and II. He lays great stress on the fact that the problems associated with each chapter are an essential part of the whole text, but one might have hoped that, coming from a physicist, the examples would have been less artificial and more of a physical nature. Moreover, the majority of numerical questions are expressed in lb.ft. units, but one is surprised to find that $g = 980{\cdot}8\ fts/ec^2$ (Problem 23.5, page 354).

It is stated in the preface that the book is written so as to enable a good student to use it unaided, and to fulfil this purpose more effectively, the author might profitably consider the inclusion, in future editions, of answers to the problems. R. W. B. S.

CONTENTS FOR SECTION B

PAGE

Dr. D. GABOR. Microscopy by Reconstructed Wave Fronts: II 449

Prof. R. V. JONES. Some Points in the Design of Optical Levers and Amplifiers . 469

Prof. G. D. WEST. Circulations Occurring in Acoustic Phenomena . . . 483

Mr. J. W. GRANVILLE and Dr. C. A. HOGARTH. A Study of Thermoelectric Effects at the Surfaces of Transistor Materials 488

Mr. W. SYLWESTROWICZ and Dr. E. O. HALL. The Deformation and Ageing of Mild Steel 495

Dr. T. R. KAISER. On the Radio-Frequency Requirements of High Energy Electron Synchrotrons 502

Mr. R. E. BURGESS. The Measurement of Fluctuation Noise by Diode and Anode-Bend Voltmeters 508

Prof. F. LLEWELLYN JONES and Dr. D. E. DAVIES. Mechanism of Secondary Ionization in Low-Pressure Breakdown in Hydrogen 519

Letters to the Editor:

Mr. W. PAUL, Mr. D. A. JONES and Prof. R. V. JONES. Infra-Red Transmission of Galena 528

Mr. N. D. CLARENCE and Dr. D. J. MALAN. Magnetic-Tape Recording of Electrostatic Field Changes 529

Prof. J. R. H. COUTTS and Dr. J. A. V. FAIRBROTHER. Poisson's Ratio and Electrical Resistance 530

DISCUSSION on papers by J. B. HIGHAM and J. M. MEEK entitled "Voltage Gradients in Long Gaseous Spark Channels" and "The Expansion of Gaseous Spark Channels" (*Proc. Phys. Soc.* B, 1950, **63**, 633 and 649) 531

Reviews of Books 533

Contents for Section A 535

Abstracts for Section A 535

ABSTRACTS FOR SECTION B

Microscopy by Reconstructed Wave Fronts : II, by D. GABOR.

ABSTRACT. The theory of diffraction microscopy is completed and extended in different directions. In this two-step method of image formation the object is reconstructed by optical means from a diffraction diagram, taken in coherent illumination with light or with electrons. The ' projection method ', originally described, and the ' transmission method ', recently proposed by Haine and Dyson, are two variants which can be treated by one theory. The process of image formation, the coherence requirements, and the conditions for a good reconstruction are discussed in detail. It is shown that the reconstructed image of extended objects suffers from some spurious detail, but this can be largely suppressed in the ' dark-field ' method of reconstruction, in which the illuminating wave is cut out after it has passed through the diffraction diagram.

Some Points in the Design of Optical Levers and Amplifiers, by R. V. JONES.

ABSTRACT. The design of optical levers with photoelectric amplifiers is examined and sources of instability are traced. Convection currents causing refraction variations are found in some circumstances to affect the light balance in the optical lever; they may be minimized by properly designed shrouds around the optical path. The better known causes of instability are discussed, and the appropriate remedies are described. The discussion is extended to the stability of galvanometers. The design of an optical lever and amplifier is given which can detect a change of 10^{-9} radian in a mirror 5 mm. in diameter with an indication time of 1 second and with a long-term drift of the order of 10^{-8} radian/hour.

Circulations Occurring in Acoustic Phenomena, by G. D. WEST.

ABSTRACT. An investigation is made, by means of smoke particles, of the movements of the air in the neighbourhood of a vibrating reed. At very low frequencies, the paths of the particles exhibit a pattern which, at first sight, resembles the lines of hydrodynamic flow. A more careful examination at sufficiently high magnification shows, however, that the particles do not move along the hydrodynamic lines but trace out small ellipses.

In addition, a mass circulation of the particles is superimposed on the above motion. At low frequencies this circulation is feeble, but with increasing frequency it strengthens and soon becomes the salient feature. Eventually yet another circulation is superimposed.

It is shown how this work connects up with that of other observers, and emphasis is placed on the common occurrence, in many acoustic phenomena, of circulatory motion in association with vibratory motion.

A Study of Thermoelectric Effects at the Surfaces of Transistor Materials, by J. W. GRANVILLE and C. A. HOGARTH.

ABSTRACT. The surfaces of various specimens of Ge and PbS have been explored with a whisker contact, and the character of the conduction mechanism in relatively small regions examined by the polarity of (*a*) the photo-voltaic effect, (*b*) the rectification, and (*c*) the thermoelectric effect. Methods (*a*) and (*b*) give results characteristic of the bulk material as determined by Hall effect measurements, whereas method (*c*) only gives results consistent with (*a*) and (*b*) for uncontaminated cleaved surfaces or for surfaces which have been etched after polishing. For polished surfaces anomalous effects are obtained and point to the existence of a layer on the surface of character different from that of the bulk semiconductor.

The Deformation and Ageing of Mild Steel, by W. SYLWESTROWICZ and E. O. HALL.

ABSTRACT. Mild steel deforms by a series of bands of plastic deformation called Lüders bands. In heavy tensile specimens a complex series of bands may arise, but in thin wire specimens it is shown that only single bands are formed. Measurements have been made of the propagation stress and Lüders strain for these single bands, and the effects which occur on ageing deformed specimens have been studied.

A critical examination of current theories of the upper yield point—the stress at which bands first appear—is also undertaken.

On the Radio-Frequency Requirements of High Energy Electron Synchrotrons, by T. R. KAISER.

ABSTRACT. A theory of the transition between betatron and synchrotron acceleration is specifically applied to high energy electron synchrotrons. The results are used to calculate the R.F. voltage required for two such machines at present being constructed. It is shown that with suitable choice of its initial rate of rise, the R.F. voltage need rise only to a peak value which is not greatly in excess of the voltage per revolution required to maintain an electron on the synchrotron equilibrium orbit.

The Measurement of Fluctuation Noise by Diode and Anode-Bend Voltmeters, by R. E. BURGESS.

ABSTRACT. The response of a diode voltmeter to a C.W. sine-wave signal and to noise is analysed for three typical diode characteristics : discontinuous linear, discontinuous parabolic and exponential. In the first type the indication is proportional to the r.m.s.value of the input voltage but the constant of proportionality is different for noise and for C.W. and depends upon the ratio of the load resistance to diode resistance. For small input signals the curvature of the diode characteristic is important and the voltmeter tends to a square-law behaviour with the result that C.W., noise or a mixture of C.W. and noise can all be measured in terms of a single calibration.

The input conductance of a diode voltmeter is in general greater for noise than for C.W. It can be very much greater in practical conditions and this represents a possible source of error in the measurement of noise.

The response of the anode-bend voltmeter to C.W. and to noise is considered for a discontinuous parabolic and for an exponential characteristic. The departure of the C.W. calibration from a square law and the difference between C.W. and noise calibrations are evaluated in terms of the characteristics.

Mechanism of Secondary Ionization in Low-Pressure Breakdown in Hydrogen, by F. LLEWELLYN JONES and D. E. DAVIES.

ABSTRACT. The breakdown mechanism was investigated by examining the dependence of the shape of the cathode emission (ω/α, X/p) curves on the deposition of electron-positive or electro-negative atoms on cathodes of nickel, aluminium, silver, copper and molybdenum. X is the electric intensity, and p the gas pressure at about 15° C., and ω is the generalized secondary ionization coefficient which includes processes of cathode emission due to impact of positive ions, of excited atoms, and of photons generated in the ionization current; α is the primary ionization coefficient due to the electrons. Deposition of positive atoms on the cathode produced sharp photoelectric peaks in the curves in the region $X/p \simeq 150$ v./cm. mm. Hg, but ω/α was not greatly affected at higher values of X/p. These results are analysed in terms of the varying effective work function of the surface due to the deposition of atoms. It is concluded that the high photoelectric emission from cathodes of low effective work function was due to low-energy photons generated in the pre-breakdown currents, but that for clean metals the secondary emission was due to impact of positive ions; photo-emission due to any high-energy photons generated in the ionization currents was negligible in comparison.